IDENTIFYING SOURCES OF LANDSCAPE VARIATION TO IMPROVE

PREDICTIONS OF POST-FIRE SAGEBRUSH STEPPE RECOVERY

by

Cara Applestein

A dissertation

submitted in partial fulfillment

of the requirements for the degree of

Doctorate of Philosophy in Ecology, Evolution, and Behavior

Boise State University

May 2023

BOISE STATE UNIVERSITY GRADUATE COLLEGE

DEFENSE COMMITTEE AND FINAL READING APPROVALS

of the dissertation submitted by

Cara Applestein

Dissertation Title: Identifying Sources of Landscape Variation to Improve Predictions of Post-fire Sagebrush Steppe Recovery

Date of Final Oral Examination: 13 March 2023

The following individuals read and discussed the dissertation submitted by student Cara Applestein, and they evaluated the student's presentation and response to questions during the final oral examination. They found that the student passed the final oral examination.

Trevor Caughlin, Ph.D   Chair, Supervisory Committee

Matthew J. Germino, Ph.D   Co-Chair, Supervisory Committee

Nancy Glenn, Ph.D   Member, Supervisory Committee

Marcelo Serpe, Ph.D   Member, Supervisory Committee

The final reading approval of the dissertation was granted by, Trevor Caughlin, Ph.D., Chair of the Supervisory Committee. This dissertation was approved by the Graduate College.

DEDICATION

This dissertation is dedicated to my parents, Marta Vogel and Eliot Applestein, who pushed me to succeed academically and supported me in doing whatever I was passionate about.

ACKNOWLEDGMENTS

ABSTRACT

Sagebrush steppe ecosystems are endangered landscapes, threated by the annual grass-fire cycle where invasion by annual grasses drives larger fires and larger fires drive invasion. Despite extensive input of resources by land management agencies, restoration of these ecosystems is notoriously variable and difficult to predict. Understanding and accounting for variation is key to effectively allocating limited resources and having success in restoring burned sagebrush landscapes. I utilized Bayesian modeling to assess how variation in weather, seed dispersal, and topography/slope/landscape position affects understanding of post-fire sagebrush-steppe recovery and how we can best incorporate sources of variation into models predicting where plant communities will most successfully recover.

We first asked how weather conditions directly after fire (in the first 4 years) during important phenological windows or during the antecedent five-years affected long-term vegetation trajectories and how inclusion of weather metrics affected the transferability of vegetation abundance models from one site to another. We found that annual grasses, perennial grasses, and sagebrush all responded differently to post-fire weather, with grasses more limited by post-fire precipitation and sagebrush more limited by post-fire temperatures. However, while including weather variables improved model transferability from one site to another for perennial and annual grass abundance (not for sagebrush), the chosen weather metrics did not matter.

Next, we aimed to assess how sagebrush seed dispersal varies across large landscapes, such as megafires. We conducted a vertical seed trapping experiment and terminal velocity measurements in the lab and combined the data to parameterize a hierarchical Bayesian model that incorporated both an empirical and mechanistic component. We determined that seed dispersal is highly variable, even at a small scale. Our seed rain projections suggest that seed dispersal from natural recovery may pose severe seed limitations for large burned areas, although natural dispersal is likely to be extremely variable. Our novel data fusion approach to seed dispersal modeling has generalizable applications to estimating seed dispersal at larger scales for other species of concern.

Finally, we asked how accuracy and precision of fractional vegetation cover estimates derived from several different satellite-derived products varied with plant cover type, scale, time, and topography in post-fire systems. We found that all gridded map products tested tended to overestimate very low cover and underestimate very high cover, although some products are more accurate than others. We also found that field-derived models of vegetation tend to agree more with satellite-derived models of vegetation at larger scale and less at a smaller scale. Finally, we found that annual herbaceous cover tends to be overestimated in higher elevation, more topographically diverse areas, whereas perennial herbaceous cover tends to be underestimated in these areas.

Together these analyses provide a means by which to better understand variability and the reliability of post-fire vegetation recovery models. Incorporation of the sources of variability we have identified here will help refine future models of recovery, whether they are based on data sources from the field, lab, or remote-sensing.

TABLE OF CONTENTS

LIST OF TABLES

LIST OF FIGURES

INTRODUCTION

Sagebrush steppe ecosystems are endangered landscapes; half of the original extent of sagebrush steppe has been lost to the annual grass-fire cycle. Invasive grasses senesce early in the season and form a continuous bed of dry plant matter that carries fire easily. They are then the first plants to reestablish after fire. Breaking the annual grass-fire cycle requires establishment of native perennial vegetation to outcompete the annual grasses. The Bureau of Land Management alone spends millions of dollars every year on restoration such as seeding and herbicide treatments aimed at reestablishing native perennial vegetation. However, past studies have found mixed results regarding the efficacy of these treatments. Mixed results indicate a high degree of variability in post-fire vegetation responses across sagebrush-steppe landscapes.

In recent decades, wildfires in the Western United States have increased in size and severity and it is no longer uncommon to observe megafires burning hundreds of thousands of acres. It is becomingly increasingly unfeasible to conduct land management treatments on every part of burned landscapes that need treatment. Therefore, managers are having to choose where and when to allocate limited restoration resources. These choices require understanding and being able to predict the variability in post-fire vegetation recovery across the landscape, a task which has historically been very difficult to do. My research sought to address this need and identify different sources of landscape variation in post-fire sagebrush-steppe vegetation dynamics to improve predictive models of recovery. I have specifically focused on comparing alterative model structures with

different variation components to determine which ones can best explain and predict post-fire plant dynamics in a generalizable way.

Sagebrush steppe ecosystems exist in a harsh climatic zone and variable weather patterns are a known driver of initial post-fire vegetation recovery. Therefore, in the first chapter, we focus on how initial weather patterns following fire affect the abundance of different functional groups (annual grass, perennial grass, and sagebrush) and if initial weather patterns better explained longer-term trajectories than more recent weather. We also asked how incorporation of weather metrics improved model transferability from one site to another. We found that annual and perennial grass abundances were best explained by initial precipitation patterns after fire, while sagebrush was more affected by initial temperature extremes. However, while including weather metrics slightly improved model transferability for grass cover types, the choice of weather metric derived from coarse-scale gridded data did not matter. This suggests that while weather is an important driver of vegetation abundances post-fire, further improving predictive models that include weather may require more spatially and temporally refined metrics.

Seed availability is yet another source of variability in post-fire plant establishment. Land managers allocate extensive resources to seeding large swaths of the landscape with sagebrush seeds under the assumption that sagebrush is seed limited after fire. However, previously little has been known or understood about sagebrush seed dispersal. Therefore, in the second chapter, we utilized field and lab data to build models of sagebrush seed dispersal, ask what scale dispersal variation was most evident at, and estimate dispersal across the landscape. We were able to determine both the typical maximum dispersal distance of sagebrush seeds and estimate density of sagebrush seed

rain near seed sources. Although we found dispersal to be extremely variable, even at a microscale, we found that natural dispersal would generally produce insufficient seed density compared with aerial seeding rates.

Finally, in the third chapter, we looked to the sources of vegetation data that most managers have readily available to them to understand post-fire recovery patterns; satellite-derived maps of fractional plant cover. We asked how the accuracy and precision of these maps varied across time, spatial scale, plant cover type, and topography. These products are becoming widely used in land management planning, but guidance for application and understanding where they may be more or less reliable has been lacking. We found that satellite-derived fractional plant cover was more reliable at mid-range abundances and less reliable at low or high abundances and that it was very unreliable for shrub cover within the first few years after fire. We found that agreement precision between field-based plant cover models and satellite-derived models generally increased with the scale of application. Additionally, annual herbaceous cover was more likely to be overpredicted in higher elevation, more topographically heterogenous areas, whereas perennial herbaceous cover was more likely to be underpredicted in these areas. Our results suggest that satellite-derived data may be most applicable for understanding larger scale trends across an entire burned areas but less reliable when applied at smaller scales.

Together these analyses provide a means by which to better understand variability and the reliability of post-fire vegetation recovery models. Incorporation of the sources of variability we have identified here will help refine future models of recovery, whether they are based on data sources from the field, lab, or remote-sensing. Future research to further refine predictive models of post-fire sagebrush-steppe recovery could focus on 1)

incorporating microscale weather into vegetation abundance trend and seed dispersal models, since we focused on coarse-scale weather metrics, 2) understanding sources of variation in sagebrush seed production, particularly over time, and 3) assess accuracy and precision of satellite-derived vegetation cover maps across burned areas of different ages.

CHAPTER ONE: WEATHER AFFECTS POST-FIRE RECOVERY OF SAGEBRUSH-

STEPPE COMMUNITIES AND MODEL TRANSFERABILITY AMONG SITES

Abstract

Altered climate, including weather extremes, can cause major shifts in vegetative recovery after disturbances. Predictive models that can identify the separate and combined temporal effects of disturbance and weather on plant communities and that are transferable among sites are needed to guide vulnerability assessments and management interventions. We asked how functional group abundance responded to time since fire and antecedent weather, if long-term vegetation trajectories were better explained by initial post-fire weather conditions or by general five-year antecedent weather, and if weather effects helped predict post-fire vegetation abundances at a new site. We parameterized models using a 30-yr vegetation monitoring dataset from burned and unburned areas of the Orchard Training Area (OCTC) of southern Idaho, USA, and monthly PRISM data, and assessed model transferability on an independent dataset from the well-sampled Soda wildfire area along the Idaho/Oregon border. Sagebrush density increased with lower mean air temperature of the coldest month and slightly increased with higher mean air temperature of the hottest month, and with higher maximum January–June precipitation. Perennial grass cover increased in relation to higher

precipitation, measured annually in the first four years after fire and/or in September–November the year of fire. Annual grass increased in relation to higher March–May precipitation in the year after fire, but not with September–November precipitation in the year of fire. Initial post-fire weather conditions explained 1% more variation in sagebrush density than recent antecedent 5-yr weather did but did not explain additional variation in perennial or annual grass cover. Inclusion of weather variables increased transferability of models for predicting perennial and annual grass cover from the OCTC to the Soda wildfire regardless of the time period in which weather was considered. In contrast, inclusion of weather variables did not affect transferability of the forecasts of post-fire sagebrush density from the OCTC to the Soda site. Although model transferability may be improved by including weather covariates when predicting post-fire vegetation recovery, predictions may be surprisingly unaffected by the temporal windows in which coarse-scale gridded weather data are considered.

Introduction

Changing global patterns of precipitation and temperature are impacting vegetation dynamics by modifying habitat suitability and disturbance regimes (Cramer et al. 2001, Griffiths et al. 2015, Kim et al. 2018). Hotter and drier conditions in the western United State are expected to increase the frequency, severity, and size of wildfires (McKenzie et al. 2004, Abatzoglou and Kolden 2011). Fire has the potential to spur much more rapid rates of change in species composition than altered weather patterns alone (Dale et al. 2001, McKenzie et al. 2004). In many ecosystems, fire disturbances combined with weather conditions are affecting recovery of key foundational native species (Keeley et al. 2005, Nelson et al. 2014, Meng et al. 2015). Understanding how

initial post-fire recovery and recruitment will affect long-term trajectories of certain functional groups, in light of weather patterns, is critical to understanding how the combination of weather and fire influence the vegetative composition of ecosystems (Keane et al. 2013).

Parameterizing weather in explanatory or predictive models can be particularly challenging because there are a myriad of weather variables which can be aggregated over any time frame. In many ecosystems, post-disturbance recruitment occurs episodically during periods of favorable weather conditions (Enright et al. 2015). Favorable weather conditions for recruitment may not be known a priori, and major community composition changes in response to weather variability can lag behind extreme events, only realized after cumulative seasons of weather conditions deviating from average (Ogle and Reynolds 2004, Wu et al. 2015). Vegetative community structure at any point in time will reflect past weather events (Anderson and Inouye 2001, Ogle et al. 2015, Wilson et al. 2017). Forecasting future vegetation responses to climate change will require quantifying the relative importance of short-term vs. longer-term weather effects for shaping plant communities.

Sagebrush steppe occupies a vast, sparsely populated, ~500,000 km2 area of western North America that includes high variability in climate, soils, disturbances, and other factors affecting plant communities (Chambers et al. 2014, McIver and Brunson 2014). Most field-based information about vegetation responses to climate and other drivers in sagebrush steppe has come from a relatively small number of locations and areas compared to this vast domain (Nelson et al. 2014, Shinneman and McIlroy 2016). Thus, knowing the generalizability of plant community and environment relationships is

critical for science and management applications in sagebrush steppe (McIver and Brunson 2014). Plant-environment models trained using site-specific data can be tested for generalizability by assessing accuracy of predictions made at different sites (Wenger and Olden 2012). Such tests are a priority need in ecology (Houlahan et al. 2017, Dietze et al. 2018). Developing ecological forecasts for restoration science will also enable transfer of knowledge from highly studied sites to sites in need of land management (Brudvig et al. 2017).

Sagebrush-steppe ecosystems provide an excellent focal system in which to consider the interplay of disturbance and climate variability. Weather at specific time periods after fire is critically important in determining whether a plant community is invaded by exotic annual grass vs. re-established with sagebrush or perennial grass (Lesica et al. 2007, Hardegree et al. 2012, Nelson et al. 2014). After burning of sagebrush steppe, exotic annual grasses compete with perennial native species for soil water or other soil resources (Melgoza et al. 1990, DiCristina and Germino 2006). Furthermore, sagebrush establishment after fire can be highly episodic, and both winter and spring precipitation are important for new seedling establishment (Nelson et al. 2014, Houlahan et al. 2017, Shriver et al. 2019). Although establishment the year directly after fire is important, sagebrush may take advantage of high precipitation for several years after fire occurrence (Lesica et al. 2007, Nelson et al. 2014). Following establishment, most sagebrush seedling mortality occurs in the first year (Donovan and Ehleringer 1991, Owens and Norton 1992), with a previous study finding that minimum spring temperatures can be a limiting factor of sagebrush survival (Brabec et al. 2017). There is also evidence that sagebrush communities display a lagged response to weather: Both

Anderson and Inouye (2001) and Pilliod et al. (2017) found that precipitation three or four years earlier was positively correlated with sagebrush or native herbaceous cover. These observations suggest that consideration of time lags could improve analyses of vegetation-water relationships.

We analyzed the relative importance of weather patterns on cover of exotic annual and perennial grasses and density of sagebrush as they varied annually over a nearly 30-yr observation period on a large landscape where multiple fires had occurred. We sought to determine how annual and perennial grass cover and sagebrush density responded to time since fire and antecedent weather using a model comparison approach that included tests of model fit, as well as transferability. Our questions were as follows:

1. How do the dominant sagebrush-steppe functional groups (perennial grass, annual grass, and sagebrush) respond to time since fire and antecedent weather conditions—either during specific post-fire windows or during a general antecedent 5-yr period?

2. Do post-fire weather conditions during specific recruitment windows leave a lasting impact on long-term vegetation trajectories or is functional group dominance more a product of recent weather, regardless of post-fire conditions?

3. Does consideration of post-fire weather or recent 5-yr weather help predict post-fire outcomes at a new site?

Materials and Methods

<u>Sites</u>

Data used to parameterize models were collected between 1989 and 2017 from monitoring plots spread across approximately 108,000 ha on the Orchard Combat Training Center (OCTC) located in the Morley Nelson Snake River Birds of Prey National Conservation Area in Southwestern Idaho (Fig. 1.1). Approximately half of the plots burned at least once between 1957 and 2014. We only included data records where monitoring occurred in consecutive years because our analysis was on year-to-year change. The dominant sagebrush type in this system is Wyoming big sagebrush (Artemisia tridentata ssp. wyomingensis). Bluebunch wheatgrass (Psuedoroegneria spicata) and Sandberg's bluegrass (Poa secunda) were the dominant bunchgrass species. According to land manager records, only 6% of plots had recorded seedlings of any type (primarily big sagebrush or shadscale, Atriplex sp.), and only two plots have seedlings recorded within 5 yr of fire. Elevation ranges from 862 and 1066 m (U.S. Geological Survey's Digital Elevation Model, 30-m pixel). Average annual precipitation (between 1989 and 2017) ranged from 199 to 307 mm, and average monthly temperature was between 10°C and 12°C (PRISM 2017). A total of 6478 plot-year entries were included in analysis.

Data for model transferability tests came from the Soda wildfire (burned in 2015) for monitoring done 2016–2018 and only 2017 and 2018 data were used to incorporate the previous year's density or cover data as a model input. The eastern edge of the Soda wildfire site is approximately 25 km from the OCTC across the Snake River (Fig. 1.1). Areas that were seeded by managers with sagebrush were excluded from this analysis

because removing these areas from this analysis primarily left lower elevation areas that
were more comparable in elevation and other site conditions to the OCTC.
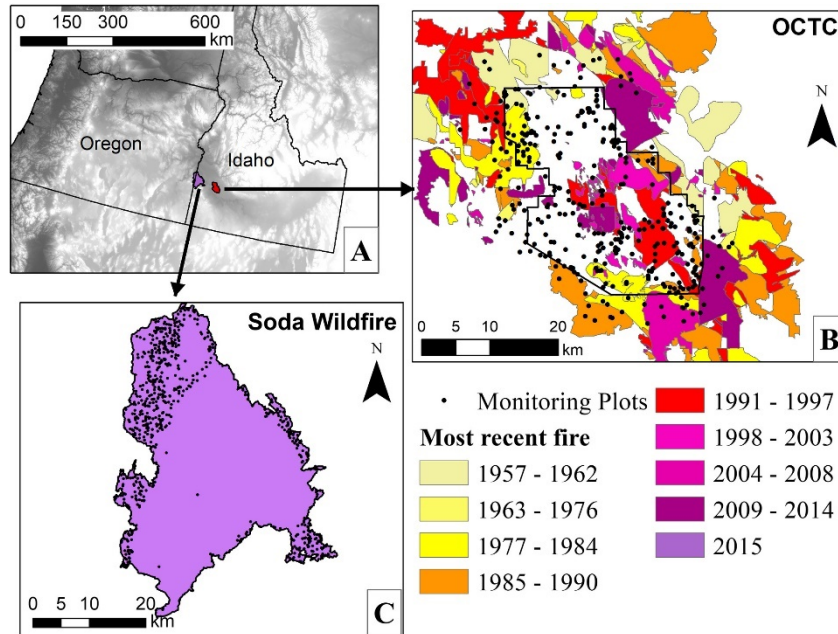
**Figure 1.1   Location of the Orchard Combat Training Center (OCTC) and Soda
Wildfire plots.**

The location of the OCTC, where data for model parameterization were collected, and

Soda wildfire, where data for model validation were collected, are shown relative to

elevation (panel A; darker shades are lower elevation based on the USGS digital

elevation model). The distribution of sampling plots and fire histories are shown for

OCTC in panel B and the Soda fire area in panel C.

The dominant sagebrush type in this system is Wyoming big sagebrush with some low sagebrush (A. arbuscula). Low sagebrush were excluded from analysis. Bluebunch wheatgrass and Sandberg's bluegrass were the dominant bunchgrass species. Among the plots included in the test dataset, about 5% and 7% were drill seeded or aerially seeded with perennial grass, respectively. The total number of plot-year entries included was 698. Elevation for the test plots selected on the Soda wildfire ranged from 747 to 1692 m (U.S. Geological Survey's Digital Elevation Model, 30-m pixel). Average annual precipitation (between 2016 and 2018) ranged from 238 to 473 mm, and average monthly temperature was between 8°C and 11°C (PRISM 2017).

<u>Data collection</u>

At the OCTC, cover data for perennial and annual grasses were derived from line point intercept monitoring (LPI). Density of sagebrush (plants/m2) came from belt transects ranging from 100 to 1400 m2.

At the Soda wildfire, cover data for perennial and annual grasses were derived from grid-point intercept (GPI) from overhead photographs (Applestein et al. 2018). We quantified sagebrush density using a frequency-density method. First, we counted individuals in a 1-m2 quadrat, and if three individuals were not found, we moved outwards in circular plots with radiuses of 5.5, 9, 13, and 18 m until we found at least three individuals within the incremental area. Then, we completed counting all the individual plants in that radius to determine density. Density was calculated as the number of individuals over the area searched (to obtain plants/m2).

Calculation of climate and landscape variables

For OCTC and Soda data, we calculated the following from 800-m resolution PRISM data from 1957 to 2018 by plot: monthly precipitation, mean daily temperature by month, maximum daily temperature by month, and minimum daily temperature by month. Time since fire was derived by extracting the date of the last fire on record from the Land Treatment Digital Library database in the Great Basin (Pilliod and Welty 2013). If there was no record of the last fire, we assumed that the last fire was more than 100 yr prior and coded this as such in the input data.

Annual and perennial grass cover were treated as continuous variables, and sagebrush density was treated as an ordinal variable. We transformed exotic annual grass and perennial grass cover as suggested by Smithson and Verkuilen (2006) to remove 0 and 1 values, which cannot be fit with a beta-distribution. The transformation is given as

$$y^n = \frac{y'(n-1) + 0.5}{n}$$

where n is the sample size, y' is the original data point, and yn is the transformed data point. We then modeled transformed grass cover values with a beta-distributed random variable using a logit link function. Density of sagebrush (number/m2) was binned into one of five possible categories: 0, <0.5, 0.5–1, 1–5, and >5 plants/m2 and modeled via ordinal regression (using the cumulative distribution with logit link). We chose to bin sagebrush density rather than model it directly because exact counts are more likely to be site-specific, whereas density bins are likely to be more generalizable across different sites. A previous assessment comparing plant cover measured as a continuous vs. ordinal variable found that using ordinal categories did not result in a significant loss of information (Irvine et al. 2019).

Model parameterization

We compared models of vegetative functional group density or cover as predicted by (1) no weather or fire effects (landscape effects only), (2) landscape and fire effects only (time since fire), (3) landscape and antecedent weather effects (with or without time since fire). We parameterized antecedent weather variability in two ways. First, we built a model that included weather variables selected a priori during specific time windows in the first several years after fire with the assumption that weather during these time periods would have lasting impacts on functional group density or cover. Secondly, we built models that included weather variables within the most recent five years, allowing the data to determine important time windows.

Cover of the target functional groups were estimated using Bayesian generalized linear models (GLMs) fit in STAN (a no-U-turn sampler) via the brms package in R (Bürkner 2017, R Core Team 2017). We also explored fitting generalized additive models (GAMs), which do not make assumptions about the linearity of response curves, but GAM model errors were higher than the GLM errors so we report on the GLMs here for the final analysis. To better interpret covariate effects and facilitate model convergence, we standardized covariates (but not response variables) using the scale package in R, which subtracts the mean from each value and divides by the standard deviation. Additional covariates (elevation, percent sand, percent clay) were incorporated into all models because they are known to affect the habitat suitability of a site for sagebrush (Schlaepfer et al. 2012, Nelson et al. 2014). These covariates were not strongly correlated with each other (Appendix A: Table A1). All models included an autoregressive term (density or cover from the previous time step). Model convergence was assessed by rhat

values and visual checks of the posterior predictive distributions (calculation given by

Brooks and Gelman 1998).

We set uninformative priors for the models from the brms package. These were as

follows: normal(0,1) for all parameters except for the beta dispersion parameter, Φ, for

which gamma(0.01,0.01) was used.

The models are as follows

$$A_{pt} \sim \text{Beta}(\mu_t^a, \Phi^a)$$

where A_{pt} is the observed annual grass cover at year t and plot p, μ_t^a is the overall mean

annual grass cover in year t, Φ^a is the annual grass dispersion parameter.

$$P_{pt} \sim \text{Beta}(\mu_t^p, \Phi^p)$$

where P_{pt} is the observed perennial grass cover at year t and plot p, μ_t^p is the overall mean

perennial grass cover in year t, Φ^p is the perennial grass dispersion parameter.

$$q_{pt} = Pr\{S_{pt} > k | X_{pt}\} = \sum_{k+1}^{5} p_{ptk}$$

where S_{pt} is the observed sagebrush density category and $k = 1, \ldots, 5$, which corresponds

to $S = 0$, $0 < S < 0.5$, $0.5 < S < 1$, $1 < S < 5$, and $S > 5$, respectively. q_{pt} is the probability

that a plot p during year t has a sagebrush density greater than that defined by k, p_{ptk} is the

probability that a plot has a sagebrush density in category k, given X_{pt} covariates at

plot p and year t. This parameterization reflects a cumulative logistic regression where

the calculation of the probability of a given density category takes into consideration the

probability of any of the other density categories occurring.

μ_t^a, μ_t^p, and q_{pt} (annual grass cover, perennial grass cover, and sagebrush density

category, respectively) are calculated using different covariates for each model, where

superscript ᵃ denotes annual grass cover covariates, superscript ᵖ denotes perennial grass cover covariates, and superscript ˢ denotes sagebrush density covariates. A_{pt-1} stands for annual grass cover at plot p one year before time t, P_{pt-1} stands for perennial grass cover at plot p one year before time t, and S_{pt-1} stands for sagebrush density category at plot p one year before time t. All models include terms β0, β1, β2, and β3, which are coefficients for elevation (elev), percent sand (sand), percent clay (clay), and the previous year's cover/density, respectively.

Model 0: null model

The null model served as a baseline with which to compare the time since fire and weather effects models with the null hypothesis that neither weather conditions nor time-since-fire covariates improve predictions of post-fire vegetative outcomes. The null model considered the year-to-year change in sagebrush, annual grass, and perennial grass cover with fixed landscape covariates (elevation, percent sand, percent clay) but no fire or weather variables. μ_t^a, μ_t^p, and q_{pt} (annual grass cover, perennial grass cover, and sagebrush density category) are calculated as such:

$$\text{logit}(\mu_t^a) = a^a + \beta0^a \times \text{Elev} + \beta1^a \times \text{Sand} + \beta2^a \times \text{Clay} + \beta3^a \times A_{pt-1}$$

$$\text{logit}(\mu_t^p) = a^p + \beta0^p \times \text{Elev} + \beta1^p \times \text{Sand} + \beta2^p \times \text{Clay} + \beta3^p \times P_{pt-1}$$

$$\text{logit}(q_{pt}) = a^s + \beta0^s \times \text{Elev} + \beta1^s \times \text{Sand} + \beta2^s \times \text{Clay} + \beta3^s \times S_{pt-1}.$$

Model 2: time since fire and post-fire weather events

The second model tested how time since fire and weather covariates in the first several years after fire would affect post-fire vegetation recovery. We hypothesized that pre-selected weather variables during specific time windows in the first several years after fire would have lasting impacts on functional group density or cover. We only

included plots that burned from 1900 to 2016 for this analysis (n = 5374). A previous analysis of weather variable effects on vegetation at the OCTC found no relationship between temperature and cheatgrass or native herbaceous cover (Pilliod et al. 2017), so we did not include temperature variables for the annual or perennial grass cover models. The two climate variables used for testing annual grass cover were fall and spring precipitation the year following fire since Bradley et al. (2016) identified these variables as directly affecting annual grass growth and biomass. Native perennial grass cover, specifically bluebunch wheatgrass and Sandberg's bluegrass, is positively correlated with higher fall and total annual precipitation (Anderson and Inouye 2001, Adler et al. 2009). Consequently, we tested fall and total annual precipitation on the year-to-year variation in perennial grass cover. Furthermore, because Anderson and Inouye (2001) identified a four-year lag for precipitation effects on total perennial grass cover, we included average annual precipitation for the first four years following fire.

We selected climate variables for sagebrush based on factors known to be important specifically for seedling recruitment and initial survival; these included average winter/spring precipitation (Shriver et al. 2019), maximum precipitation January–June, spring temperature (Brabec et al. 2017), mean temperature of the coldest month, and mean temperature of the hottest month. All of these variables were assessed during the first four years after the fire. μ_t^a, μ_t^p, and q_{pt} (annual grass cover, perennial grass cover, and sagebrush density category) are calculated as such:

$$\text{logit}(\mu_t^a) = a^a + \beta 0^a \times \text{Elev} + \beta 1^a \times \text{Sand} + \beta 2^a \times \text{Clay} + \beta 3^a \times A_{pt-1} + \beta 4^a \times \text{Yrs}$$
$$+ \beta 5^a \times \text{MMPYr1} + \beta 6^a \times \text{SNPYr0}$$

$$\text{logit}(\mu_t^p) = a^p + \beta0^p \times \text{Elev} + \beta1^p \times \text{Sand} + \beta2^p \times \text{Clay} + \beta3^p \times P_{pt-1} + \beta4^p \times \text{Yrs}$$

$$+ \beta6^p \times \text{SNPYr0} + \beta7^p \times \text{APYr14}$$

$$\text{logit}(q_{pt}) = a^s + \beta0^s \times \text{Elev} + \beta1^s \times \text{Sand} + \beta2^s \times \text{Clay} + \beta3^s \times S_{pt-1} + \beta4^s \times \text{Yrs}$$

$$+ \beta8^s \times \text{JAP14} + \beta9^s \times \text{JJP14} + \beta10^s \times \text{MJT14} + \beta11^s \times \text{MnCMn14}$$

$$+ \beta12^s \times \text{MxHMn1}$$

where β5 is the coefficient for March–May precipitation in the first year after fire (MMPYr1), β6 is the coefficient for September–November precipitation in the year of fire SNPYr0, β7 is the coefficient for annual precipitation years one through four after fire APYr14, β8 is the coefficient for mean January–April precipitation years one through four after fire (JAP14), β9 is the coefficient for the maximum January–June precipitation years one through four after fire JJP14, β10 is the coefficient for the mean March–June precipitation in years one through four after fire (MJT14), β11 is the coefficient for the mean temperature of the coldest month in years one through four after fire (McCMn14), and β12 is the coefficient for the mean temperature of the hottest month in years one through four after fire (MxHMn14).

Model 3: recent five-year weather using random forests to weigh the importance of weather during antecedent months

The third model used a moving window approach to assess how antecedent weather at certain times of the year affects density or cover of sagebrush, annual grasses, and perennial grasses with no hypothesis concerning what times of year would have the most impact (Fig. 1.2). We allowed the data to inform which weather windows affected functional group density or cover.
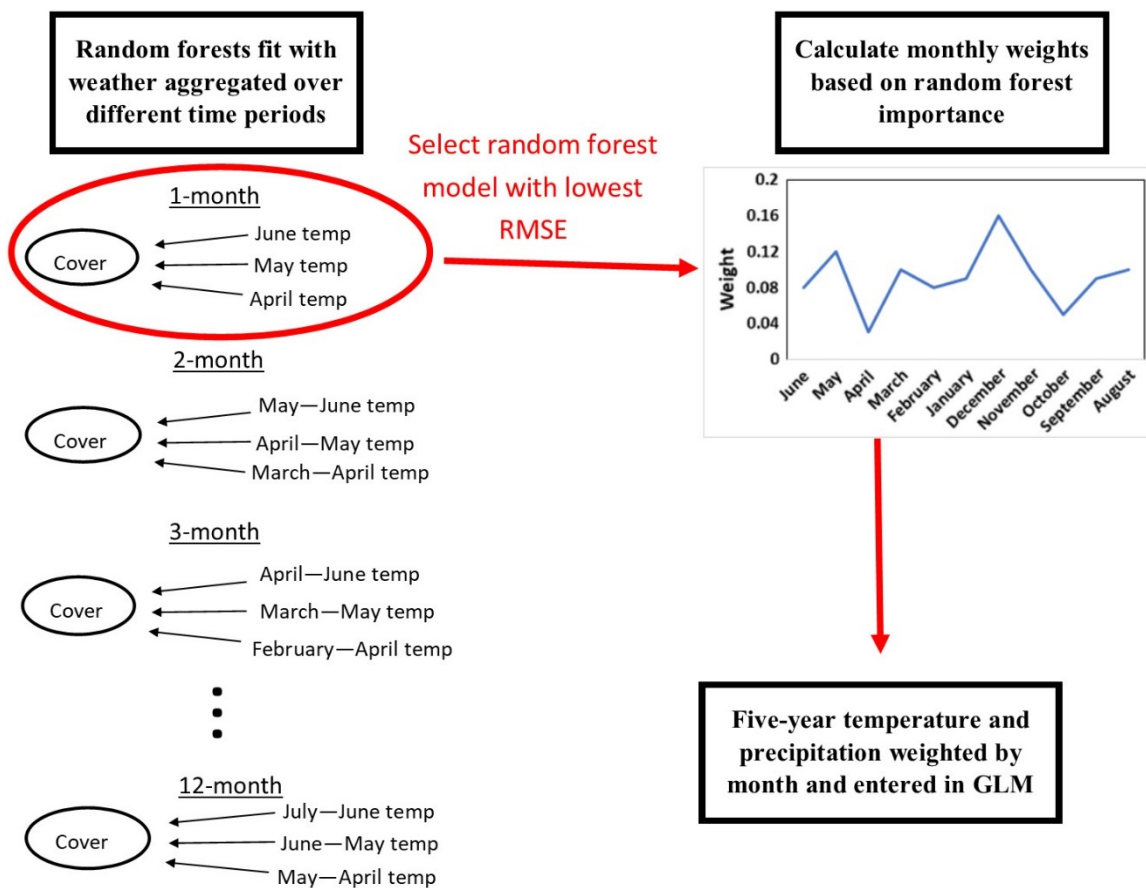
Figure 1.2   Conceptual example of analysis used to fit Models 3 and 4.

Only temperature is shown as an example on the diagram, although precipitation was also

included.

Our approach is conceptually similar to the ecological memory models fit by Ogle et al. (2015), but with weather weights calculated via random forest importance instead of from a fitted Dirichlet distribution. Deriving monthly weather weights from this distribution makes the assumption that there is a point in time in the past that is most important for predicting current plant responses and that the importance of weather events before or after this point declines along a specified parametric curve. We anticipated that there might be multiple spikes of importance during times of the year that were particularly important to plant growth and that using a method with sufficient flexibility to represent these spikes would help to determine certain periods of time that had the most impact on current plant density or cover.

Random forests

To determine how to weigh specific time periods of past weather, we fit random forests to predict the response variables (annual grass, perennial grass, and sagebrush density) from summed monthly precipitation and average monthly temperature combined across different time period lengths. A similar technique to identify temporal lags and time period lengths has previously been used for looking at climate effects in a remote sensing context (Lamberty et al. 2012). Random forests were trained using the caret package in R using the parRF model.

In the first step, we fit random forests with monthly precipitation and monthly average temperature as the independent variables aggregated over 1-, 2-, 3-, 4-, 5-, 6-, or 12-month time periods. In each iteration, all five years of previous weather data were included but the window length determined the level of temporal aggregation (for instance, the random forest with 1-month windows included a variable for each month in

the five-year time period, whereas the random forest with 6-month windows included an averaged variable for each overlapping 6-month time period). The random forest with the lowest out-of-bag (OOB) root mean square error (RMSE) was selected (for all three functional groups, it was the 1-month time period random forest). OOB is the prediction error on average of each sample predicted by those trees which did not use the sample for training. In the second step, importance values for each of these 1-month time periods were then calculated using the varImp function in the caret package (Kuhn 2012). Monthly weights were calculated scaled based on variable importance values from the random forest with all weights summing to 1. In the final step, cumulative five-year average temperature and monthly precipitation were calculated using monthly weights. A conceptual example of this method is shown in Fig. 1.2. To facilitate model-fitting in random forest models, we considered sagebrush density as a continuous response variable for this step.

<u>Full GLM model using monthly weights derived from random forest</u>

We assigned proportional weights to each window relative to the importance of each window from the random forest with all weights equaling 1 (this was done separately for each functional group). μ_t^a, μ_t^p, and q_{pt} (annual grass cover, perennial grass cover, and sagebrush density category) in the final model are thus defined as:

$$\text{logit}(\mu_t^a) = a^a + \beta 0^a * \text{Elev} + \beta 1^a * \text{Sand} + \beta 2^a * \text{Clay} + \beta 3^a * A_{\text{pt-1}} + \beta 13^a *$$
$$\sum_{i=1}^{n} \text{ppt} * \text{wp}_i^a + \beta 14^a * \sum_{i=1}^{n} \text{tmp*wt}_i^a * \beta 15^a * \text{int}(\sum_{i=1}^{n} \text{ppt} * \text{wp}_i^a, \sum_{i=1}^{n} \text{tmp*wt}_i^a)$$

$$\text{logit}(\mu_t^p) = a^p + \beta 0^p * \text{Elev} + \beta 1^p * \text{Sand} + \beta 2^p * \text{Clay} + \beta 3^p * P_{\text{pt-1}} + \beta 13^p *$$
$$\sum_{i=1}^{n} \text{ppt} * \text{wp}_i^p + \beta 14^p * \sum_{i=1}^{n} \text{tmp*wt}_i^p * \beta 15^p * \text{int}(\sum_{i=1}^{n} \text{ppt} * \text{wp}_i^p, \sum_{i=1}^{n} \text{tmp*wt}_i^p)$$

$$\text{logit}(q_{\text{pt}}) = a^s + \beta 0^s * \text{Elev} + \beta 1^s * \text{Sand} + \beta 2^s * \text{Clay} + \beta 3^s * S_{\text{pt-1}} + \beta 13^s *$$

$$\sum_{i=1}^{n} \text{ppt} * \text{wp}_i^s + \beta 14^s * \sum_{i=1}^{n} \text{tmp} * \text{wt}_i^s * \beta 15^s * \text{int}(\sum_{i=1}^{n} \text{ppt} * \text{wp}_i^s, \sum_{i=1}^{n} \text{tmp} * \text{wt}_i^s)$$

where wp_i is the month-specific and functional group-specific precipitation weight and wt_i is the month-specific and functional group-specific temperature weight. $\beta 13$ is the coefficient of the weighted sum of precipitation ($\sum_{i=1}^{n} \text{ppt}$), $\beta 14$ is the coefficient of the weighted sum of temperature ($\sum_{i=1}^{n} \text{tmp}$) and $\beta 15$ is the coefficient of an interaction term between precipitation and mean monthly temperature (int).

Model 4: time since fire and recent five-year weather using random forests to weigh the importance of weather during antecedent months

Model 4 was the same as model 3, but with an added term for time since fire ($\beta 4 \times \text{Yrs}$) for each functional group, in order to test if including timing of fire as a covariate (but not specifically post-fire weather conditions) improved predictions of post-fire outcomes in a recent weather model.

Model fit and significance of effect sizes

We assessed model fit using leave-one-out (loo) cross-validation from the brms package (Bürkner 2017). For annual and perennial grass cover, we evaluated model fit using RMSE (root mean squared error), NRMSE (normalized root mean squared error), and squared bias. RMSE is calculated as

$$\text{RMSE} = [\frac{\sum_{i=1}^{n}(P_i - A_i)^2}{n}]^{0.5}$$

where n is the sample size, P_i is the predicted value, and A_i is the actual value (Willmott 1981). NRMSE is calculated by dividing the RMSE by the range of the observed response variable. For sagebrush density, probability predictions were made for

each density category and the category with the highest probability was taken to be the

density prediction. From these predictions, we calculated a confusion matrix and

evaluated model fit using overall accuracy, and Cohen's kappa (referred to just as kappa

hereafter) using the caret package in R (Kuhn 2012). Kappa is calculated as

$$\text{kappa} = \frac{P_o - P_e}{1 - P_e}$$

where Pe is the chance of proportional agreement between the predicted and

actual data and Po is the actual proportional agreement between the predicted and actual

data for categorical variables (Cohen 1960).

To determine the significance of effect sizes, we used the bayestestR package to

calculate the probability of direction (pd, or maximum probability of effect; Makowski et

al. 2019). The pd is correlated with frequentist P values where pd values of 0.95, 0.975,

0.995, and 0.9995 are approximately equivalent to two-sided P values of 0.1, 0.05, 0.01,

and 0.001, respectively. For the purposes of this analysis, we define a significant effect

size as one with a pd of 0.975 or greater.

<u>Model transferability</u>

We calculated predictions of each model for the 2017 and 2018 Soda wildfire data

and then calculated error metrics as described above in the previous section. Comparing

the transferability of each model allowed us to assess our last question of whether post-

fire weather or recent antecedent 5-yr weather helped predict post-fire outcomes.

Results

<u>Vegetation responses to time since fire and antecedent weather</u>

<u>Model 1: time since fire</u>

Annual grass cover increased by a small amount (1.5% over 100 yr, pd = 1, Table 1.1) and perennial grass cover did not change with time since fire (pd = 0.73, Table 1.2). Sagebrush density was more likely to increase with time since fire (13% more likely to have density higher than 0 plants/m2 over 100 yr, pd = 1, Table 1.3). However, including time since fire did not improve fit (model 0 vs. model 1 comparison between NRMSE, Table 1.4).

<u>Model 2: time since fire and historical post-fire weather events</u>

Annual grass cover increased by 3.7% as March–May precipitation in the year after fire increased from 31.2 to 146 mm (pd = 1, Fig. 1.3A, Table 1.1), but not significantly with September–November precipitation in the year of fire (pd = 0.91, Table 1.1). Perennial grass cover increased by 14% as mean annual precipitation increased from 160.1 to 415.7 mm in the first four years after fire (pd = 1, Fig. 1.3C, Table 1.2) and increased by 2.6% as September–November precipitation in the year of fire increased from 20.9 to 152.7 mm (pd = 1, Table 1.2, Fig. 1.3B).

In the OCTC data, sagebrush density was negatively related to mean temperature of the coldest month (34% higher probability of no sagebrush present at 1°C vs -5.4°C, pd = 1, Figure 1.4B, Table 1.3) and slightly positively related to mean temperature of the hottest month in the first four years after fire (34% higher probability of sagebrush density >0 at 27.01°C, pd = 0.99, Table 1.3, Figure 1.4C). There was a 30% higher probability of sagebrush density >0 as maximum January-June precipitation in the first

four years after fire increased from 77.2 mm to 325.3 mm (pd = 0.99, Table 1.3, Figure
1.4A).

Table 1.1   Modelled marginal responses of annual grass cover to spatial or temporal predictors

Estimates are the median of the posterior probability distribution, "l-95% CI" stands for the lower 95% credible interval and the "U-95% CI" standards for the upper 95% credible interval. "pd" is the probability of direction (the Bayesian equivalent of a frequentist p-value, where 0.975 is equivalent to 0.05 p-value). "Estimate of change in cover" is the amount of change in cover of the functional group predicted between the maximum and minimum covariate value. Positive values mean an increase in cover and negative values mean a decrease in. Significant pd-values (≥0.975) are italicized.

Covariate	Minimum Covariate value	Maximum Covariate estimate	Estimate of Change in Cover	l-95% CI	u-95% CI	pd
Model 0: Null model						
Prior year's annual grass cover (%)	0	98	70.11	68.06	72.07	1.00
% Clay	7.5	37.5	71.48	68.73	73.89	0.86
% Sand	11.4	67.3	72.7	70	75.2	0.99
Elevation (m)	862.7	1065.6	72.1	69.6	74.4	0.98
Model 1: Time Since Fire						
Prior year's annual grass cover (%)	0	98	71.98	69.98	73.85	1.00
% Clay	7.5	37.5	2.68	2.1	3.33	0.94
% Sand	11.4	67.3	3.27	2.39	4.21	0.99
Elevation (m)	862.68	1065.58	2.55	2.25	2.89	0.95
Time since fire (years)	1	100	1.5	1.54	1.45	1.00
Model 2: Post-fire weather effects						
Prior year's annual grass cover (%)	0	98	73.04	70.44	75.4	1.00

% Clay	7.5	37.5	4.55	3.66	5.52	0.85
% Sand	11.4	67.3	6	4.8	7.33	1.00
Elevation (m)	862.68	1065.58	3.73	3.21	4.31	0.55
Time since fire (years)	1	100	4.33	4.03	4.62	0.99
March-May ppt (year after fire)	31.2	145.7	3.66	3.39	3.94	1.00
Sep-Nov ppt (year of fire)	20.9	152.7	4.54	3.82	5.34	0.91

Model 3: Recent five-year weather						
Prior year's annual grass cover (%)	0	0.98	78.34	76.21	80.26	1.00
% Clay	7.5	37.5	8.64	7.41	9.97	0.94
% Sand	11.4	67.3	12.07	10.24	14.18	0.99
Elevation (m)	862.68	1065.58	3.34	2.8	3.85	0.95
Weighted Mean Temp	9.71	11.78	2.54	1.47	4.02	1.00
Weighted Mean Precip	13.79	32.35	9.01	8.2	9.9	1.00

Model 4: Time since fire + recent five-year weather						
Covariate	Minimum Covariate value	Maximum Covariate estimate	Estimate of Change in Cover	l-95% CI	u-95% CI	pd
Prior year's annual grass cover (%)	0	98	78.45	76.25	80.36	1.00
% Clay	7.5	37.5	8.95	7.67	10.27	0.51
% Sand	11.4	7.3	12.26	10.47	14.3	1.00
Elevation (m)	862.68	1065.58	3.15	2.69	3.69	1.00
Time since fire (years)	1	100	10.15	9.26	11.05	1.00

Weighted mean temp	9.71	11.78	2.63	1.5	3.97	1.00
Weighted mean precip	13.79	32.35	8.92	8.1	9.73	1.00

Table 1.2   Modelled marginal responses of perennial grass cover to spatial or temporal predictors across the range of each predictor.

Estimates are the median of the posterior probability distribution, "l-95% CI" stands for the lower 95% credible interval and the "U-95% CI" standards for the upper 95% credible interval. "pd" is the probability of direction (the Bayesian equivalent of a frequentist p-value, where 0.975 is equivalent to 0.05 p-value). "Estimate of change in cover" is the amount of change in cover of the functional group predicted between the maximum and minimum covariate value. Positive values mean an increase in cover and negative values mean a decrease in. Significant pd-values (≥0.975) are italicized.

Covariate	Minimum Covariate value	Maximum Covariate estimate	Estimate of Change in Cover	l-95% CI	u-95% CI	pd
Model 0: Null model						
Prior year's perennial grass cover (%)	0	83	64.44	62.14	66.59	*1.00*
% Clay	7.5	37.5	-1.7	-2.08	-1.29	*0.99*
% Sand	11.4	67.3	1.3	0.33	2.38	0.96
Elevation (m)	862.68	1065.58	14.22	13.11	15.38	*1.00*
Model 1: Time Since Fire						
Prior year's perennial grass cover (%)	0	83	64.16	61.85	66.31	*1.00*
% Clay	7.5	37.5	-1.89	-2.19	-1.59	*0.99*
% Sand	11.4	67.3	1.08	0.25	2.01	0.96
Elevation (m)	862.68	1065.58	14.15	13.06	15.27	*1.00*
Time since fire (years)	1	100	-0.19	-0.07	-0.31	0.73
Model 2: Post-fire weather effects						
Prior year's perennial grass cover (%)	0	83	58.38	55.55	61.12	*1.00*
% Clay	7.5	37.5	-1.68	-2.09	-1.24	*0.98*
% Sand	11.4	67.3	1.8	0.81	2.89	*0.99*
Elevation (m)	862.68	1065.58	6.25	5.42	7.19	*1.00*

Time since fire (years)	1	100	-1.63	-1.5	-1.76	*1.00*
Average annual precip (4 years post-fire)	160.1	415.7	14.38	13.09	15.74	*1.00*
Sep-Nov ppt (year of fire)	20.9	152.7	2.63	2.02	3.31	*1.00*

Model 3: Recent five-year weather

Prior year's perennial grass cover (%)	0	83	63.96	61.57	66.19	*1.00*
% Clay	7.5	37.5	-2.12	-2.47	-1.73	*0.99*
% Sand	11.4	67.3	0.83	-0.14	1.81	0.96
Elevation (m)	862.68	1065.58	12.84	11.71	14.16	*1.00*
Weighted Mean Temp	9.61	11.76	7.99	7.22	8.73	*1.00*
Weighted Mean Precip	13.53	31.57	10.68	9.82	11.54	*1.00*

Model 4: Time since fire + recent five-year weather

Covariate	Minimum Covariate value	Maximum Covariate estimate	Estimate of Change in Cover	l-95% CI	u-95% CI	pd
Prior year's perennial grass cover (%)	0	83	63.84	61.53	66.11	*1.00*
% Clay	7.5	37.5	-2.16	-2.54	-1.77	*1.00*
% Sand	11.4	67.3	0.78	-0.17	1.77	0.86
Elevation (m)	862.68	1065.58	13.02	11.77	14.28	*1.00*
Time since fire (years)	1	100	-0.35	-0.2	-0.47	0.87
Weighted mean temp	9.61	11.76	7.99	7.24	8.85	*1.00*
Weighted mean precip	13.53	31.57	10.84	9.98	11.75	*1.00*

Table 1.3 Modelled marginal responses of sagebrush abundance to spatial or temporal predictors across the range of each predictor.

Estimates are the median of the posterior probability distribution, "l-95% CI" stands for the lower 95% credible interval and the "U-95% CI" standards for the upper 95% credible interval. "pd" is the probability of direction (the Bayesian equivalent of a frequentist p-value, where 0.975 is equivalent to 0.05 p-value). The change in the probability of occurrence of each density category predicted between the maximum and minimum covariate values is given. Positive values mean an increase in density and negative values mean a decrease in density. Significant pd-values (≥0.975) are italicized.

	Minimum Covariate value	Maximum Covariate value	Cat 1 (0 plants /m^2)	Cat 2 (<0.5 plants /m^2)	Cat 3 (>0.5-1 plants /m^2)	Cat 4 (1-5 plants /m^2)	Cat 5 (>5 plants /m^2)	pd
Model 0: Null model								
Prior year's Sagebrush Category	1	5	93%	-7%	0%	66%	34%	*1.00*
% Clay	7.5	37.5	-9%	8%	1%	0%	0%	0.94
% Sand	11.4	67.3	1%	-1%	0%	0%	0%	0.59
Elevation	862.68	1065.58	-17%	15%	2%	0%	0%	*1.00*
Model 1: Time Since Fire								
Prior year's Sagebrush Category	1	5	93%	-7%	0%	69%	31%	*1.00*
% Clay	7.5	37.5	-12%	11%	1%	0%	0%	*0.99*
% Sand	11.4	67.3	-2%	2%	0%	0%	0%	0.68
Elevation (m)	862.68	1065.58	-16%	14%	2%	0%	0%	*1.00*
Time since fire (years)	1	100	-13%	12%	1%	0%	0%	*1.00*
Model 2: Post-fire weather effects								
Prior year's Sagebrush Category	1	5	-94%	-6%	0%	75%	25%	*1.00*

	Minimum Covariate value	Maximum Covariate value	Cat 1 (0 plants /m²)	Cat 2 (<0.5 plants /m²)	Cat 3 (>0.5-1 plants /m²)	Cat 4 (1-5 plants /m²)	Cat 5 (>5 plants /m²)	pd
% Clay	7.5	37.5	-11%	10%	1%	0%	0%	0.95
% Sand	11.4	67.3	-6%	5%	0%	0%	0%	0.84
Elevation (m)	862.68	1065.58	-20%	19%	1%	0%	0%	*0.99*
Time since fire (years)	1	100	-23%	21%	1%	0%	0%	*1.00*
Max Jan-Jun ppt (4 years post-fire)	77.2	325.3	-30%	28%	1%	0%	0%	*0.99*

	Minimum Covariate value	Maximum Covariate value	Cat 1 (0 plants /m²)	Cat 2 (<0.5 plants /m²)	Cat 3 (>0.5-1 plants /m²)	Cat 4 (1-5 plants /m²)	Cat 5 (>5 plants /m²)	pd
Mean temp coldest month (4 years post-fire)	-5.4	1	34%	-32%	-2%	0%	0%	*1.00*
Mean temp hottest month (4 years post-fire)	21.8	27.01	-34%	31%	2%	0%	0%	*0.99*
Mean Jan-April precip (4 years post-fire)	58.95	180.1	16%	-15%	-1%	0%	0%	0.92
Mean March-June temp (4 years post-fire)	10.46	14.12	-2%	2%	0%	0%	0%	0.59

Model 3: Recent five-year weather

	Minimum	Maximum	Cat 1	Cat 2	Cat 3	Cat 4	Cat 5	pd
Prior year's Sagebrush Category	1	5	-93%	-7%	0%	68%	32%	*1.00*
% Clay	7.5	37.5	-6%	5%	1%	0%	0%	*1.00*
% Sand	11.4	67.3	-1%	1%	0%	0%	0%	0.56
Elevation (m)	862.68	1065.58	-7%	6%	1%	0%	0%	0.88

Weighted mean temp	9.25	11.29	11%	-10%	-1%	0%	0%	0.96
Weighted mean precip	13.43	32.14	-17%	15%	2%	0%	0%	*1.00*

Model 4: Time since fire + recent five-year weather

Prior year's sagebrush category	1	5	-93%	-7%	0%	72%	28%	*1.00*
% Clay	7.5	37.5	-9%	8%	1%	0%	0%	0.96
% Sand	11.4	67.3	-4%	4%	0%	0%	0%	0.81
Elevation	862.68	1065.58	-5%	5%	0%	0%	0%	0.82
Time since fire (years)	1	100	-14%	13%	1%	0%	0%	*1.00*
Weighted mean temp	9.25	11.29	9%	-8%	-1%	0%	0%	0.93
Weighted mean precip	13.43	32.14	-20%	18%	2%	0%	0%	*1.00*

Table 1.4   Model fit metrics.

Error for grass cover values and accuracy of sagebrush density class (from by leave-one-out cross validation on the OCTC data set) for each generalized additive model. For annual and perennial grass cover, root mean squared error (RMSE) and normalized root mean squared error (NMSE), calculated by dividing the RMSE by the range of the observed response variable, as given. For sagebrush density class, overall accuracy, kappa and p-values are given.

	Sagebrush Density Class			Perennial Grass Cover			Annual Grass Cover		
	Overall Accuracy	Kappa	P-value	RMSE	NRMSE	Bias	RMSE	NRMSE	Bias
Model 0: Null model	90%	0.83	<0.0001	0.12	14%	0.004	0.14	15%	0.001
Model 1: Time Since Fire	90%	0.83	<0.0001	0.12	14%	0.004	0.14	15%	0.001
Model 2: Post-fire weather events	91%	0.84	<0.0001	0.12	14%	0.003	0.14	14%	0
Model 3: Recent five-year weather	90%	0.83	<0.0001	0.12	13%	0.004	0.14	14%	0.001
Model 4: Time since fire + recent five-year weather	90%	0.83	<0.0001	0.12	13%	0.004	0.14	14%	0.001

34
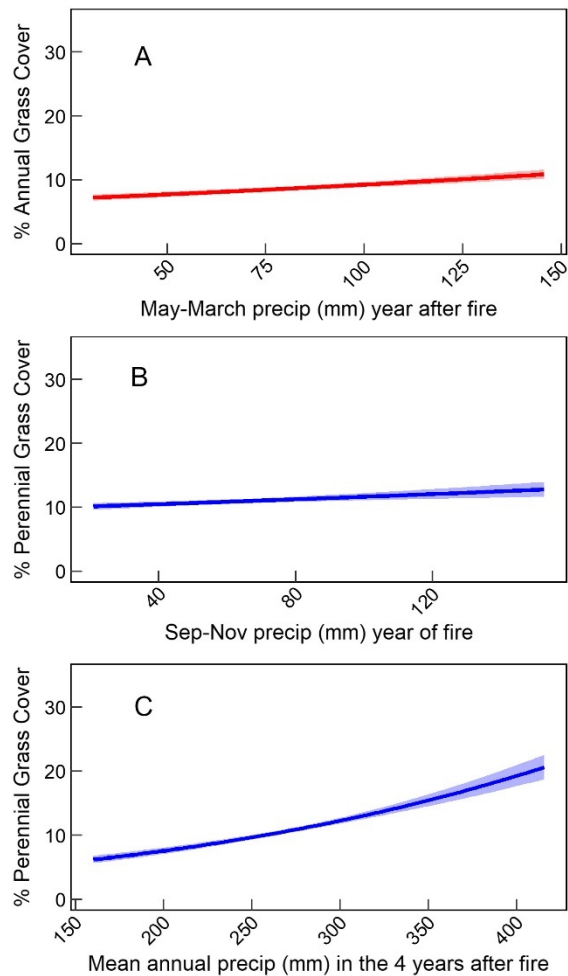
Figure 1.3   Marginal effects from Model 2 of three post-fire weather covariates on annual grass cover and perennial grass cover.

Precipitation ("precip") is given in millimeters (mm). The center line shows the median of the posterior probability distribution, the shaded ribbons show the 95% credible interval.
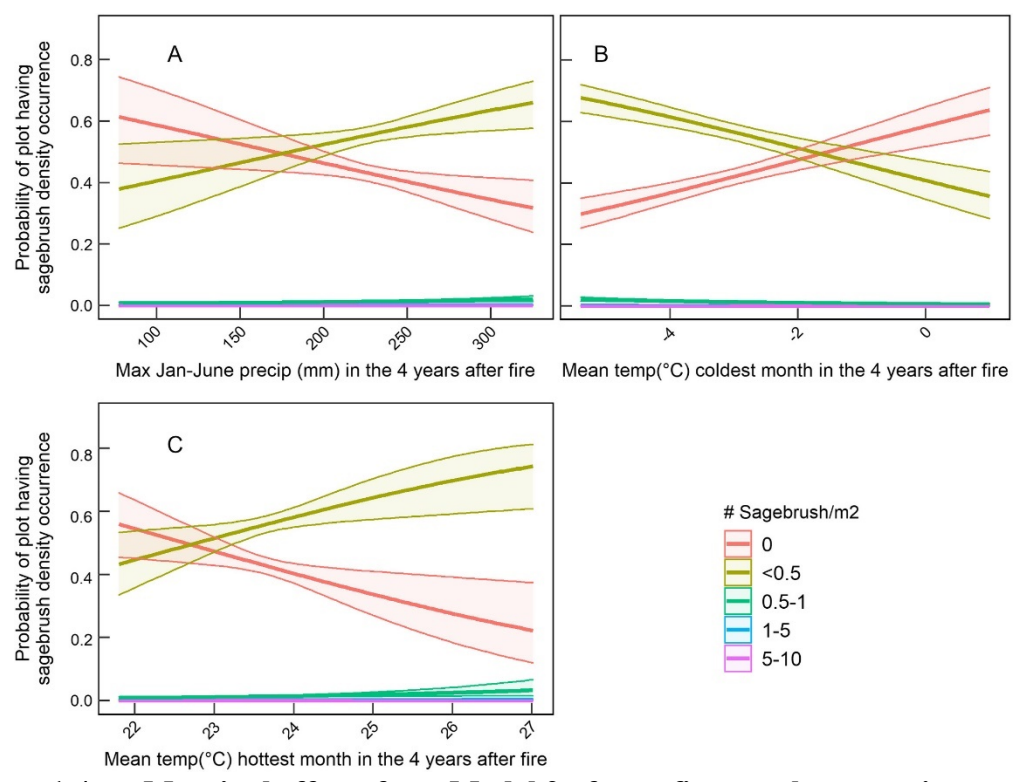
Figure 1.4   Marginal effects from Model 2 of post-fire weather covariates on the probability of a plot having sagebrush density in a certain category.

Sagebrush density category is given as number of sagebrush per m^2. "Precip" stands for precipitation and is measured in millimeters (mm). "Temp" stands temperature and is measured in degrees celcius (^{o}C).

Model 3: Recent five-year weather using random forests to weigh the importance
of different months

All three functional groups showed increases in cover or density with increased
precipitation weighted by month over the five years preceding each observation (Figure
1.5A,1.5B,1.5C, Tables 1-3). Both annual and perennial grass cover increased by 2.5%
and 8% respectively as prior 5-year mean temperature weighted by increased by from
~9.6°C to 11.8°C (pd = 1 for both, Tables 1.1 and 1.2). Sagebrush density was not
significantly affected by mean temperature weighed by month (pd = 0.96, Table 1.3).

Model 4: Time since fire and recent five-year weather using random forests to
weigh the importance of different months

Adding a term to model 3 to incorporate time since fire did not result in any
appreciable changes to the effect sizes of weighted averages of precipitation and
temperature on functional group density or cover.

Do post-fire weather conditions or recent five-year weather better explain functional
group abundances? Model fit

The models which included weather had very similar accuracy to the null no-
weather model, which underscores the importance of considering and comparing
hypothesis-driven models with null effect models when trying to predict future vegetation
composition dynamics (Harvey et al. 1983). With a one exception, functional group
abundances overall were no better explained by post-fire weather conditions during
specific intervals than they were by recent five-year antecedent weather (Tables 1.4 and
1.5). Model 2 (post-fire weather events) was 1% more accurate at predicting sagebrush
density class than the other models. The models that included weather at all (either post-

fire or recent 5-year weather) were better at predicting perennial grass cover by 1% (as measured by a decrease in NRMSE) over the models which did not include weather (models 0 and 1) and the five-year recent weather (3-4) were 1% better at predicting annual grass compared to the others (Table 1.4).

<u>Does consideration of post-fire weather or recent weather help predict post-fire outcomes at a new site? Model transferability.</u>

No model emerged as most transferable over all of the three plant functional groups, indicating no consistent landscape, disturbance, or weather drivers in post-fire abundances across all functional groups. Instead, transferability varied among the plant types. The models that included weather (2-4) were better at predicting perennial grass (by 7-10% decrease in NRMSE) and annual grass (by 1-4% decrease in NRMSE) cover on the Soda wildfire than the models which did not include weather (models 0 and 1) (Table 1.5). The differences in model transferability between the two different weather parameterizations (model 2: post-fire weather events and model 3: five-year weather) when predicting perennial or annual grass cover were minimal: 1% error for perennial grass, 2% error for annual grass (Table 1.5). No model was more transferable than any other for predicting sagebrush density.
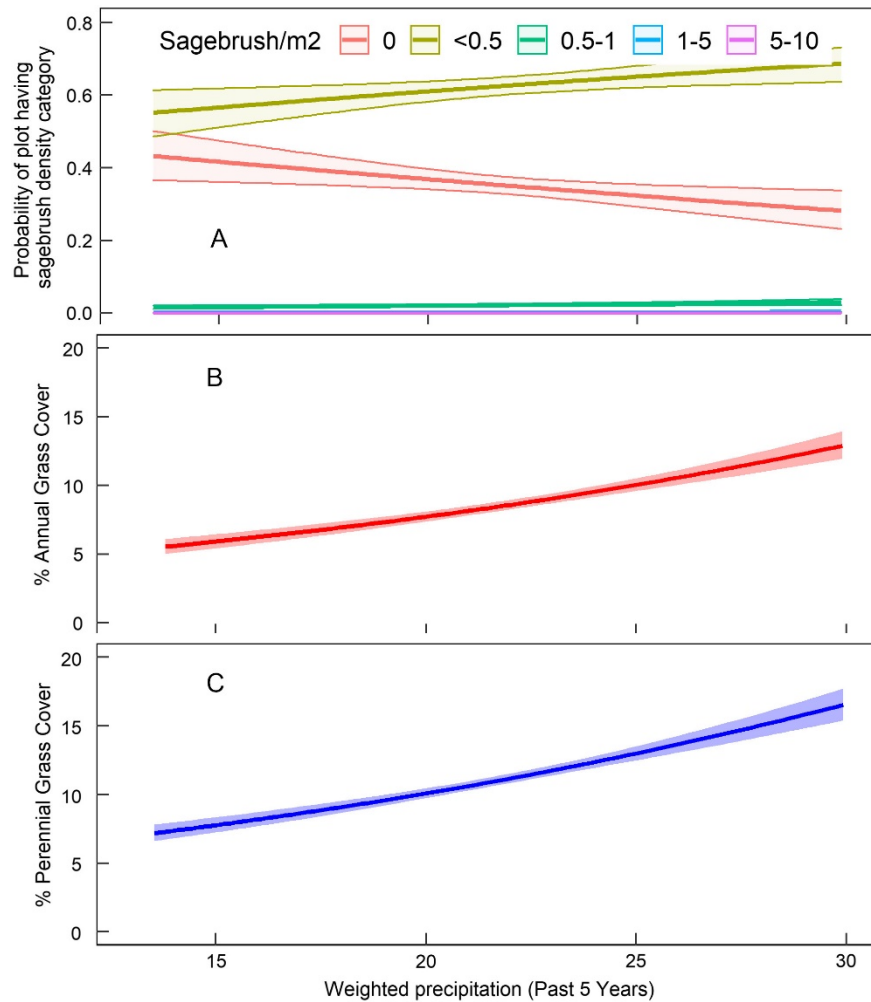
Figure 1.5   Marginal effects of average monthly precipitation in the most recent five years weighted by random-forest derived importances (from Model 3).

Effects are shown on sagebrush density category (top), annual grass cover ("% AG Cover" - middle), and perennial grass cover ("% PG Cover" - bottom). Precipitation is given in millimeters (mm). The center line shows the median of the posterior probability distribution, the shaded ribbons show the 95% credible intervals.

Table 1.5 **Transferability error for grass cover values and accuracy of sagebrush density class (from validation error on the Soda Wildfire data set) for each generalized linear model.**

For annual and perennial grass cover, root mean squared error (RMSE) and normalized root mean squared error (NMSE), calculated by dividing the RMSE by the range of the observed response variable, as given. For sagebrush density class, overall accuracy, kappa and p-values are given.

	Sagebrush Density Class			Perennial Grass Cover			Annual Grass Cover		
	Overall Accuracy	Kappa	P-value	RMSE	NRMSE	Bias	RMSE	NRMSE	Bias
Model 0: Null model	89%	0.71	<0.0001	0.42	55%	-0.27	0.36	36%	-0.02
Model 1: Time Since Fire	89%	0.71	<0.0001	0.42	55%	-0.27	0.35	35%	-0.01
Model 2: Post-fire weather events	89%	0.71	<0.0001	0.35	45%	-0.20	0.34	34%	-0.02
Model 3: Recent five-year weather	89%	0.71	<0.0001	0.35	46%	-0.21	0.32	32%	0.07
Model 4: Time since fire + recent five-year weather	89%	0.71	<0.0001	0.36	47%	-0.21	0.32	32%	0.07

Discussion

We sought to assess how time-since-fire and antecedent weather affected long-term functional group abundances, and how sensitive within-site and across-site predictions of abundance were to weather during specific post-fire windows or in general antecedent five-year period. We found mostly positive relationships between post-fire precipitation and abundance of all functional groups, and mixed effects of temperature. Post-fire weather in specific time periods critical for recruitment did not explain long-term vegetation trajectories better than did recent five-year weather conditions, although incorporating weather during either time period improved perennial and annual grass cover predictions at a new site.

<u>Vegetation responses</u>

Post-fire precipitation is a key factor directing plant community development following fire disturbances (Shryock et al. 2015, Young et al. 2019, McIlroy and Shinneman 2020). Indeed, we found that post-fire precipitation had significant positive effects on abundances of all three functional groups. As expected, sagebrush density increased with maximum Jan-June precipitation in the first four years after fire (post-fire weather model, Model 2) and with precipitation in the preceding 5 years (recent five-year weather models), which may be indicative of drought thresholds on seedling establishment, such as the threshold of -2.5 MPa in mean soil-water availability in the March after fire found by O'Conner et al. (2020). A previous study found a relationship between fall precipitation and cheatgrass (the most common annual grass species in the Western US) outside of a specific post-fire context (Bradley et al. 2016). We found that annual grass cover increased with precipitation in the spring of the year after fire but not

with fall precipitation in the year of fire (post-fire weather model). This may reflect the fact that fire usually reduces the annual grass seedbank (Pyke 1994), and thus propagule arrival to a burned site could be delayed. There was a positive effect of post-fire fall precipitation on perennial grass cover, which indicates a different life cycle strategy between annual and perennial species. Perennial grasses can frequently resprout after fire (Wright 1985) and can immediately take advantage of available soil moisture. Indeed, perennial grass cover increased with precipitation during all of the time periods analyzed. This finding is consistent with previous research that has indicated that precipitation is strongly related to germination and cover of perennial grasses (Pilliod et al. 2017, James et al. 2019). Furthermore, Adler et al. (2009) found that survival of several common perennial bunchgrass species was 90% or higher after 3-4 years, so both seedlings and resprouts that emerge during critical post-fire time periods are likely to subsist long after fire.

Freezing temperatures during critical growing periods can reduce sagebrush seedling establishment and survival (Brabec et al. 2017). However contrary to Brabec et al. (2017), we observed an increase in sagebrush density in relation with lower mean temperature of the coldest month and higher mean temperatures in the hottest month in the first four years after fire. The OCTC has a relatively warm climate for sagebrush and low winter temperatures may be less of a selective factor here than in colder climates (Lazarus et al. 2019). The lack of an effect of mean monthly temperature (from the five-year weather model) on sagebrush density is consistent with the findings of Brabec et al. (2017) and Kleinhesselink and Adler (2018), who suggest that temperature extremes are more often the limiting factor for establishment. However, weather effects on sagebrush

seedling establishment and early survival may not translate into long-term effects on population dynamics because of size-structure effects (Shriver et al. 2019) and negative density dependence (Chu and Adler 2015) and because susceptibly to minimum temperature appears to decrease as plants age (Germino et al. 2019).

We modeled year-to-year change in grass cover or sagebrush density class, and incremental change each year was generally small. In particular, shifts from one sagebrush density class to another may occur more slowly than the temporal resolution and focus of our models, ultimately diminishing change detection. This finding is in agreement with Anderson and Holte (1981), who reported negligible change in shrub density in relatively undisturbed sagebrush steppe over a 9-year period of time, even as precipitation varied year-to-year. Sagebrush cover in that study did increase with precipitation, suggesting that established plants may display greater response to weather variability (i.e. growth or shedding of biomass) without concomitant changes in recruitment or mortality.

Explanatory factors for post-fire vegetation recovery: how does weather fit in?

Our coarse-scale consideration of weather provided only marginal gains in explaining long-term vegetation trajectories, nor did it reveal that weather during specific post-fire recruitment periods had a lasting impact relative to the effects of antecedent weather at any time before or after fire. Variation in vegetation over time can frequently be partly accounted for by temporal autocorrelation. For instance, in remote sensing vegetation cover trend analysis, normalized difference vegetation index (NDVI) in prior months or years can be used to better predict future NDVI (i.e. Fernández-Manso et al. 2011, Adeyeri et al. 2017). The fact that our null model that only incorporated landscape

variables performed nearly as well as our models that included weather suggests that a significant amount of variation in future vegetative trajectories can be explained by knowing past abundances.

<u>Generalizing weather effects on post-fire vegetation recovery across sites</u>

There has been a recent call in ecology to develop and apply iterative forecasting approaches in predicting ecosystem responses to disturbance and changing climate, especially near-term forecasting (Dietze et al. 2018). Our findings suggest that although including weather covariates may improve transferability of predictions of post-fire vegetation recovery for some functional groups, predictions may not be sensitive to the choice of weather variables when the weather data is spatially and temporarily coarse. We used PRISM data for this study, which is the most readily available and frequently used weather data set but also has a coarse spatial scale of 250 m pixel sizes and is available only in monthly increments (PRISM 2017). Previous studies have shown that microsite vegetative structure and topographic position can change the suitability for perennial seedling establishment in semi-arid ecosystems (Franzese et al. 2009, Boyd and Davies 2010), which means that local conditions may moderate larger scale weather effects. Furthermore, soil moisture thresholds for plant establishment or survival can occur on the scale of days, rather than months, as shown for sagebrush (O'Connor et al. 2020). The choice of weather variable parametrization may increase in importance as data becomes more fine-scale, both temporally and spatially.

The approach we used illustrates how ecological forecasting can be applied to restoration ecology, including leveraging data from highly studied sites to inform predictions at sites with limited data. These sorts of studies can help fill in the gap for

management-applicable predictions on a useful temporal and spatial scale; many ecological forecasts currently rely on long-term simulations at regional scales (Pouyat et al. 2010, Dietze et al. 2018), despite a land manager need for near-term predictions at a local scale (Dilling and Lemos 2011). Our analysis found that weather effects (either post-fire or recent antecedent) were more important for predicting post-fire perennial and annual grass cover at a new site than they were for explaining variability at a single site. Our analysis did not directly address weather effects on specific post-fire demographic stages. Future analyses could consider other population dynamics which may affect longer term outcomes, such as size structure or negative density dependence (Chu and Adler 2015, Shriver et al. 2019). Furthermore, we only present two ways of considering the temporal dynamics of weather variability (ie post-fire weather during the growing season or recent antecedent five-year weather) here but acknowledge that other temporal windows or weather variables (such as soil-water deficit, temperature extremes) could be considered.

Conclusions

While we consistently found some effects of precipitation on vegetation recovery, the temporal dynamics of weather variation in relation to time since fire were not important for predicting annual or perennial grass cover or sagebrush density at a new site, at least for the models we tested that relied on coarse-scale weather data. Coarse-scale seasonal weather forecasts may provide some utility for predicting whether precipitation will be sufficient for successful vegetation recovery after fire. However, developing models with finer-scale weather data (ie daily, such as in O'Connor et al. 2020) will be an important next step for leveraging our methods to forecast vegetation

dynamics. Land managers often have to make decisions on post-fire management treatments without site-specific knowledge of the subject plant communities, and model predictions is one of the only ways the information can be obtained. We have shown a method of transferring information at one area affected by historic fires to predict outcomes at another burned area, and our basic approach could be adopted for similar applications made elsewhere. The information gained could be useful for helping to predict both post-fire restoration outcomes, or other applications such as fire vulnerability based on fuel predictions. Long-term monitoring in particular can provide important information about weather variability for transferring quantitative forecasts from well-studied sites to new sites.

Acknowledgements

CHAPTER TWO: POST-FIRE SEED DISPERSAL OF A WIND-DISPERSED SHRUB

DECLINED WITH DISTANCE TO SEED SOURCE, YET HAD HIGH LEVELS OF

UNEXPLAINED VARIATION

Abstract

Plant-population recovery across large disturbance areas is often seed-limited. An understanding of seed-dispersal patterns is fundamental for determining natural-regeneration potential. However, forecasting seed dispersal rates across heterogeneous landscapes remains a challenge. Our objectives were to determine (1) the landscape patterning of post-disturbance seed dispersal, and underlying sources of variation and the scale at which they operate, and (2) how the natural seed dispersal patterns relate to a seed augmentation strategy. Vertical seed-trapping experiments were replicated across two years and five burned and/or managed landscapes in sagebrush steppe. Multi-scale sampling and hierarchical Bayesian models were used to determine the scale of spatial variation in seed dispersal. We then integrated an empirical and mechanistic dispersal kernel for wind-dispersed species to project rates of seed dispersal and compared natural seed arrival to typical post-fire aerial seeding rates. Seeds were captured across the range of tested dispersal distances, up to a maximum distance of 26 m from seed-source plants, although dispersal to the furthest traps was variable. Seed dispersal was better explained by transect heterogeneity than by patch or site heterogeneity (transects were nested within

patch within site). The number of seeds captured varied from a modelled mean of ~13 m^{-2} adjacent to patches of seed-producing plants, to nearly none at 10 m from patches, standardized over a 49-day period. Maximum seed-dispersal distances on average were estimated to be 16-m according to a novel modelling approach using a "latent" dispersal distance based on seed trapping heights. Surprisingly, statistical representation of wind did not improve model fit and seed rain was not related to the large variation in total available seed of adjacent patches. The models predicted severe seed limitations were likely on typical burned areas, especially compared to the mean 95 to 250 seeds m^{-2} that previous literature suggested were required to generate sagebrush recovery. More broadly, our Bayesian data fusion approach could be applied to other cases that require quantitative estimates of long-distance seed dispersal across heterogeneous landscapes.

Introduction

Seed dispersal sets the spatial template for patterns of plant population recovery across disturbed landscapes (Leland Russell and Roy 2008; Caughlin et al. 2016; Snell et al. 2019; Gill et al. 2020). Seedling recruitment after disturbance is often related to proximity to seed sources (Webber et al. 2010; Leirfallom et al. 2015). Seed source patches in disturbed areas drive recolonization, including expansion of remnant islands as new recruits establish around existing reproductive plants (Corbin and Holl 2012). To predict how and where plant populations will reestablish after disturbance, we need to understand the sources of heterogeneity in seed dispersal events (Ozinga et al. 2005; Clark et al. 1999; Caughlin et al. 2014; San-José et al. 2019).

Small-scale spatial heterogeneity in post-disturbance seed dispersal can be a major determinant of plant population recovery (DiVittorio et al. 2007). Understanding

this heterogeneity through spatially explicit seed-dispersal predictions can inform spatial prioritization of limited restoration resources and thus cost-effectiveness of restoration (Neeson et al. 2015; Jones et al. 2018; Strassburg et al. 2020). Many past seed trapping experiments needed to make these sorts of dispersal predictions have focused on intensive trapping at short distances from seed sources (Greene and Calogeropoulos 2002). Longer distance travel of seeds across landscapes is rare and difficult to detect via experimental methods, however, is hypothesized to have an oversized impact on plant colonization (Clark et al. 1998, Cain et al. 2002). For instance, a prior study on dispersal of an invasive plant using seed traps found that mean dispersal distance was only 0.26 m, an insufficient distance to explain the continental-scale of ongoing range expansion; models demonstrated that only one-in-a-million seeds moving kilometers further than the mean was sufficient to replicate the observed distribution of the plant (Neubert and Caswell 2000). These infrequent, but critically important, long-distance dispersal events challenge field-based methods for quantifying dispersal distance.

Previous researchers have modeled how seed density decreases with distance from remnant seed sources in many disturbed landscapes, including heath lands, tropical forests, and subalpine forests (Hammill et al. 1998; Holl 1999; Gill et al. 2020). These models can help answer questions about whether or not seeds will arrive at certain landscape locations and where to prioritize direct seeding for restoration (Peeler and Smithwick 2020). However, variability in seed dispersal during succession contributes to model uncertainty (e.g. Shive et al. 2018) and disentangling the sources of variability will be necessary to operationalize models for restoration decision support.

Direct seeding ("active restoration") of desired species is common practice on disturbed landscapes to increase the pace of natural regeneration and ensure that propagules of desired species arrive before or at least concurrently with invasive species (Palma and Laurance 2015). However, when disturbed landscapes are not seed limited, supplemental seedings can be ineffective at increasing the rate of vegetative recovery or even suppress natural regeneration (Schoennagel and Waller 1999; James and Svejcar 2010; Peppin et al. 2010).

Wind is a common agent of seed dispersal across many different ecosystems and taxa (Nathan et al. 2011; Sullivan et al. 2018). Wind strength and direction varies seasonally and the timing of major wind events in relationship to the timing of seed ripening can have significant effects on dispersal distances (Heydel et al. 2015). Furthermore, seed functional traits, landscape characteristics, and weather can all affect wind-driven dispersal of seed across landscapes. Seeds with specific wind dispersal mechanisms, such as a pappus or wings, have a higher propensity towards long-distance or widespread seed dispersal (Ozinga et al. 2005; Dauer et al. 2007; Tamme et al. 2014). Small seed mass can also contribute to longer wind dispersal distances (Hoppes 1988; Tamme et al. 2014). Additionally, wind energy for seed dispersal can be both constrained and/or modified by landscape characteristics including canopy density and structure (Nathan et al. 2009), which can be particularly heterogeneous in disturbed areas.

Sagebrush-steppe provides an excellent system for studying how wind-driven seed dispersal from remnant patches varies across scales because these ecosystems are experiencing unprecedented habitat disruption from megafires (Miller et al. 2011) and tens of millions of dollars are spent each year on burned area rehabilitation, particularly

purchasing of sagebrush seed (as a representative example, the US Bureau of Land Management allocated $20 million USD to burned area rehabilitation in Fiscal Year 2018). Sagebrush is considered a keystone species in these ecosystems, as the shrub supports subsequent recovery of many wildlife and plant species (Beck et al. 2012). Investment in aerial seeding of sagebrush assumes that sagebrush regeneration is primarily limited by seed availability owing to short longevity of the sagebrush seed bank (Wijayratne and Pyke 2012). The capacity for unburned remnants or edges to provide seed is relatively unknown and implicitly assumed to be negligible. While several studies have examined post-fire regeneration of big sagebrush, these studies have not specifically addressed the impact of unburned remnant patches (or newly created patches) within a larger burn context (DiCristina and Germino 2006; Lesica et al. 2007; Ziegenhagen and Miller 2009; Nelson et al. 2014). Young and Evans (1989) and Welch and Nelson (1995) asserted that seed dispersal distances of sagebrush stands are < 1-2 m from the maternal plant (Young and Evans 1989; Welch and Nelson 1995). Despite this, seedling recruitment can occur several hundred meters from remnant adults into burned areas and on unseeded landscapes (Mueggler 1956; Nelson et al. 2014).

Our questions in this study were:

1) How far do sagebrush seeds disperse and how variable is sagebrush seed dispersal?

2) Which landscape scales best explain variation in seed dispersal (trap, transect, patch, site)? Do wind direction metrics help explain variation in seed dispersal?

3) How does seed dispersal from seed source patches compare with aerial seeding rates?

Methods

We conducted a seed trapping study around sagebrush patches during the winters of 2018/2019 and 2019/2020. Our vertical wind traps were designed to catch seeds at any height in the wind from the ground to approximately the height of release (i.e., the height of flowers on seed-source plants). Big sagebrush flowers in the fall (typically November, depending on the elevation and weather) and seeds mature and release in early to mid-winter. Seeds weigh 0.25 mg or less and are approximately 1.5 mm in diameter (Jacobs et al. 2011). Seed traps were arrayed on two transects per patch of sagebrush plants that were adjacent to (or surrounded by) areas with no sagebrush and instead were dominated by grasses. Multiple patches (and thus, transects) were evaluated in each of six sites. Three of the sites were sampled in the first year of the study and the three other sites were sampled in the second year. We evaluated seed dispersal under and away from sagebrush patches.

We used vertical seed traps as opposed to ground traps for several reasons. First, sagebrush seed dispersal occurs during the winter when snow cover may be present. Our small ground traps directly beneath the canopy were fairly sheltered from snow but any ground traps set outside of the canopy would have accumulated snow and been non-functional. Secondly, we anticipated that seed density would be very low and that we would therefore need a large trap area to capture seeds. Creating greater surface area for vertical traps was more feasible than for ground traps. We account for our trap design using a novel modeling approach with a latent ground distance term (see below).

<u>Sites</u>

Study sites for the first year of trapping were the Soda Wildfire (113 kHa, burned 2015), Alkie Wildfire (814 ha burned 2018), and the Botanical Garden in Boise (at a planted sagebrush patch in a disturbed area otherwise dominated by grasses). Study sites for the second year of trapping were the Soda Wildfire, the Pony Wildfire (60 kHa, burned 2013), and Table Rock fire (1 kHa, burned 2016) (Fig. 2.1). The two trapping locations on the Soda Wildfire were at different locations on the fire (Year 1 location in the southeast, Year 2 location in the central west) and thus were considered separate sites. The seed trap size, dates of trapping, and site summary information, including sample sizes, are given in Table 2.1.

Patches (n = 22) were selected by reconnaissance at each site based on the following criteria: there had to be at least 5 individual reproductive plants in each patch, slopes in and around the patches had to be less than twenty degrees, and patches had to be isolated enough from other patches so that no other seed-bearing sagebrush plants in the surrounding area could be any closer to the traps than the individuals in the patch. In a few cases, all flower stalks were clipped from single individual sagebrush that were located outside of a patch to satisfy these criteria. Patches could either be unburned remnants or created from planting seedlings or aerial seeding.

Most sites were dominated by *Artemisia tridentata* ssp. *wyomingensis*, although the dominant subspecies at the Pony wildfire site was *A. tridentata* ssp. *xericensis.* The surrounding vegetation for the sites during the first year was exotic annual grasses at the Soda site, a mixture of perennial and annual grasses at the Botanical Garden, and the Alkie site was freshly burned and had no vegetative cover. The surrounding vegetation

for sites during the second year was mixed low sagebrush (*Artemisia arbuscula*) and low-statured grasses at the second Soda fire site, exotic annual grasses at Table Rock, and mixed low sagebrush and low-statured grasses at the Pony site.

<u>Seed traps</u>

During the first winter, traps (n = 79) were located under canopy, 2 m, 4 m, 7 m, 10 m, and 13 m from the patch. Since seeds were found at all distances in the first year, we increased the distance of the farthest traps in the second year. During the second winter, traps (n = 275) were located, under canopy, 2 m, 4 m, 6 m, 10 m, 14 m, 18 m, 22 m, and 26 m from the patch. Traps were arranged along two transects per patch (except for the one patch at the Botanical Gardens, for which there were four transects) with angles chosen based on the following criteria: first, all transects had to be isolated enough so that no reproductive individuals were any closer to the traps than the plants in the patch. Given this requirement, the first angle was aligned as close as possible against the prevailing wind direction at the site and the second angle was aligned as close as possible towards the prevailing wind direction at the site (these wind directions were taken from prior year weather station data – actual wind directions during trapping season were not always as expected). Trap distances were measured from the base of the individual reproductive individual sagebrush plant where each transect began (termed "base individual plant" below).

Table 2.1   Number and sizes of seed-collection traps, their spatial deployment and trapping dates by year.

Alkie was excluded due to seed crop failure and no seeds trapped. The total number of vertical patches and traps excludes those lost to animals or weather.

	Year 1	Year 2
Vertical trap size (cm)	50 x 91 rectangle	50 x 76 rectangle
Under-crown trap size (cm)	25.4-radius pan (with 2.5 center hole)	10 x 10 square
Trap distances (m)	2, 4, 7, 10, 13	2, 4, 6, 10, 14, 18, 22, 26
Sites	Soda, Botanical Garden, Alkie	Soda, Table Rock, Pony
Number of patches	4	15
Total number of vertical traps	36	237
Total number of under-crown traps	6	30
Dates of Collection		
Soda	24 November 2018 to 21 December 2018	Round 1: 22 November 2019 to 17 December 2019; Round 2: 17 December 2019 to 10 January 2020
Botanical Garden	4 December 2018 to 22 December 2018	-
Alkie	26 November 2018 to 3 January 2019	-

Table Rock	-	Round 1: 22 November 2019 to 14 December 2019; Round 2: 14 December 2019 to 6 January 2020
Pony	-	Round 1: 23 November 2019 to 18 December 2019; Round 2: 18 December 2019 to 7 January 2020
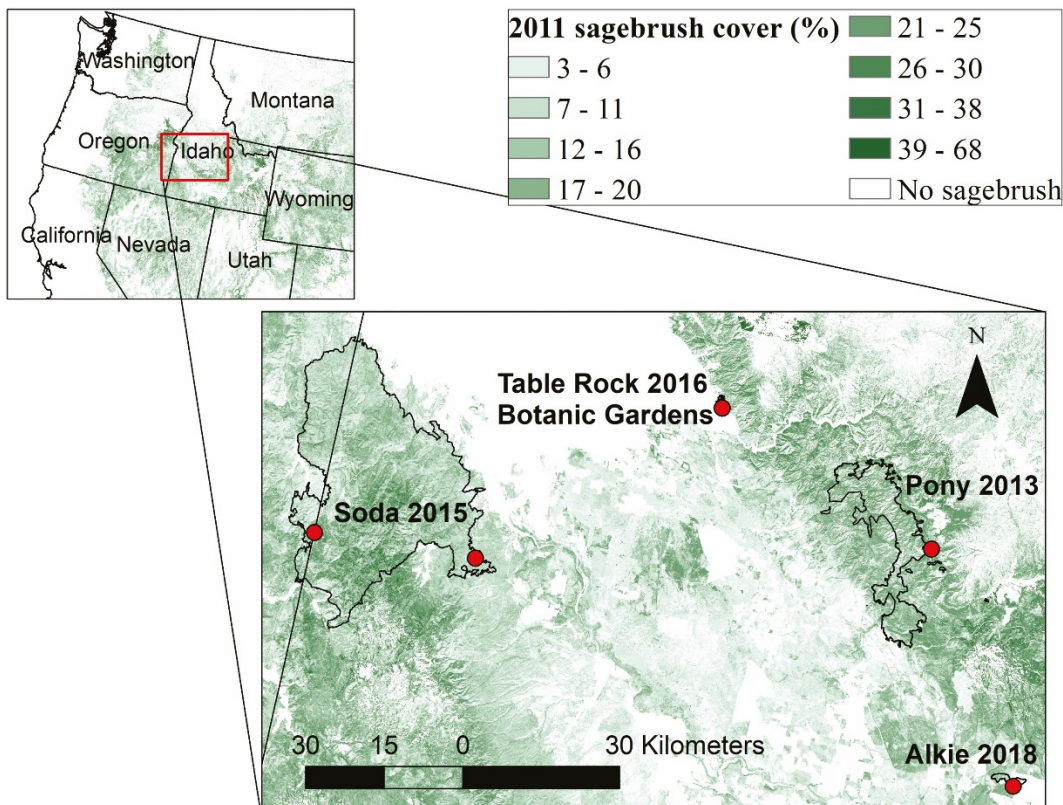
Figure 2.1   Locations of fires (black outlines) and trapping sites (red dots) for dispersal study.

Shown as an inset map on western United States and 2011 sagebrush cover (%) from the National Land Cover Database (NLCD) (Rigge et al. 2020).

Vertical traps were constructed from two 5x5 cm wooden stakes that were either 1.23 m tall (Year 1) or 0.91 m tall (Year 2). The stakes were set 50 cm apart with 0.55 oz white AgFabric (Wellco Industries, Corona, CA) stapled between the stakes (Appendix B, Fig. B.1). The AgFrabic was then sprayed with Tanglefoot (Scotts Miracle Gro, Grand Rapids, MI) to provide a persistently adhesive surface. Under-crown traps were circular cake bundt pans (25.4 cm radius with 2.5 cm center hole) filled with marbles to prevent seeds from blowing out (Year 1) or square 10x10 cm frames with sprayed AgFabric stapled on (Year 2) and were set directly under the crown of the base individual plant.

Some vertical traps failed because of weather or animal interference (including all traps at three of the six patches at Pony) and these were excluded from analysis, resulting in some missing data values. Excluding Alkie and failed traps, the total sample size was 5 sites, 19 patches, 40 transects, and 309 traps.

Patch characteristics

At each patch, we recorded the following information for ten individual plants (or all plants if the patch was composed of fewer than 10 plants): number of flowering stalks, and average length of flowering stalks (of 3 representative stalks). If there were more than 10 individual plants in the patch, the first two plants measured were the base individual plants for the transects, then the three tallest plants in the patch, then five additional representative plants. If there were fewer than 50 plants in a patch, the number of reproductive and non-reproductive plants were counted directly. If there were more than 50 plants in a patch, we estimated number of individuals by counting the number of plants in randomly distributed subplots (the number of which were proportional to the size of the patch) and scaling this number up to the patch size. We also visually estimated surrounding vegetation canopy height in bins outside of the patch (<30cm, 30-50cm, 50-75cm, >75cm), which was used to parameterize the WALD wind model.

Estimating maximum seed production

We estimated maximum seed production per individual by multiplying number of stems by the average stem length by 8.2 (mean number of flower heads per 1-cm stalk length) by 3.7 (mean flowers per head). The mean number of flower heads and mean flowers per head were taken from Winward and Tisdale (1977) morphological

measurements on *A. tridentata wyomingensis.* Seed production was estimated during the same season as trapping (upon trap deployment).

Terminal velocity

We collected samples of sagebrush seeds from reproductive plants at each site in areas outside of the patches for assessment of terminal velocity (3 inflorescences each from 3 plants). We followed the protocol for Sullivan et al. (2018) to measure terminal velocity by dropping seeds down a measurement tube containing two arrays of LED lights and sensors to estimate the speed of seed falls. We conducted 7 trial drops of pooled sagebrush seeds using either 500 or 1000 seeds per drop. Terminal velocity measurements ranged from 0.19 to 2.11 m/s. We selected the median terminal velocity of 0.41 m/s for use in our models.

Data Analysis

Our modeling approach was composed to two parts. The first part involved fitting simplified negative binomial regressions to determine which sources of landscape variance best explained trapped seed density. The second part involved combining an empirical 2dt dispersal model (Clark et al. 1999) with a mechanistic WALD wind model (Katul et al. 2005) to estimate latent ground distance for seeds caught above the ground (described below). Fitting models to quantify the influence of scale in a generalized linear model framework (negative binomial regression) enabled us to leverage a well-understood statistical approach to test covariate importance and develop random effect structures (Warneke et al. 2022) for our field data.

How far do sagebrush seeds disperse and how variable is sagebrush seed dispersal?

We calculated the seed density ("seeddens") for each trap by dividing the number of seeds caught by trap area and a standardized term for the number of days deployed (stdays). The standardized day term (stdays) was calculated for each trap as the number of days deployed over the maximum number of days any trap was deployed (n = 49). After calculating the seed density for each trap, we calculated the relative standard error (RSE) of seed density for each trap distance across sites, years, and patches. RSE is calculated as the standard error over the mean seed density for each distance. Typically, effects with a RSE >20% are considered highly variable in ecology (McCune and Grace 2002).

<u>Which landscape scales best explain variation in trap seed density?</u>

We fit negative binomial regressions using the R package *brms* (Burkner 2017) of trap seed density as a function of capture height, capture distance, and total available seed. The overall model is described as follows:

$$\text{Nseeds} \sim \text{negbin}(\mu, \phi) \tag{1}$$

where the number of seeds (Nseeds) is a random variable drawn from a negative binomial distribution, with mean µ and overdispersion parameter ϕ.

$$\text{Log}(\mu) = \gamma 0 + \gamma 1 * \text{ht} + \gamma 2 * \text{dist} + \gamma 3 * \text{ht} * \text{dist} + \gamma 4 *$$
$$fecund + \log(stdays) + \log(Area) \tag{2}$$

In Equation 2, *γ0, γ1, γ3*, and *γ4* are fitted parameters. *ht* is the capture height, *dist* is the capture distance, and *fecund* is the total available seed in the patch. An interaction term between *ht* and *dist* is included. The total available seed term is described as:

$$fecund = \text{seeds}_p * \text{nrem} \tag{3}$$

where *seeds_p* is the average maximum seed production per plant and *nrem* is the number of reproductive plants per patch. The trap area (*Area*) and *stdays* term function as offsets (Hilbe 2011), constant terms that scale the mean based on sampling effort.

To determine how trapped seed density varied across different landscape scales, we fit different versions of the basic model, allowing $\gamma 0$, $\gamma 1$, $\gamma 2$, and $\gamma 3$ to vary by group levels as follows:

1) No landscape effects

2) Site only

3) Site x Patch

4) Patch only

5) Patch x Transect

6) Transect only

7) Site x Patch x Transect

No site was monitored across both years (the location of the trapping at Soda in year 2 was in a completely separate part of the fire) so "Site" actually refers to a site-year effect. Total available seed, distance, and trapped height were all centered around 0 and scaled by 1 standard deviation to improve convergence. We calculated the leave-one-out cross validation metric using the *loo* package to compare models with different variations in slope. Model convergence was assessed by assuring all $\hat{r}$ values were no greater than 1.05 and visual inspection of chain mixing (Monnahan et al. 2017). Priors are given in Appendix B, Table B.2.

<u>Do wind direction metrics help explain variation in seed dispersal?</u>

We considered if wind direction could help explain variation in seed dispersal. We reviewed wind data from the closest NOAA weather station to each site and determined the dominant wind directions of gusts greater than or equal to 32 km per hour during the trapping time (Table 2.2). Assuming that traps set at angles 180 degrees from the dominant wind direction (i.e. facing the wind) would be most likely to collect seeds, we recorded the smallest absolute difference between the transect angle and the direction the dominant wind gusts were blowing towards. The wind orientation was then scaled (for each value, we subtracted the mean and multiplied the standard deviation) and given as the variable *windorient*. This wind effect was described by a new parameter, $\gamma 5$, which we added as an additional effect to the best-fitting landscape model. The updated equation 2 for the model with wind effect is then:

$$\log(\mu) = \gamma 0 + \gamma 1 * \text{ht} + \gamma 2 * \text{dist} + \gamma 3 * \text{ht} * \text{dist} + \gamma 4 * fecund + \gamma 5 * windorient + \log(stdays) + \log(Area) \qquad (4)$$

We also considered wind direction as a binary variable with traps either facing towards (within 45 degrees facing a dominant wind direction) or away from the wind as variable windbinary. In this model, the wind effect (*windface*) was described by the parameter, $\gamma 6$.

$$\log(\mu) = \gamma 0 + \gamma 1 * \text{ht} + \gamma 2 * \text{dist} + \gamma 3 * \text{ht} * \text{dist} + \gamma 4 * fecund + \gamma 6 * windface + \log(stdays) + \log(Area) \qquad (5)$$

How does seed dispersal from remnant patches compare with aerial seeding rates?

We combined a 2dt empirical dispersal kernel (Clark et al. 1999) with a mechanistic WALD dispersal kernel (Katul et al. 2005). The 2dt kernel is a bivariate model used to describe decreasing seed or recruit density as distance from the seed source increases and fit using empirical data, while the WALD kernel is a mechanistic model describing the expected movement of a seed in the wind given an understanding of wind movement and seed properties. Our resulting fusion model was used to simulate landscape-scale dispersal of sagebrush seeds. The 2dt kernel was chosen over other dispersal kernels through an initial exploration looking at capture distance (BIC and AIC kernel comparisons are given in Appendix 2). Similar to other studies of long-distance dispersal, the maximum distance of seed traps was limited by logistical constraints. Fusing lab-based estimates of wind dispersal via the WALD model with our 2dt dispersal model, informed by field data, enabled us to develop dispersal predictions that made full use of our vertical trap design. In this study, the WALD parameters were set (i.e. we did not propagate uncertainty in wind speed, canopy density, or terminal velocity).

The overall model is described as follows:

$$\text{Nseeds} \sim \text{negbin}(\mu, \phi 2) \tag{6}$$

$$\mu = \text{Area} * disp * (f * \frac{fecund}{1000}) * \text{stdays} \tag{7}$$

$$disp = a_{transect}(\frac{1}{\pi b_{transect} * \left(1 + \frac{dist_{ground}^2}{b_{transect}}\right)^{a_{transect}+1}}) \tag{8}$$

$a_{transect}$ and $b_{transect}$ are fitted parameters that determine the shape of the 2dt kernel allowed to vary by transect where;

$$a_{transect} = a + \omega_{transect} * v1 \tag{9}$$

$$b_{transect} = b + \delta_{transect} * v2 \tag{10}$$

a and b are the global parameters for the 2dt kernel, $\omega_{transect}$ and $\delta_{transect}$ are the deviation of each transect from a and b respectively, and $v1$ and $v2$ are the transect-level variance for the a and b parameters.

f is a fitted parameter describing the effect of total available seed on seed density. Total available seed was divided by 1,000 to scale it for model convergence. $Dist_{ground}$ is the estimated latent ground distance of a seed caught at a certain height on a trap (i.e. the distance we expected a seed to travel to the ground based on its captured height at a certain distance). $Dist_{ground}$ was set at the trap distance ($dist_{trap}$) for seeds caught below 20cm in height (we assumed the additional distance these seeds would travel would be negligible). For seeds caught 20cm above the ground or higher:

$$dist_{ground} = dist_{trap} + dist_{wald} \qquad (11)$$

$$dist_{wald} \sim Wald(\rho, \lambda) \qquad (12)$$

where ρ and λ are parameters calculated from wind speed, vegetation canopy height, canopy density, and terminal velocity. Katul et al. (2005) and Sullivan et al. (2018) describe the calculation of these parameters, including validation with post-dispersal data on spatial patterns of seedling recruitment.

$$\rho = \left(\frac{ht}{\sigma}\right)^2 \qquad (13)$$

where ht is the height of seed capture. σ is a parameter calculated as:

$$\sigma^2 = kc\left(2\frac{\sigma_w}{U}\right) \qquad (14)$$

where k is a scaling coefficient set between 0.3 and 0.4 to describe canopy density. We set k at 0.38 for sparse, heterogeneous canopies typical of post-fire systems. c is the canopy height surrounding the patch based on our visual estimates from the field at each specific patch. We set σ_w (a measure of boundary conditions) to half of U based on Sullivan et al. (2018). U is the average daily maximum wind speed during the time periods in which the traps were deployed taken from the closest NOAA or RAWS weather station.

$$\lambda = \frac{htU}{V} \qquad (15)$$

where V is the terminal velocity of sagebrush seeds. Priors are given in Appendix 2, Table 2.

After fitting the combined empirical mechanistic model, we created a forward version in R that sampled from the posterior distributions of our parameters and ran 10000 simulations to estimate seed dispersal at distances between zero and 100 meters.

Table 2.2   Dominant wind direction for gusts > 32 km h−1 (given in degrees) during the trapping dates at the NOAA weather station closest to the site.

Alkie was excluded due to seed crop failure and no seeds trapped.

Site and year	Dominant wind direction (°) for gusts > 32 km h−1	NOAA weather station
Soda Year 1	200, 250–270	Rome
Botanical Garden Year 1	120–140, 160–170	Boise Airport
Soda Year 2	220–240, 160–170	Rome
Table Rock Year 2	120–140	Boise Airport
Pony Year 2	100–130, 290–310	Mountain Home

Results

How far do sagebrush seeds disperse, and how variable is sagebrush seed dispersal?

No seeds were caught on vertical seed traps at the Alkie fire, despite extending the trapping time several weeks past the initial ~3-week observation period. Seeds on patch plants appeared not to develop at the Alkie site, and thus it was excluded from analysis. At the other sites, 31% of traps captured seeds. Two seeds were detected on each on two of the traps at the maximum distance of 26 m from the seed-source patches. Relative standard errors (RSE) of seed density for each trap distance across sites and years were large, ranging from 24% to 77% (Fig. 2.2). RSE tended to increase with distance of traps from seed-source patches ($R^2 = 0.47$), indicating that dispersal became more variable the farther the distance from the patch.

Which landscape scales best explain variation in seed dispersal (trap, transect, patch, site)? Do wind direction metrics help explain variation in seed dispersal?

The total number of available seeds produced by the sagebrush present in each patch varied across years and sites, with the greatest mean total observed at the Table Rock Fire in year 2 (Fig. 2.3). However, available seed abundances did not relate to the number of seeds caught per trap, nor were there consistent relationships of available seeds to abundance of seeds captured by seed traps in each patch (90% credible interval for total available seed [-0.14, 0.66]) (Fig. 2.4). On average, the most seeds per trap were caught at the lowest elevation site, the Botanical Garden in year 1.

Model performance increased as the landscape scale of variance decreased with best model performance at the transect level, the finest spatial scale in this study (Table 2.3). Models incorporating multiple levels of variance did not perform better than models

with single lower levels of variance. This indicates that the primary source of spatial variability in seed rain occurred at a small-scale level (different sides of patches) rather than either at the scale of 1) the five sites across two years or 2) patch level.

As expected, distance had the strongest effect on trapped seed density (Fig. 2.4). Estimated seed density decreased from a mean of ~ 13 seeds m^{-2} [90% credible interval 0-66] to < 1 seeds m^{-2} [90% credible interval: 0-4] as distance increased from 0 to 10 m from the source, holding all other predictors constant. Neither total available seed nor height had a consistent effect on trapped seed density (90% credible intervals crossed zero) (Fig. 2.4). However, there was a positive interaction between trap distance and trapped height on seed density, with more seeds caught at higher heights at distances near the source (Fig. 2.5). For example, at a distance of ~0.3 m, more than 160 seeds m^{-2} were predicted to be trapped at 65 cm height, as opposed to 11 or <1 seeds m^{-2} at 40 and 15 cm height, respectively.

The random intercept varied more between transects than did the slope of distance, height, or the interaction between distance and height (Fig. 2.4). This indicates that the effects of distance and height on seed density were less variable between transects than overall seed density differences. Including either continuous or a binary metric of wind direction did not improve model performance (Table 2.3).
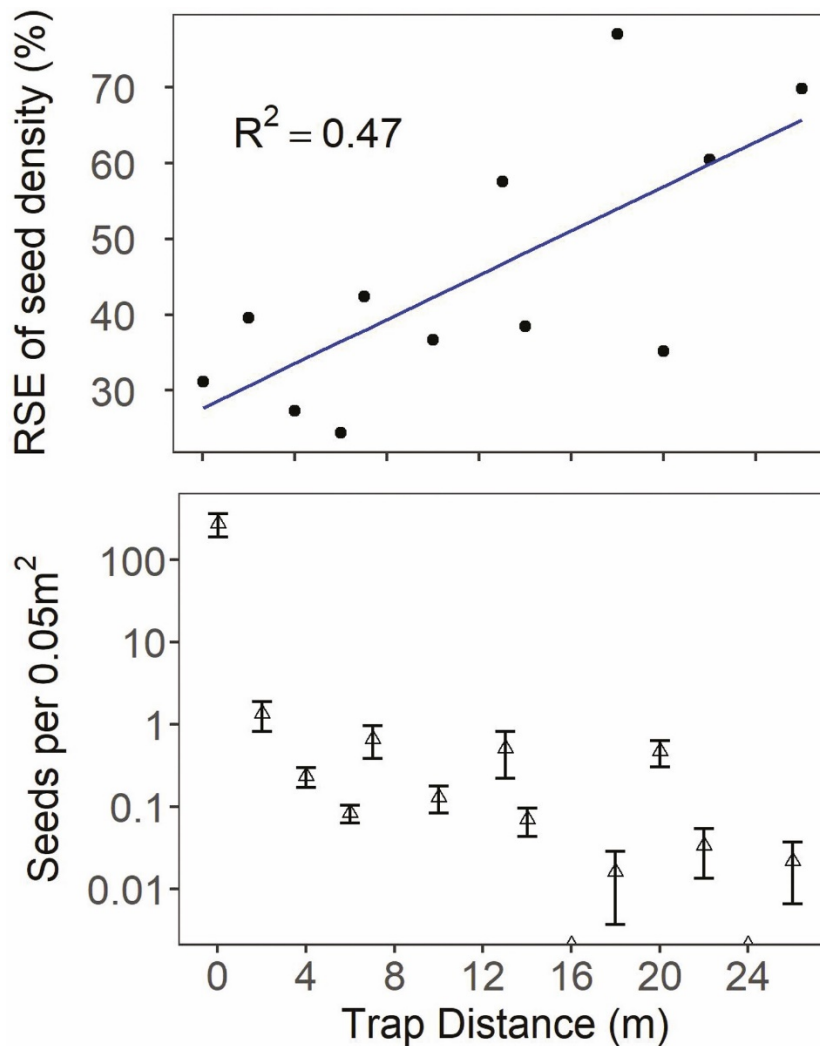
Figure 2.2 **Relationship of mean trap abundance (bottom panel) and variability (RSE, top panel) of the density of seeds captured (per 0.05 m2 of vertical trap area) relative to the distance of seed traps from seed source patch.**

Seed density is standardized by the number of days in each collection interval period shown as the mean per trap ± the standard error (bottom). Alkie was excluded due to seed crop failure and no seeds trapped.
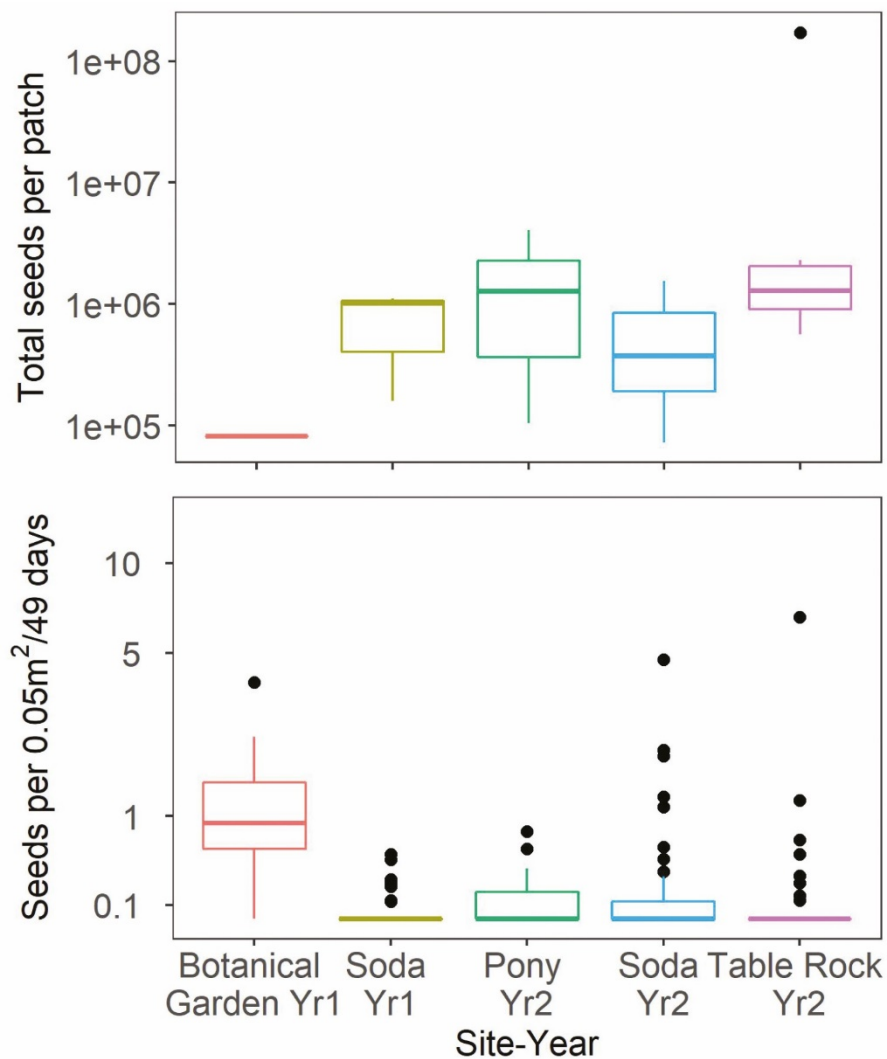
Figure 2.3   Box plots of the estimated total available seeds per patch (fecundity x number of reproductive plants) across sites (top) and number of seeds across traps of all distances caught per 0.05 m2 trap area standardized by 49 days deployed (bottom).

The graphs do not include under-crown traps. The unit of measure for the top graph is a patch (n = 19) and the unit of measure for the bottom graph is a trap (seed counts aggregated across heights, n = 273). Alkie was excluded due to seed crop failure and no seeds trapped.
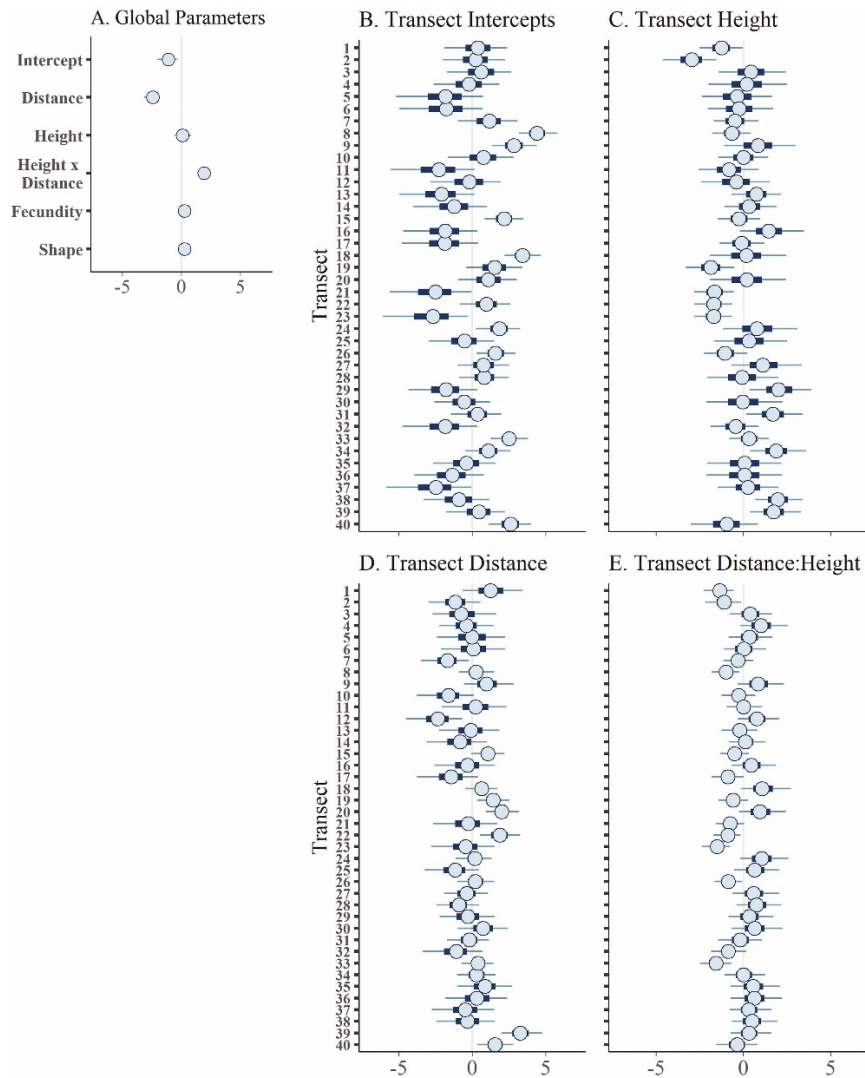
Figure 2.4   Posterior distributions intervals for parameters of the landscape negative binomial seed density model with intercepts and slopes varied by transect.

The center blue circle of each distribution shows the median, the dark blue bars show the 50% credible interval, and the thin blue lines show the 90% credible interval. Predictors were scaled prior to analysis so that parameter values represent relative effect size of each predictor on trapped seed density. A) Global parameters, B) Varying intercepts by transect, C) Varying slope of the height parameter by transect, D) Varying slope of the distance parameter by transect, and E) Varying slope of the height:distance parameter by transect.
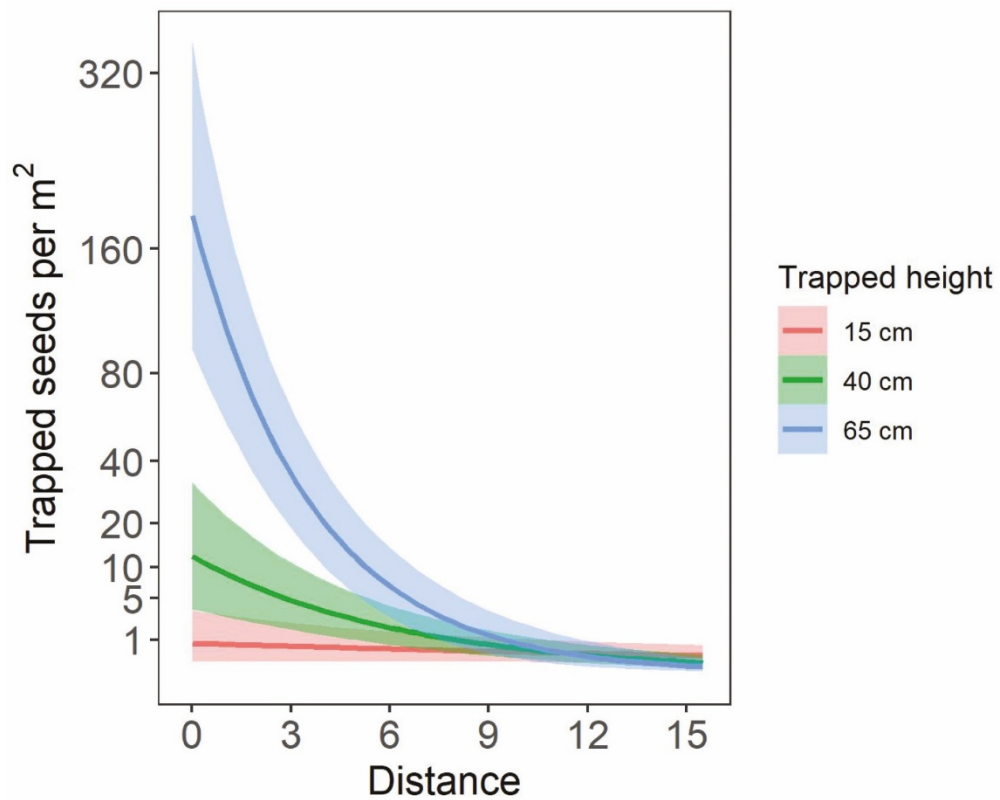
Figure 2.5   Mean number of trapped seeds per m2 area predicted from the landscape model with slope varied by transect, showing the interacting effects of trapped height and trapped distance on seed density.

The shaded ribbons show the 90% credible intervals.

Table 2.3 **Comparison of leave-one-out information criteria between different landscape models.**

Model	loo IC
Model 1: No landscape variation	1927.1
Model 2: Site only	1803.7
Model 3: Site × Patch	1795.5
Model 4: Patch only	1780.1
Model 5: Patch × Transect	1770
Model 6: Transect	1756.1
Model 7: Site × Patch × Transect	1766.3
Wind Model 1: Wind Angle with Transect	1760.7
Wind Model 2: Binary Wind with Transect	1766.7

How does seed dispersal from remnant patches compare with aerial seeding rates?

Seed dispersal predicted for a median transect with a fecundity of 30,000 seeds/individual and a patch size of 25 individuals (750,000 total available seed) would decrease to 0 seeds m^{-2} capture area at a distance of ~16 m distance from the patch, based on the median of 10000 simulations (Fig. 2.6). However, in the top 5% of simulations, there were still 48 seeds m^{-2} at 100 m distance and in the lower 5% of simulations, there was no dispersal at any distance. These seed dispersal simulations were highly variable. For example, the 90% quantiles for modeled seed dispersal to 5 m from patches ranged from 0 seeds m^{-2} to >100,000 seeds, and the median value was 12 seeds m^{-2}. For comparison, on the Soda wildfire, the aerial sagebrush seeding rate was between approximately 95 and 250 aerial pure live seeds m^{-2}.
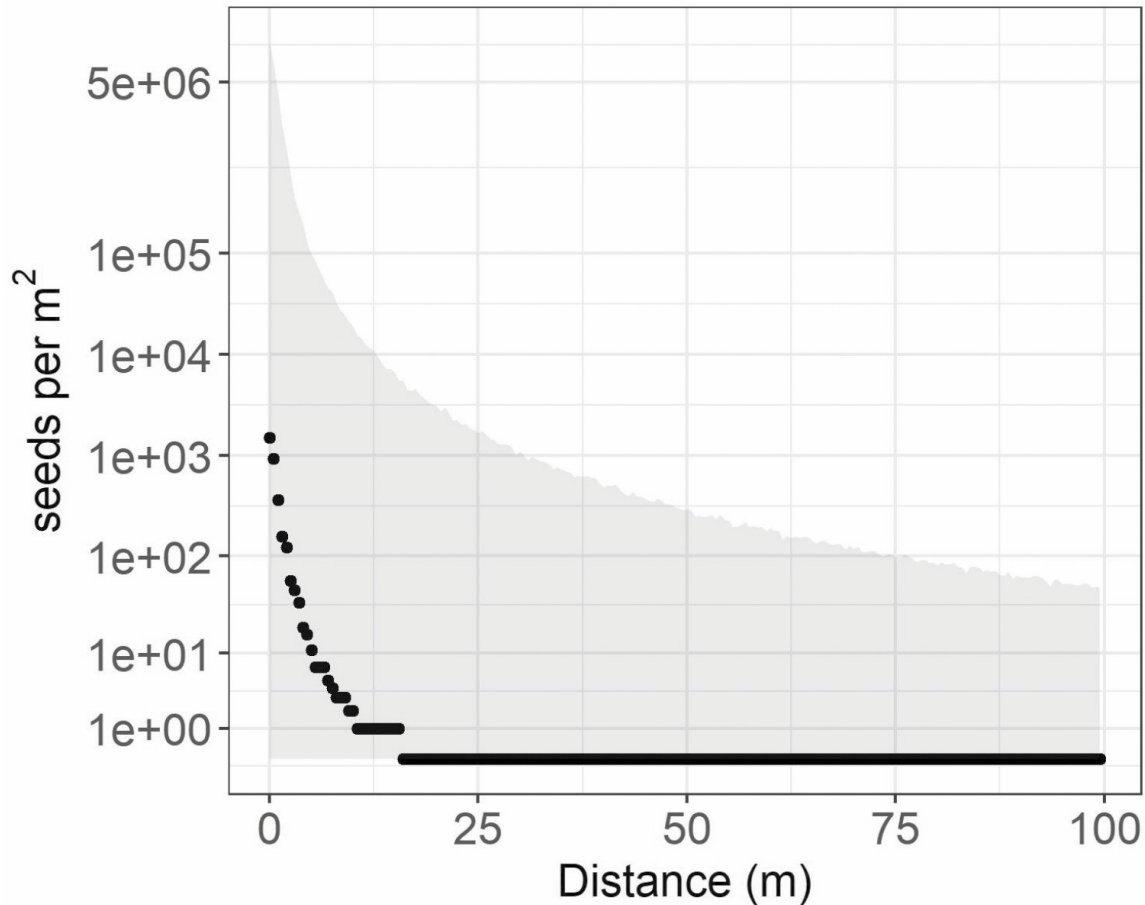
Figure 2.6   Simulated median seed dispersal (seeds m-2) estimated using the seed dispersal model with transect-level variation in dispersal kernel (1000 simulations).

Based on global parameters for the p and u parameters of the 2dt kernel, and assuming an average of 30,000 seeds per reproductive plant, and 25 individuals per patch. The grey ribbon shows the 90% quantiles of the simulations.

Discussion

Seed availability is an important component of restoration and rehabilitation of disturbed areas, particularly for foundational species like sagebrush that can only reestablish from short-lived seeds. Insufficient seeding could cause missed recovery opportunities, while unnecessary seeding of areas with adequate natural seed could waste resources and carry unnecessary collateral ecological risks (e.g. potential introduction of

maladapted genotypes, Seaborn et al. 2021). Therefore, there is a pressing ecological need to develop better methods of predicting natural seed dispersal across disturbed landscapes. Our study presents a rare attempt to quantify seed dispersal at management-relevant scales by integrating both empirical and mechanistic modeling. Although our seed dispersal predictions indicated a high degree of uncertainty, they revealed that seed dispersal from unburned remnant sagebrush or actively created sagebrush patches is a major source of variability in natural post-fire regeneration of sagebrush. Even areas very close to these patches may experience limited seed dispersal.

Landscape variability

Although we found a measurable amount of seed dispersal from sagebrush patches, there was a high degree of variability in dispersal between transects, even when total available seed and patch size were accounted for. Differences in canopy heights and plant densities can strongly affect wind movement and wind-transported seeds (Nuttle and Haefner 2005; Bohrer et al. 2008). These previous studies from forested studies show that strong bursts of vertical wind (influenced by the structure of the canopy) are particularly important to long-distance seed dispersal. In comparison to forests, recently burned sagebrush-steppe ecosystems have minimal canopy structure, and wind movement near the ground is less likely to be strongly affected by remaining vegetation (Driese and Reiners 1997). Furthermore, although we found clear evidence that sagebrush seeds are dispersed by wind, they lack a true wind-dispersal mechanism (such as a pappus; in spite of being in the Asteraceae family) that would allow them to remain aloft in vertical wind lifts for extended transport. The predictive strength of models that account for variability at different directions from the patch has implications for theoretical and applied research

on seed dispersal, where isotropy (equal probability of dispersal in all directions) is often assumed (van Putten et al. 2012).

Sagebrush steppe often occurs in topographically complex areas, and even though our sampling areas were relatively flat, airflow patterns caused by the surrounding hills could have contributed to the high variability in seed dispersal we observed across different transects. The greater variation in seed dispersal at the transect level than at the site or patch level, combined with the lack of explanatory power of coarse ("average") wind-direction metrics suggests that transect identity may have been a proxy for canopy structure, topography and stronger and unaccounted-for wind variability within sites. Due to the difficulty in controlling for these factors in the field, the question of how topography and vegetative structure influences seed dispersal could be addressed in follow-on investigation using mechanistic modeling (Nathan et al. 2009).

Height of seed release is another factor that can contribute to differences in dispersal distances (Thomson et al. 2011, Schupp et al. 2019). In canopies with variable heights of plant crowns (as was the case in our patches), assessing maternal plant height effects on dispersal can be difficult because plants may not contribute equally to seed dispersal, and tracing seeds to specific source plants requires genetic analysis via DNA microsatellites (Ashley 2010). However, the effect of sagebrush height on dispersal distance could be addressed in an experimental context by trapping around individual plants of different heights. In many semiarid landscapes, mound-like features are created by mammals, insects, or geomorphic processes, such as the very common "mima mounds" of sagebrush steppe that host relatively tall and fecund plants elevated above the

surrounding sagebrush population (Hill et al. 2005). These microtopographic effects would be important considerations in modeling height of seed release.

Phenology is another important factor in determining seed dispersal by wind. Some tree species with specific wind dispersal mechanisms synchronize seed ripening and release with meteorological conditions that promote long-distance seed dispersal (Heydel et al. 2015). Although species in open vegetative habitats, including many Asteraceae species, do not display such targeted release patterns (Tackenberg et al. 2015), the timing of seed ripening and release can still have an impact on dispersal distances. In our second year of trapping, initial seed development was delayed, possibly due to above-average rain in October. A significant wind event occurred at Table Rock in mid-November during our first three weeks of trapping yet there were few seeds collected in traps. Seeds did not appear fully developed or easy to remove from the inflorescences at that time, and appreciable seed capture was not detected until later in December. An improved understanding of how seed development coincides with major wind events may help elucidate differences in patch and site seed dispersal.

Estimating landscape scale dispersal distance

Predicting seed dispersal becomes more difficult as distance from the maternal plant increases (Bullock and Clark 2000; Fig. 2.2) but can be particularly critical to vegetative recovery in disturbed systems when seed sources are limited (Hammill et al. 1998; Urza and Sibold 2017; Borchert et al. 2003). We attempted to address this problem by utilizing vertical traps, measuring height of seed capture, and integrating a mechanistic wind dispersal model into our empirical dispersal kernel to simulate latent ground distance a seed would travel. Our approach allowed us to estimate a range of dispersal

distances without actually placing traps at locations where seed dispersal was expected to be so rare that we were unlikely to detect it. We believe this approach could be further refined and used to estimate landscape-scale wind dispersal of other species of restoration or conservation concern. The key point is that height of seed capture can be used as a proxy by which to estimate dispersal distance, if certain properties of the seed and system are known (seed terminal velocity, average wind velocity, canopy density). We used a modestly parameterized approximation of a WALD dispersal kernel in this study and incorporating microsite-specific wind measurements and site-specific terminal velocity metrics could further improve predictions (Sullivan et al. 2018).

On the Soda wildfire, widespread aerial sagebrush seeding of a rate between ~95-250 aerial pure live seeds m^{-2} (not applied at the time of our study) generally overcame seed limitations to allow for significant seedling establishment in the first year after fire (Germino et al. 2018). Establishment was strongly limited by topographic features, absence of "fertile islands" (high organic-content areas where sagebrush existed pre-fire and burned), and dominance of exotic annual or perennial grasses (Germino et al. 2018). While our seed dispersal models show that it is possible that remnant sagebrush islands could generate as much seed as aerial seeding in some rare instances close to the patch, it is highly unlikely that this seed dispersal would reach the microsites needed for significant population re-establishment.

One further consideration is the potential role of negative density dependence inside and near remnant sagebrush patches (Zaiats et al. 2020). Given that the majority of sagebrush seeds fall within a few meters of the mother plant, many of the seeds will be establishing with the zone of influence of not only the mother plant but possibly other

individuals in the patch. Strong negative density dependence is likely to further negate the seed contribution of remnant sagebrush patches to landscape scale sagebrush regeneration.

Conclusions

Developing quantitative models for spatial prioritization of restoration efforts is a major research objective with immediate applicability to land management. Small scale and near-term forecasting of vegetative regeneration is an integral part of making decisions about where and when to actively manage landscapes (Dietze et al. 2018). In this study, we demonstrated how empirical and mechanistic dispersal models can be integrated to predict post-fire seed dispersal from undisturbed seed sources and that large burned areas in sagebrush-steppe likely receive little or no natural sagebrush-seed deposition across most of their area. These results can be utilized in predictions of post-fire regeneration for determining which areas of the landscape to actively manage.

Data Availability

Data will be released with publication of this paper to the Forest Service Research Data Archive and can be accessed here: https://www.fs.usda.gov/rds/archive/Catalog/RDS-2021-0073. Code for the models is available here: https://zenodo.org/badge/latestdoi/537824506

Acknowledgements

CHAPTER THREE: HOW DO ACCURACY AND MODEL AGREEMENT VARY

WITH VERSIONING, SCALE, AND LANDSCAPE HETEROGENEITY FOR

SATELLITE-DERIVED VEGETATION MAPS IN SAGEBRUSH STEPPE?

Abstract

Maps of the distribution and abundance of dominant plants derived from satellite data are essential for ecological research and management, particularly in the vast semiarid shrub-steppe. Appropriate application of these maps requires an understanding of model accuracy and precision, and how it might vary across space, time, and different vegetation types.For a 113 k Ha burn area, we compared modeled maps of different vegetation cover types created from satellite data to 'benchmark" models based on intensive field sampling (~1500-2000 plots resampled annually for 5 years) for three new satellite-derived models: USDA Rangeland Analysis Platform (RAP), the USGS Rangeland Condition Monitoring Assessment and Projection (RCMAP), and USGS fractional estimate of exotic annual grass cover (USGS-fractional-EAG). We assessed out-of-sample point accuracy and asked if and how accuracy changed each year due to vegetation shifts, new images, and model improvements (i.e. model versions). We also assessed how map agreement between satellite-based and field-based models changed with scale of application, topography, and time since fire.

Accuracy and map agreement varied considerably among the vegetation types and across time and space (r^2 ranging from 0 to 0.54), and some of the variability was predictable. All models tended to over- or underestimate cover when field-measured cover was relatively low or high, respectively, i.e. a "false moderating effect". Accuracy was greater and improved with newer versions of RAP (+ 0.05 to 0.29 r^2) compared to RCMAP and USGS fractional model estimates, and in some cases was greater than field-based models. Variability in map agreement tended to decrease with larger areas sampled (particularly in areas > 12km), and this scale dependency was more evident in RAP and USGS-fractional-EAG models. Creating a "fair" basis for comparison of spatial models of low-statured semiarid vegetation derived from satellite compared to field data is not trivial because scaling the field data to the scale of large satellite pixels (or downscaling satellite-based models to field scale) requires modeling and associated model uncertainty. Accuracy can vary considerably and understanding the variation can help guide application of the models to the appropriate time, place, and variables.

Introduction

Maps of plant abundance are fundamental to terrestrial ecology and management, such as evaluating vegetation responses to disturbance, weather, or management (e.g. Elmore et al. 2003, Costello and Kenworthy 2011, Bradley et al. 2018). The spatial models used to generate maps of the distribution and abundance of plant types can be created by 1) collecting field-data at point locations and interpolating values across landscapes (e.g. Mkrtchyan 2004), 2) using field-data to train predictive models of cover based on environmental covariates (e.g. McNellie et al. 2021), 3) modeling plant cover based on spectral reflectance measured with remote sensing, often from satellites (e.g. Yu

et al. 2014, Boswell et al. 2017), or 4) some combination of these methods (e.g. Miller 2005, Wilson et al. 2011, Xu et al. 2018, Barnard et al. 2019).

Knowing the reliability of satellite-based vegetation models is essential for their appropriate application in land management and science, and estimating the underlying error requires comparison to field-based estimates of vegetation (Ludwig et al. 2007). However, field-based plant inventory cannot match the complete landscape coverage provided by remote sensing, and ground-based monitoring is often insufficient to create accurate maps of species or functional group abundance that are comparable to those generated from remote sensing, considering their commonly large pixel sizes (e.g. 30 m; Lechner et al. 2012, Valley 2016, Bradley et al. 2018). Creating a fair basis for comparison of field- to satellite-based vegetation models thus requires either downscaling satellite data from large pixels to field points, and/or using interpolative modeling to upscale field point data to the pixel, or pixel-cluster level (Ludwig et al. 2007, Wilson et al. 2011, Barnard et al. 2019). Both upscaling and downscaling introduce model assumptions and error to the accuracy assessments (Dark & Brom 2007, Lechner et al. 2012). Accuracy of vegetation models and maps is also expected to vary with the scale of model application, typically negatively (Ludwig et al. 2007), and among vegetation types and contexts. In many systems, we still lack an understanding of how scale and landscape heterogeneity affect agreement between field data and satellite-derived data.

Vegetation maps derived from models based on satellite data are particularly valuable in the vast semiarid rangeland landscapes that cover a substantial portion of the terrestrial earth, where field-based data tend to be scarcest. Stressors such as climate change, altered wildfire regimes, and exotic plant invasions can entail rapid vegetation

changes over large areas that transgress jurisdictional or ecological boundaries (e.g. Beever et al. 2019). Semiarid landscapes seem to be suited to remote sensing, partly because aridity confers less complications of cloud cover for remote-sensing data capture (Hansen and Loveland 2012). However, there are also challenges to employing remote sensing classification techniques on semiarid rangelands. Low canopy cover results in increased noise from bare soil and discriminating between different functional groups or species can be challenging because of similar spectral properties of the vegetation (Smith et al. 1994, Mansour et al. 2012, Smith et al. 2019). These challenges can be particularly prominent during early post-fire successional stages, which happens to be a context where rapid assessment of large areas possible with satellite-based vegetation models is particularly needed (Applestein & Germino 2021). Moreover, high dominance of temperature and moisture on variability in plant growth in dry environments means that even subtle topographic or edaphic differences can cause important spatial variation in species' abundances (Passey et al. 1982, Mitchell et al. 2017). The temporal overlap of suitable moisture and temperature needed for growth each year can be narrow, causing the green and remotely sensible presence of herbaceous or deciduous leaves to happen quickly, often a month or few weeks (Svoray et al. 2013). Thus, the relatively high frequency of data capture made simultaneously over large areas by satellite sensors such as Landsat make them indispensable tools for assessing broadscale vegetation patterns in semiarid settings.

Three new satellite-derived products for mapping functional group cover back in time are now available for western United States rangelands and related semiarid landscapes. They include the USDA Rangeland Analysis Platform (RAP) cover for

annual herbaceous, perennial herbaceous, shrubs, trees, and bareground (Allred et al. 2021), USGS Rangeland Condition Monitoring Assessment and Projection (RCMAP) time-series for annual herbaceous, bare ground, herbaceous, litter, non-sagebrush shrub, perennial herbaceous, sagebrush and shrub (Rigge et al. 2021), and a USGS-produced fractional estimate of exotic annual grass cover (Devendra et al. 2021). RAP and RCMAP are novel in their large-scale coverage, temporal completeness (30+ years), dispersed ground truthing, and scaling relevant to management applications. The USGS-produced fractional estimates address a different need; they are produced as real-time data for immediate land management action. These products have been increasingly used for land management applications, despite limited assessments of scale of applicability.

We capitalized on an intensively field-sampled landscape that offered a rare opportunity to attain high-accuracy upscaling for comparison to satellite-derived vegetation maps for understanding changes in accuracy and map agreement across time, scales, and landscape heterogeneity.

We asked:

1) How does accuracy compare between field-based and satellite-derived map models, does accuracy change over time?

2) How does map agreement between our field-based and each satellite-derived map model product change with the scale of aggregation (scaling up)?

3) How does map agreement between satellite-derived and field-based model maps relate to spatial co-variates (e.g., topography of pastures) and time (e.g. time-since-fire disturbance)?

We expected that out-of-sample point accuracy would be higher for field-based than satellite-derived map models. We expected agreement between field-based and satellite-derived maps to increase with: 1) larger scale of aggregation (larger sample area), 2) more time since fire, and 3) with less topographic heterogeneity of focal areas. Moreover, we anticipated that modeling versioning changes, which are typical and ongoing for many or most modeling efforts, would lead to greater accuracy.

Materials and Methods

<u>Field data collection</u>

The study landscape was 113,000 ha of sagebrush steppe that burned in the 2015 Soda Wildfire in Idaho and Oregon USA, which was a nearly unpopulated rangeland setting with considerable topographic variation including mountains, basins, plateaus, and canyons (Fig. 1). The Boise District Bureau of Land Management (BLM) conducted several imazapic herbicide applications, aerial seeding of grasses, sagebrush, and forbs, and drill seeding of perennial bunchgrasses between 2015 and 2018 to stabilize the soil, improve sage-grouse habitat, reduce risk of invasion by exotic annual grasses, and increase resilience to future fires. Some areas were treated multiple times. Training data collection occurred between mid-April and October in 2016 and between late-April and mid-August in 2017-2020. Plot location coordinates were generated via a stratified-random method at 1 plot per 54.5 ha or denser and were moved if they overlapped roads, had >20% trail area within an 18-m radius, or fell within 0.40 km of water troughs or ponds. Plot locations were recorded using a Juniper Mesa 3 tablet (typical accuracy ~ 3m). In 2016, to quantify the percent cover of each species, we took aerial photographs of 6-m^2 of rectangular areas around the plot center captured from nadir at 2-m height (with

Nikon Coolpix AW130, 16 megapixel). We then analyzed species cover using the grid-point intercept (GPI) software, Samplepoint (v 1.43, Booth et al. 2006), via visual interpretation based on a list of species collected in the field. Training data collection was similar in 2017-2020, however, in order to adjust for parallax distortion on plants as they grew taller each year since fire, we took two overhead photographs instead of one (the second photograph at 5.5m directly south of the first) and cropped each photograph to a 3m^2 area. We used 100 points/image for the single photo analysis in 2016 and 49 points/image for a total of 98 points per plot for the double photo analysis in 2017-2020. We then aggregated species cover into functional group (annual herbaceous, perennial herbaceous, and shrub) cover for the purpose of analysis.

Two additional, independent test datasets collected between 2016-2020 were available to assess accuracy of our maps and compare them with satellite-based products (see Germino et al. 2018, other datasets unpublished). Test data were composed of samples using the same Samplepoint-GPI described above. The first set of data was collected for a study to assess sagebrush seed source effects and was composed of plots that were well-distributed across the fire from 2016-2018 (n = 418 for 2016, n = 513 for 2017, and n = 450 for 2018), and the second set of data was collected to assessment treatment layering effects in 2020 (n = 141) (Fig. 1). Test data in 2016 was collected during peak phenological conditions (in the same weeks as the satellite imagery and field-training data set), whereas test data collected in 2017-2020 was collected primarily in August, weeks after peak phenological conditions but when cover is readily identified and similar to peak season. We excluded one test plot from 2016 that was composed of >80% shrub cover (all other plots had <20% shrub cover).
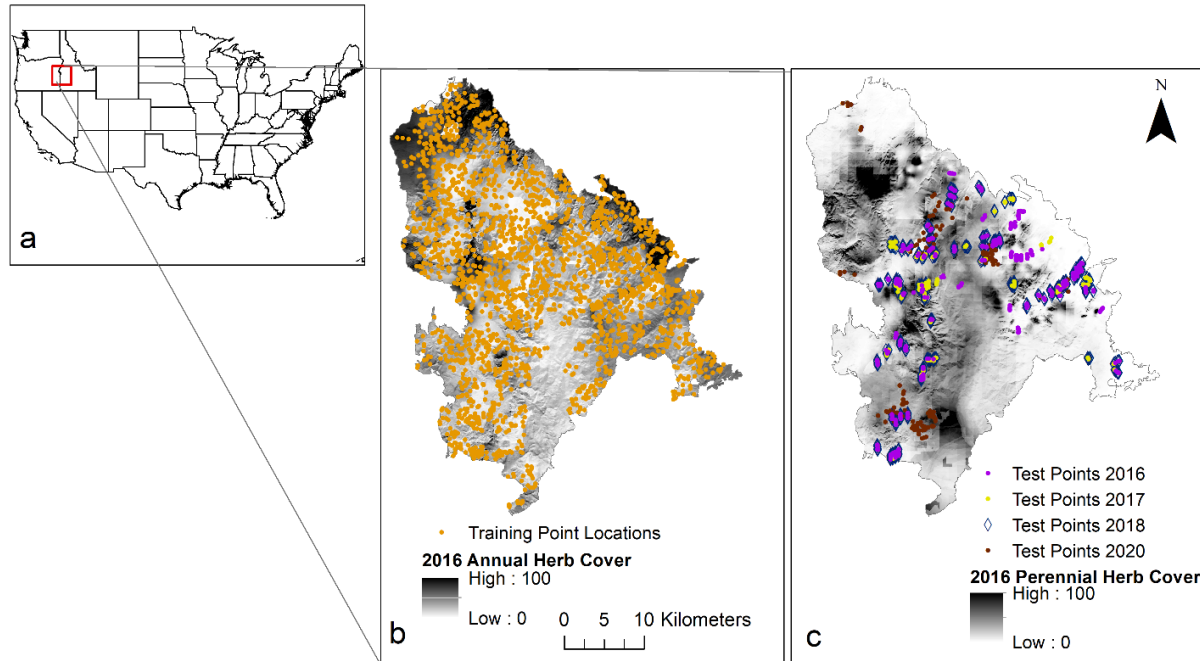
Figure 3.1   a. Location of study area shown on the continental United States with a red box. b. Location of training points (repeatedly sampled) with 2016 annual herbaceous cover. c. Locations of test points with 2016 perennial grass cover.

Annual and perennial herbaceous cover displayed in tiles b and c were derived using empirical Bayesian kriging regression (EBK).

Mapping functional groups

Empirical Bayesian kriging (EBK) regression is a geostatistical fusion method which combines ordinary least squares regression (OLS) with kriging; explanatory landscape variables are used to predict the dependent variable mean, while the error is modeled with a semivariogram describing the strength of the correlation between locations of different distances (Krivoruchko and Gribov 2019). This combination approach can make more accurate predictions than either regression or kriging individually. For each functional group and year, we conducted an EBK regression in ArcGIS Pro at 31.5 m pixel resolution with the following covariates used as predictors: mean annual precipitation (800m pixels, monthly PRISM data), heatload (calculated from

USGS Elevation DEMs, 31.5m pixels), number of herbicide treatments (derived from

vector data and set at 10m pixels), and number of drill treatments (derived from vector

data and set at 10m pixels). The resolution of the EBK regression was set to match the

heatload data raster grid and was chosen because it was similar to the 30m pixel size of

RAP, RCMAP, and USGS-produced fractional estimate data (as opposed to the scale of

800m PRISM data). In the EBK routine in ArcGIS Pro, predictor variables are

transformed into their principal components prior to the least-squares regression. The

dependent variable was log empirically transformed (with a constant – 0.01 added to all

values to remove zeros), the semivariogram model type was K-Bessel, the minimum

neighbors was set at 5 and the maximum neighbors was set at 15. The resulting maps

were constrained to be between 0 and 100 percent cover.

Accuracy

We extracted the pixel value of the test plot location from each field-based and

satellite-derived map model product and calculated r^2 values between the field data and

singular pixel value.

Scaling effects on map agreement between field-based and satellite-derived models

We evaluated how satellite-to-field modeled map agreement varied at different

scales, specifically for 1000 randomly centered samples ranging in circular area from 0.2-

44 km^2, specifically using 15 different radii ranging from 0.25-3.75 km, located entirely

within the boundary of Soda Fire, using ArcMap 10.1. The 3.75 km cutoff was chosen as

the largest size area that would allow five non-overlapping samples to fit within the fire

boundary. The pool of samples was then filtered to eliminate same-size samples that

overlapped. Next, we used the zonal.stats function in the *SpatialEco* package to calculate

the mean functional group cover in each sample area for both our field-based and the satellite-derived map models. We then calculated the average difference, standard deviation, and relative standard error between the field-based and remote-sensing maps for each polygon size.

<u>Landscape variability effects on map agreement</u>

To assess how landscape variability affected agreement between maps, we assessed functional group cover at the pasture level (n=101, mean = 1457 ha, stdev = 1562 ha), a spatial scale widely applicable to management decisions across western United States rangelands. A previous study on the same area found that the mean and SD of elevation and slope and pasture size were important sources of heterogeneity among pastures, and thus they were used as our "landscape variables" (Applestein et al. 2017). We calculated the difference in mean cover and the mean and SD of the landscape variables between the satellite- and field-based maps, for each pasture within the Soda wildfire using the zonal.stats function in R. Linear mixed models were used to determine the significance of the satellite-to-field model map differences to the landscape variables for sampling year and cover type. We included time since fire as an additional variable to assess map agreement over time. Pasture identity was included as a random intercept effect to account for resampling and thus avoid pseudoreplication (repeated polygons each year).

Results

<u>Accuracy assessment: comparison of map model estimates to test field data</u>

The patterns in accuracy of models relative to field test data were generally similar among the years (Fig. 2 compared to Appendix C), so we focus here on the variability in modeled compared to plot-scale field test data in 2016. Slopes of the relationships of cover determined in the field with satellite-derived or field-derived model estimates of cover (x and y, respectively) were typically much smaller than one, and had positive intercepts. This indicated that vegetation cover was generally overestimated by the models, especially the satellite-derived models, relative to field data when cover was low, and conversely under-estimated by the models when cover was high (Fig 2). Shrub cover was extremely sparse and patchy, especially in 2016, and was not well represented by any models, including the field-based maps (Fig 2). After then, from 2017-2020, r^2 tended to be greatest for the RAP estimates compared to field plots, except for perennial herbaceous cover in 2018 (i.e., in 8 of 9 comparisons for annual or perennial herbs or bareground; Table 1, Appendix C Fig. C.1-C.3). Field-based maps were nearly always more accurate than RCMAP and the USGS fractional cover estimates, often by 2x or more, for all plant types except shrubs (2017-2020) and bareground in 2020 (Table 1). Model accuracy was much lower in the reduced sample set of 2020 compared with 2016-2018 (Table 1).

Version 2 of RAP was more accurate than the version 1 map at predicting test data cover for all functional groups and years, except shrubs in 2018 (Fig. 3). Specifically, increases in r^2 among the RAP versions ranged from 0.05 for bareground in 2016 and 2017, to 0.29 for annual herbaceous cover in 2018. Version 2 of RCMAP had

greater accuracy than version 1 for bareground in 2016 (increase in $r^2 = 0.003$) and

perennial herb and shrub cover in 2017 (increases in r^2 of 0.13 and 0.03, respectively; Fig.

3). Otherwise, there were no other accuracy improvements and several reductions in

accuracy, for other functional groups in other years.
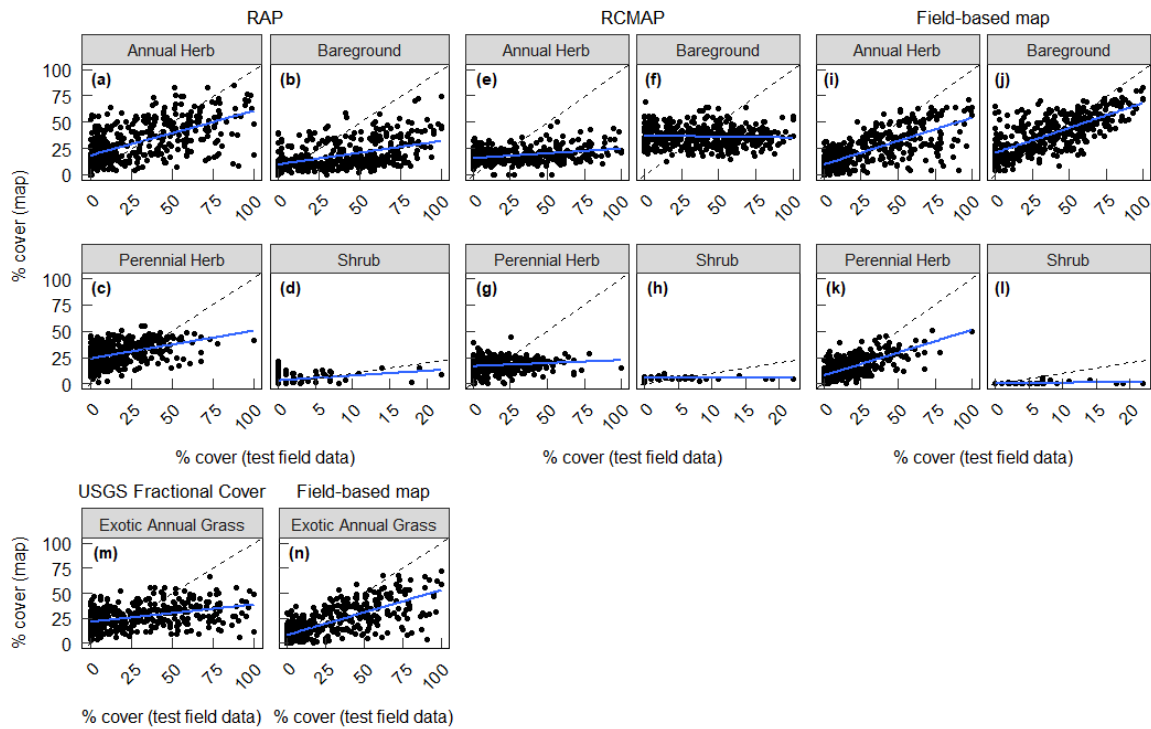
Figure 3.2   Relationship of satellite- or field-derived modeled vegetation cover (Y) to test field data (X) in 2016.

Models included the Rangeland Analysis Platform (RAP, **a** through **d**), Rangeland

Condition Monitoring Assessment and Projection (RCMAP, **e** through **h**), a field-based

benchmark map (**i** through **l** & **n**), or the USGS fractional cover estimate (**m**). The

diagonal dashed line on each plot shows the one-to-one correspondence (perfect

accuracy) and the blue line shows the linear regression line fit for each functional group.

Table 3.1 **Out-of-sample R^2 values for the comparison of cover estimates from spatial models to field test data that were set aside a priori and thus not used to parameterize the models.**

RAP is Rangeland Analysis Platform, and RCMAP is Rangeland Condition Monitoring Assessment and Projection.

Spatial model type, Data source	Cover type	Year 2016	2017	2018	2020
Field-based,					
Empirical Bayesian Kriging Regression	Annual Herbaceous	0.52	0.24	0.30	0.03
	Perennial Herbaceous	0.49	0.38	0.32	0.03
	Bareground	0.53	0.30	0.30	0.04
	Shrub	0.20	0.02	0.00	0.00
	Exotic Annual Grass	0.53	0.24	0.29	-
Satellite-based,					
RAP (Version 2)	Annual Herbaceous	0.36	0.31	0.54	0.26
	Perennial Herbaceous	0.18	0.46	0.23	0.16
	Bareground	0.20	0.42	0.40	0.29
	Shrub	0.08	0.03	0.02	0.02
RCMAP (Version 2)	Annual Herbaceous	0.12	0.01	0.12	0.10
	Perennial Herbaceous	0.03	0.16	0.05	0.00
	Bareground	0.00	0.01	0.16	0.19
	Shrub	0.01	0.05	0.00	0.03
Fractional Estimate USGS	Exotic Annual Grass	0.16	0.08	0.19	-
	Annual Herbaceous	-	-	-	0.00
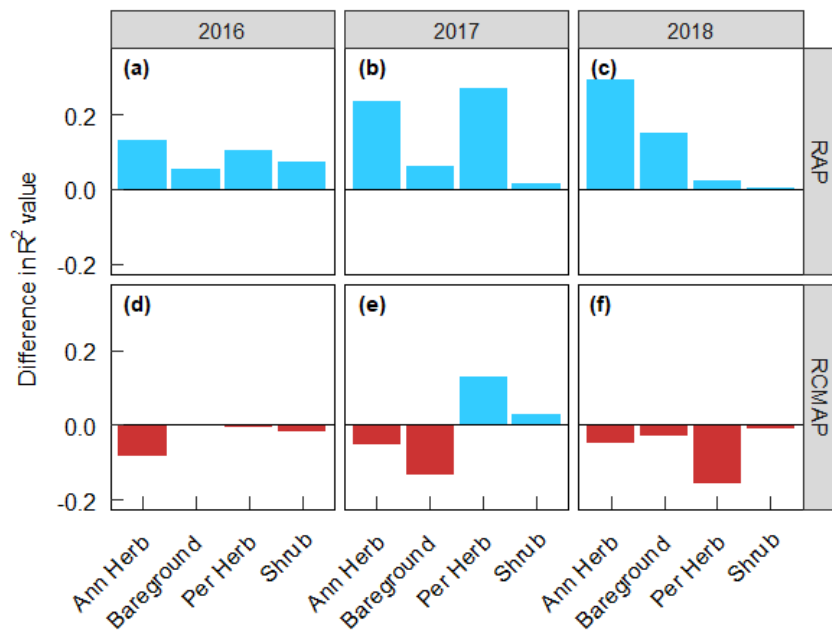
Figure 3.3 **Differences in r² values for vegetation cover between the original and updated versions of Rangeland Analysis Platform (RAP) or Rangeland Condition Monitoring Assessment and Projection (RCMAP) in 2016 (a and d), 2017 (b and e), and 2018 (c and f).**

Blue and red indicate an improvement or reduction in accuracy. "Ann Herb" is annual herbaceous cover, "Per Herb" is perennial herbaceous cover.

<u>Map agreement between field-based and satellite-derived models at different scales</u>

Standard deviations and especially relative standard errors (RSE) of the difference between satellite- and field-derived model estimates became closer to zero with increased size of polygons (and, thus, number of pixels) for which the comparisons were made, especially in the RAP and USGS fractional cover estimates of annual grasses (Figs. 4-6). Variability (given by standard deviations and RSE) in differences between RCMAP and field-based maps did not consistently decrease with greater scale and was extremely high at some scales, particularly in 2016. These high RSE values resulted in many cases from

mean cover differences being close to zero (numerator) but having high variability between samples (denominator).

In many combinations of year and cover type, RSE decreased most as the sample radii increased to ~2-3 km (Fig. 4-6). Exceptions included RAP estimates of annual herbaceous cover in 2018 and all RCMAP estimates in 2016 except shrub cover (Figs. 4, 5). RAP estimates of plant cover were ~5-10 percentage points (i.e. difference between percentages) greater compared to field-based model maps, whereas estimates of bareground progressively ranged from 20 (in 2016) to 5 percentage points (in 2020) lower than field-based model maps (Fig. 4). RCMAP estimates of plant cover were initially (in 2016) on average very similar to field-based estimates of herb cover and bare soil and ~6 percentage points different for shrubs, but the differences increased in subsequent years to ~12 percentage points greater for annual herbs, shrubs, and bare soil, and ~15 percentage points less for perennial herbs (Fig. 5). USGS-fractional-EAG estimates of annual grasses or herbs were 10-15 percentage points greater than field model estimates (Fig. 6).
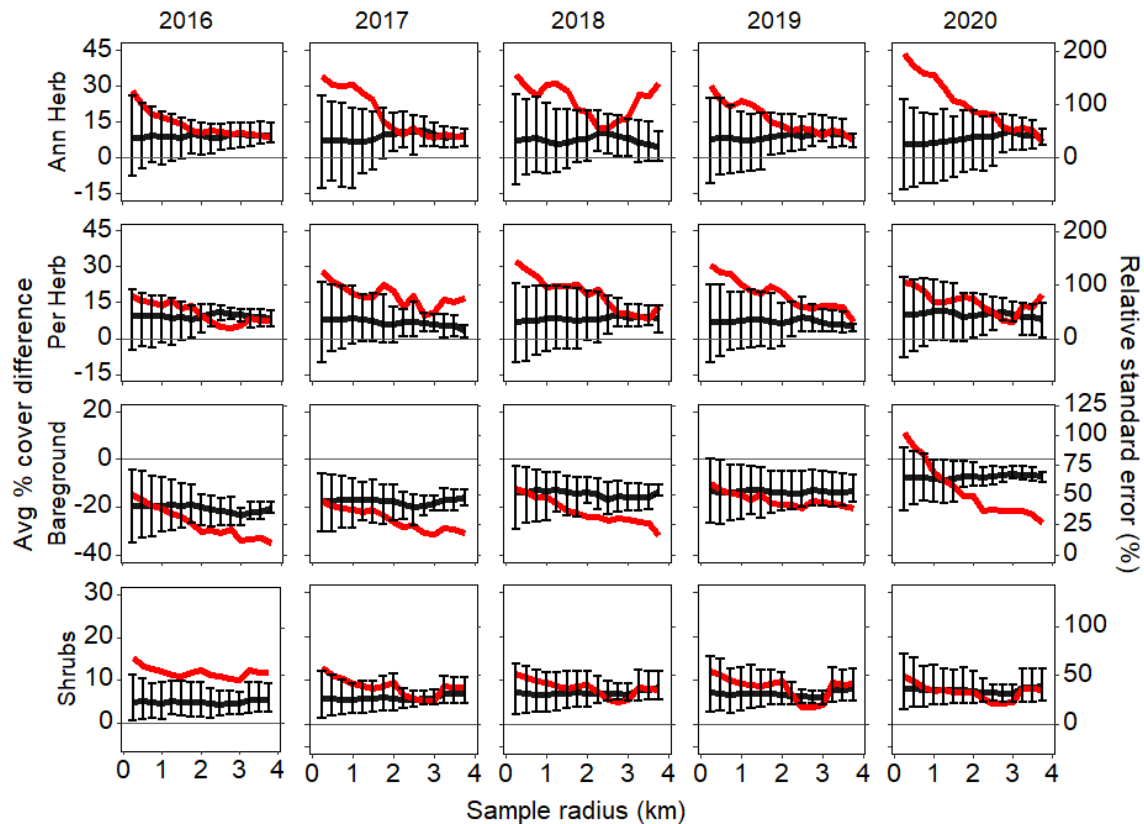
Figure 3.4   Mean ± 1 SD difference in vegetation cover as Rangeland Analysis Platform (RAP) cover minus field-based modelled cover (black), and relative standard error (red)., across a gradient of sample-area sizes.

Each row of panels is a functional group, from top-to-bottom: annual herbaceous (Ann Herb), perennial herbaceous (Per Herb), bareground, and shrubs. Each column is a sampling year, from 2016 to 2020.

Figure 3.5   Mean ± 1 SD difference in vegetation cover as Rangeland Condition Monitoring Assessment and Projection (RCMAP) cover minus field-based modelled cover (black), and relative standard error (red), across a gradient of sample-area.

Each row of panels is a functional group, from top-to-bottom: annual herbaceous (Ann Herb), perennial herbaceous (Per Herb), bareground, and shrubs. Each column is a sampling year, from 2016 to 2020. Bareground RSE in 2016 for sample areas with 0.25 km radiuses was >20,000% owing to a mean difference near zero but high variation (not shown).
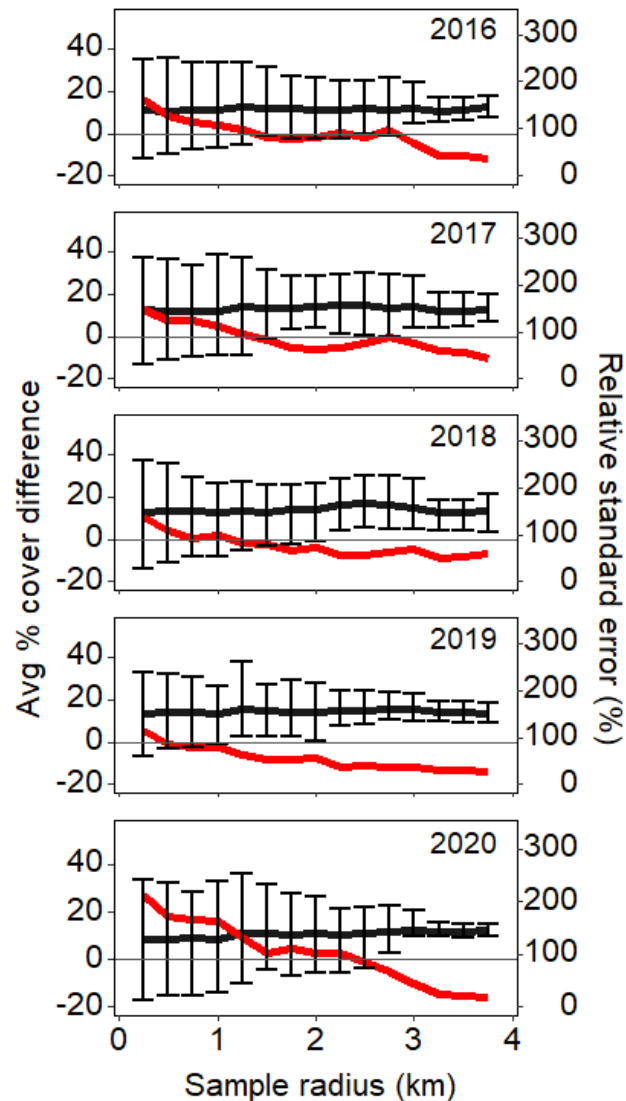
Figure 3.6   **Mean ± 1 SD difference in exotic annual grass cover (or annual herbaceous in 2020) as the USGS fractional cover minus field-based modelled cover (black), and relative standard error (red), across a gradient of sample-area sizes.**

Landscape heterogeneity and map agreement

Whether and how pasture-level cover differences between the satellite- and field-based models related to landscape variables depended on the identity of plant type and satellite-based model (Figs. 7-9). There was not enough variance in RCMAP shrub cover map differences to fit a landscape heterogeneity model. Marginal pseudo-r^2 values (variance described by fixed effects only) for the linear mixed models describing the

difference between RAP and field-based map vegetation cover were 0.065, 0.101, 0.364, and 0.375 for annual herbaceous, perennial herbaceous, bareground, and shrub cover, respectively. Marginal pseudo-r^2 values for the linear mixed models describing the difference between RCMAP and field-based map vegetation cover were 0.40, 0.35, and 0.40 for annual herbaceous, perennial herbaceous, and bareground, respectively. The marginal pseudo-r^2 value for the linear mixed models describing the difference between USGS fractional cover estimates and field-based map vegetation cover was 0.16 for exotic annual grass cover (annual herbaceous in 2020).
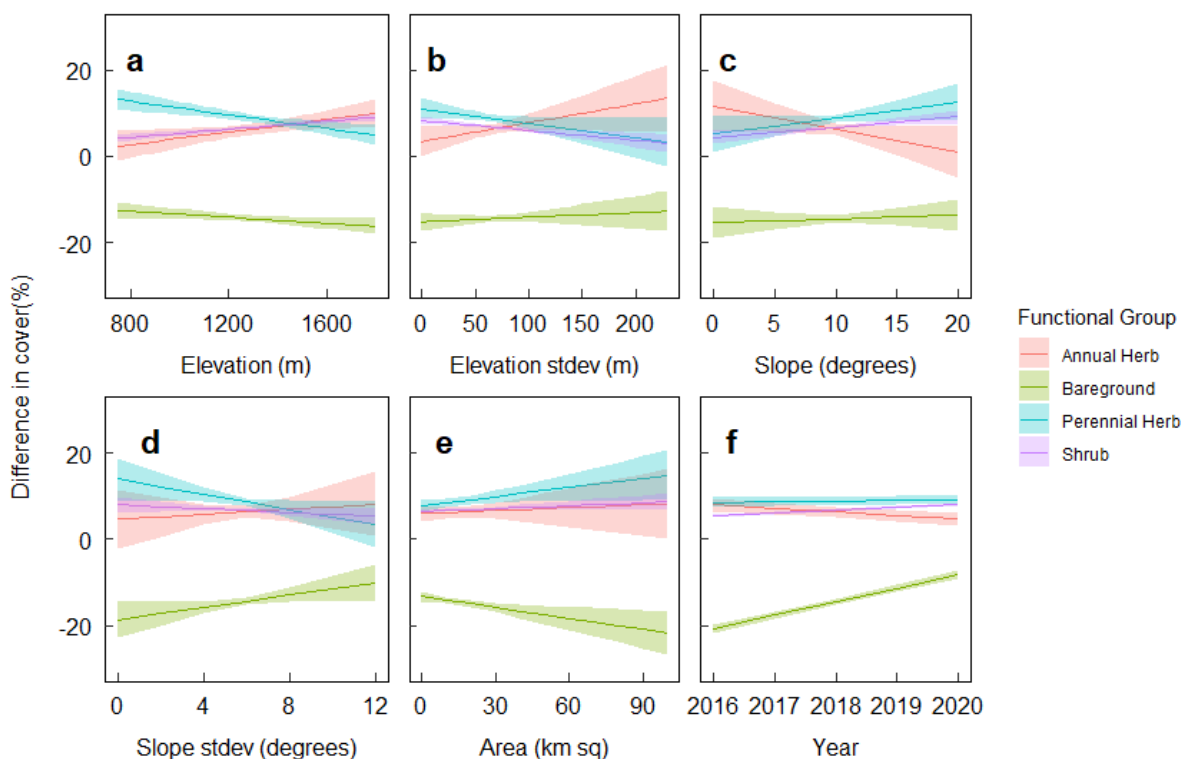
Figure 3.7   Linear-mixed modelled relationships of differences in cover as the Rangeland Analysis Platform (RAP) cover minus field-based modeled cover (Y) to landscape variables (X), using pastures as the unit of analysis.

Variables for each pasture included mean and standard deviation (stdev) of elevation or
slope, pasture size and year. Lines are average marginal effects and shaded ribbons are
95% confidence intervals.
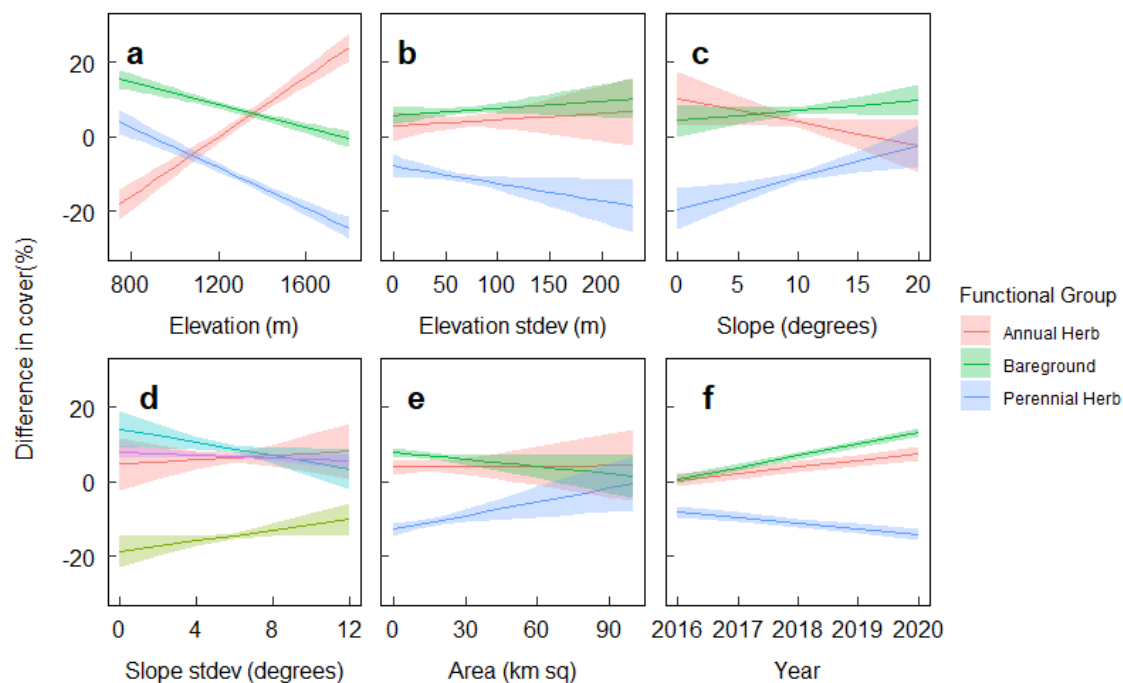
**Figure 3.8   Linear-mixed modelled relationships of differences in cover as
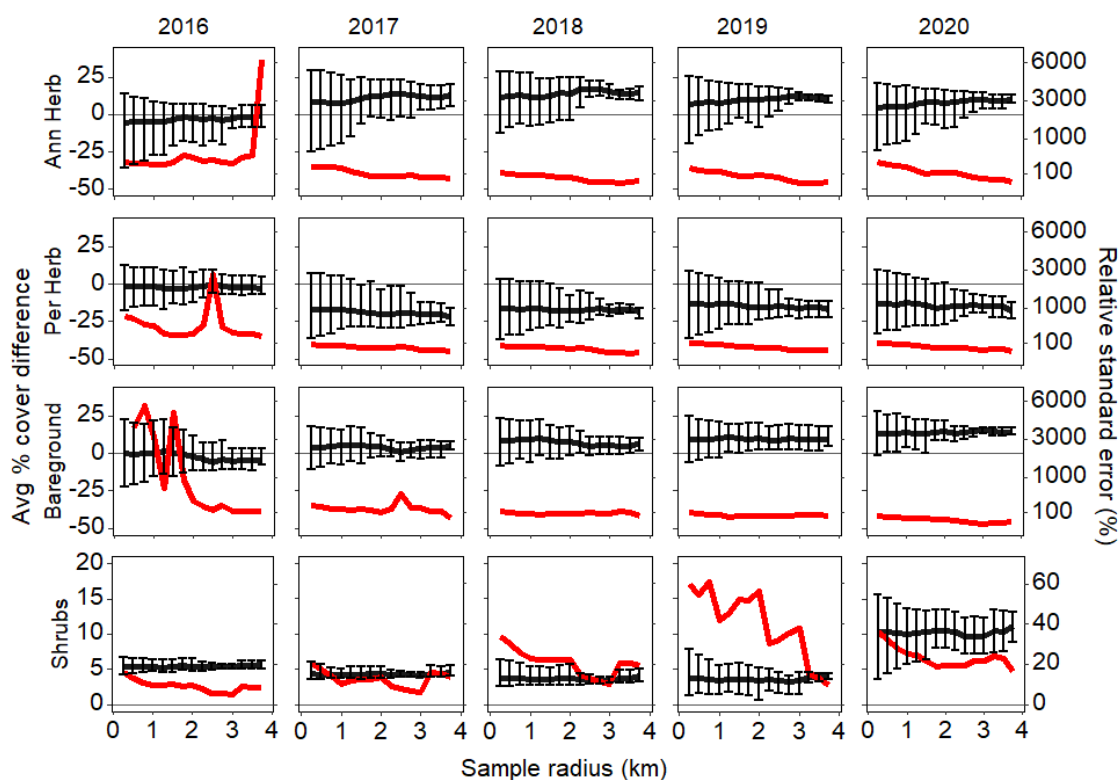Rangeland Condition Monitoring Assessment and Projection (RCMAP) cover
minus field-based modelled cover (Y) landscape variables (X), using pastures as the
unit of analysis.**

Variables for each pasture included mean and standard deviation (stdev) of elevation or
slope, pasture size and year. Lines are average marginal effects and shaded ribbons are
95% confidence intervals. Relationships for shrubs are not shown because there was not
enough variance in shrub cover differences to assess landscape variability effects on
model agreement.
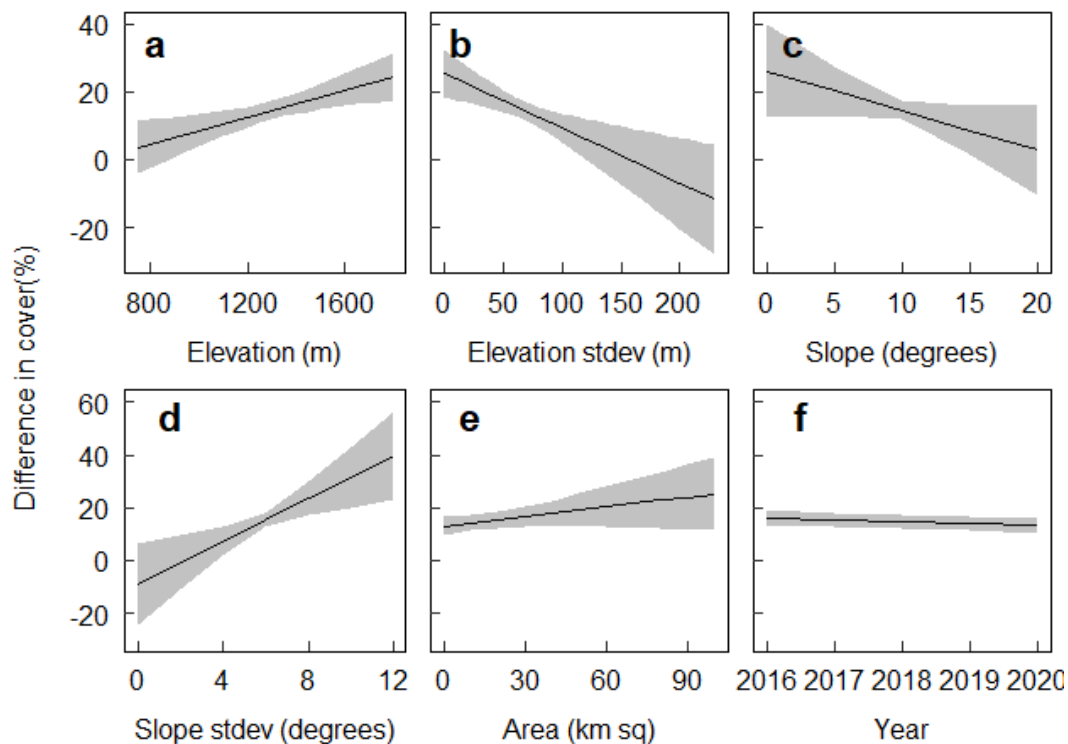
Figure 3.9   Linear-mixed modelled relationships of differences in exotic annual grass (annual herbs for 2020) cover as USGS fractional cover minus field-based modelled cover (Y) to landscape variables (X), using pastures as the unit of analysis.

Variables for each pasture included mean and standard deviation (stdev) of elevation or slope, pasture size and year. Lines are average marginal effects and shaded ribbons are 95% confidence intervals.

Model differences for annual herbs were positively related to elevation for all models, increasing from 2 to 10 percentage points for RAP (p = 0.02) and from 4 to 25 percentage points for USGS fractional estimates (p = 0.003) as elevation increased from 750 to 1800 m elevation (Figs. 7, 9), whereas the differences changed strongly in sign and magnitude from -18 to +24 percentage points across these elevations for RCMAP (p <0.001, Fig. 8). Model differences in annual herb cover showed inconsistent responses to increased standard deviation in elevation, with RAP and RCMAP predicting slight increases in annual herb cover as standard deviations increased (<10% change as standard

deviations increased from 0 to 200 m) and USGS fractional estimates predicting strong decreases in exotic annual grass cover (~20% as standard deviations increased from 0 to 200 m). Slope (average and standard deviation) had no effect on annual herb cover map differences for RAP and RCMAP ($p>0.05$) but slope standard deviation was positively related to annual herb differences for USGS fractional estimates; differences increased and changed sign from -9 to 40 percentage points as standard deviation of slope increased from 0 to 12 degrees ($p = 0.003$, Fig. 9). Pasture size was not related to annual herb cover differences ($p > 0.05$ for all comparisons).

Model differences for perennial herbs were negatively related to average elevation and elevation standard deviation and sometimes changed sign across elevational ranges. Model differences decreased from 13 to 5 percentage points for RAP ($p < 0.001$) and from 4 to -24 percentage points for RCMAP ($p < 0.001$) as elevation increased from 750 to 1800 m and from 11 to 3 percentage points for RAP ($p = 0.05$) and from -9 to -18 percentage points for RCMAP ($p = 0.03$) as standard deviation in elevation increased from 0 to 230 m. Model differences for perennial herb cover decreased with increasing slope variability: from 14 to 3 percentage points for RAP ($p = 0.04$) and from 0 to 22 percentage points for RCMAP ($p < 0.0001$) as standard deviation in slope increased from 0 to 12 degrees (Fig. 7,8). Perennial herb model differences were unrelated to average slope for RAP ($p = 0.09$) but increased from -20 to -2 percentage points as slope increased from 0 to 20 degrees from RCMAP ($p = 0.002$). Model differences for perennial herbs increased with larger pasture size, from 8 to 15 percentage points for RAP ($p = 0.04$) and from -13 to near parity (< -1 percentage point) for RCMAP ($p = 0.005$) as pasture size increased from 0 to 100 km^2 (Fig. 7,8).

Model differences in bareground cover were negatively related to average elevation but not with standard deviation in elevation. Model differences decreased from -12 to -16 percentage points for RAP (p = 0.05) and from 15 to near parity (< -1 percentage point) for RCMAP (p = 0.05) as elevation increased from 750 to 1800 m (Fig. 7 and 8). Model differences for RAP increased from -19 to -10 percentage points as slope standard deviation increased from 0 to 12 degrees, but there were no other relationships found between slope and bareground model differences (p > 0.05 for all other comparisons). Model differences of bareground cover for RAP decreased with larger pasture area from -13 to -22 percentage points (p = 0.003) and from 8 to 1 percentage point for RCMAP (p=0.06) as pasture size increased from 0 to 100 km^2 (Fig. 7,8).

Model differences in shrub cover for RAP increased from 4 to 9 percentage points as average elevation increased from 750 m to 1800 m (p < 0.001) and decreased from 8 to 3 percentage points as elevation standard deviation increased from 0 to 230 m (p < 0.001) (Fig 7) and decreased estimated for RAP shrub cover by 2.3% (p < 0.001) per 100 m increase in standard deviation in elevation (Fig. 7 and 8). Model difference in shrub cover for RAP increased from 4 to 9 percentage points as average slope increased from 0 to 20 degrees (p = 0.002) but slope standard deviation had no effect on shrub cover differences (p = 0.17) (Fig. 7). Model differences in shrub cover for RAP also increased from 6 to 9 percentage points as pasture size increased from 0 to 100 km^2 (p = 0.04) (Fig. 7).

RAP map agreement for perennial herbaceous cover did not change over time (p = 0.40). RAP map estimate differences with field-based maps for bareground and annual herbaceous cover progressively became closer to zero over the five years of analysis. For

bareground, RAP estimates increased compared with field-based maps from -20% to 8 percentage points between 2016 and 2020 ($p < 0.001$) and for annual herbaceous cover RAP estimates decreased 8 to 4 percentage point during these years ($p < 0.001$, Fig. 7). Shrub cover overestimation by RAP maps increased from 6 to 8 percentage points between 2016 and 2020 ($p < 0.001$, Fig. 7). RCMAP map estimate differences with field-based maps diverged from zero for all functional groups over the five years of analysis. RCMAP map differences for annual herbaceous cover increased from near parity to 8 percentage points in 2020, for perennial herbaceous from -8 to 14 percentage points, and for bareground from 1 to 13 percentage points between 2016 and 2020 ($p < 0.001$ for all comparisons, Fig. 8). USGS fractional estimate differences showed a slight trend towards parity over time with cover differences decreasing from 18 to 15 percentage points between 2016 and 2020 ($p = 0.004$).

Discussion

Our study addressed key questions for applying spatial vegetation models derived from satellite data to ecological and land-management problems with a focus on the most basic and commonly used parameter, plant-cover. Our analysis revealed that determining accuracy of spatial vegetation models derived from satellite data such as Landsat is not trivial, because field data must be upscaled in order to create a fair comparison of the data sources, and, thus, error is introduced into the benchmark needed for estimating vegetation model accuracy. We found that both accuracy and model agreement between satellite-derived maps and benchmark field-based maps was highly variable and varied with plant cover type, model versioning, scale, and topographic heterogeneity. Thus, accuracy and model agreement are dynamic and contextual to the user's application in

ways that cannot be satisfied with a singular estimation of error or accuracy of a spatial vegetation model.

Accuracy

Only up to about half of the variance in our benchmark model of vegetation cover derived from the intensive field sampling could be accounted for in our test assessment of its accuracy, meaning there was considerable imperfection in the benchmark data we used to evaluate the satellite-derived models. In some cases, RAP ver. 2 had greater accuracy than field-based models. Ground observers can detect fine-scale characteristics unobservable to a satellite, but variation between observers can add additional uncertainty to field data (e.g. Spanhove et al. 2012). Furthermore, in highly heterogeneous areas, a $6m^2$ area may not be representative of a $900m^2$ area (when comparing field to pixel data) and vice versa. A prior study in burned and treated sagebrush steppe indicated that between 6 and 9 $3m^2$ GPI quadrats were generally sufficient to represent a 1 ha area (Pilliod and Arkle 2013), so we might expect 2 GPI quadrats to represent a 0.09 ha area (the area of a 30m pixel) reasonably well on average. However, future studies could compare more GPI quadrats per pixel to assess whether there is a threshold number of subsamples needed to obtain greater concordance. All maps predicted annual or perennial herb cover or bare ground cover with much greater accuracy than shrub cover. Annual herbs typically have rapid initial colonization of burned and other disturbed areas, and many perennial bunchgrasses (comprising the dominant component of the perennial herbaceous community) can resprout quickly, but shrubs such as big sagebrush cannot resprout and shrubs that can resprout are slower to regenerate (Davies et al. 2012). As a result, shrub recovery is typically very patchy (Germino et al. 2018), which often requires

high-resolution aerial or satellite imagery to capture (e.g. 1 m^2, Sant et al. 2014, Rasanen

& Virtanen 2019). Consider that a 2x3 m photo area with two individual shrubs could

contain > 70% shrub cover, while a 30 x 30 m pixel could almost never have more than

5% in a recently burned area and most often will have <1%. RAP and RCMAP classify

cover in terms of whole percentage points but at the landscape level, big sagebrush (the

dominant shrub) cover may be <1% for several years post-fire (Porensky et al. 2018,

Applestein & Germino 2021). Also, a large range of seedling densities can occur in pixels

that have cover ranging from 0-1%, and the differences could determine long-term

population extirpation or sustained growth (Shriver et al. 2019). Thus, remote-sensing

map products display spatial coarseness relative to the grain of shrub patchiness and the

establishment processes relevant to postburn recovery across the landscape.

All maps, including the field-based maps (to a lesser extent), suffered from a

"false moderating effect" (Applestein & Germino 2021) in which cover was

overestimated where field-estimates of cover were low, and underestimated where cover

was relatively high. This effect is attributable to the "modifiable areal unit problem"

(MAUP) because data from point locations deviating significantly from the surrounding

neighborhood are less evident as the data are aggregated with neighboring locations

(Fotheringham & Wong 1991, Dark & Brom 2007). For land management

considerations, the consequences of overestimation of low abundances are often much

greater than underestimation of high abundances. Decisions related to land management

are frequently triggered by lower-end thresholds; for instance, application of an herbicide

where exotic plants are beginning to invade, or additional seeding if a desirable

functional group has low cover (Pyke et al. 2002, Briske et al. 2006). Therefore, more

intensive field monitoring may be needed in situations where low cover of a functional group is expected and knowing that cover with a high degree of precision is needed for management decisions. Indeed, a previous analysis of sample size on the Soda wildfire showed that when cover of exotic annual grass or perennial bunchgrass was low, more samples were needed to reduce variance to an acceptable level of precision for each respective cover type (Applestein et al. 2018).

Map agreement across scale

Our point accuracy assessments were a conservative estimate of accuracy because our test data was much finer scale than our map data. Therefore, we also assessed map agreement between satellite and field-derived maps as both were scaled-up to larger and larger units. Sagebrush-steppe rangelands, particularly burned areas, are examples of ecosystems where small differences in landform (and thus resulting microclimates) can result in important differences in species composition across a landscape (Passey et al. 1982, Mitchell et al. 2017). Theoretically, when plant abundances are aggregated over increasingly larger spatial scales, we would expect the influence of microsite to decline and thus, more agreement between different methods of mapping (satellite-derived or field-based models). Such a pattern would suggest that functional group cover can be considered a "type I" metric as defined by Wu (et al. 2002): a metric that has a predictable response to changing scale (as opposed to a staircase like or erratic response).

Variance in map agreement generally decreased with greater aggregation of pixels (larger scale), but some idiosyncrasies in scaling relationships were evident. Differences between RCMAP and field-based maps in the first year after fire (2016) showed seemingly random "spikes" in sample error at a variety of different scales and RCMAP

overestimation of shrub cover increased in later years (2019 and 2020). This finding extends the analysis of a smaller study focused on sagebrush cover assessment of a version 1 of RCMAP, where commission error was much more frequent several years after fire than it was initially (Applestein & Germino 2021). It suggests that as vegetation recovers post-fire, RCMAP may misclassify other functional groups as shrub or sagebrush cover. Overall, RAP and the USGS fractional estimates showed more consistent and predictable scaling effects when compared with field-based maps than did RCMAP.

Map agreement across heterogeneous landscapes

Topographic heterogeneity (in elevation and slope) can introduce additional noise into remote-sensing measurements, as well as shape plant community distributions (Myneni et al. 1995, Jin et al. 2008). We therefore asked if topographic metrics could help us explain variance in differences between field-based and remotely sensed maps. We did find some consistent trends where the remote-sensing maps tended to estimate annual herbaceous cover as higher and perennial herbaceous cover as lower with greater topographic heterogeneity (higher elevation and more variation in elevation and slope across a pasture) when compared with field-based maps. This suggests that in higher elevation and more topographically diverse areas of the landscape additional field plots may be needed for monitoring annual herbaceous cover, while more plots may be needed in lower elevation, less topographically diverse areas when monitoring perennial herbaceous cover. This finding largely agrees with a previous study considering field sample size for annual and perennial grasses (Applestein et al. 2018).

Conclusions

For some vegetation cover variables and certain models, satellite-derived maps can have an accuracy that rivals field-based maps in post-fire landscapes. However, care and supplementary field data are recommended when greater precision is needed, such as determining whether to undertake a management action based on threshold cover of vegetation or when high or low amounts of the vegetation are involved (e.g., incipient invasions). Rather than reliance on either satellite or field data, combining them may help overcome their tradeoffs and may most efficiently result in the most accurate maps (Barnard et al. 2019). Applications of spatial models of vegetation are best guided by error estimates, and the data presented here suggest that the tendency of accuracy or error to be communicated with a singular term (e.g. 6% accurate) will often be inadequate. Maps of model uncertainty are sometimes provided with spatial models of vegetation, which are useful, but they do not necessarily capture the error associated with match to ground conditions. We propose that providing a suite of accuracy estimates for representative functional group and environmental contexts with each model will provide end users with a starting point from which to gauge how model or map error relates to their application.

REFERENCES

Abatzoglou, J.T., and C.A. Kolden. 2011. Climate change in Western US deserts: Potential for increased wildfire and invasive annual grasses. Rangeland Ecology and Management 64(5): 471-478.

Adeyeri, O.E., F.O. Akinluyi, and K.A. Ishola. 2017. Spatio-temporal trend of vegetation cover over Abuja using Landsat datasets. International Journal Environmental Research 3(3) 3084-3100.

Adler, P.B., J. HilleRisLambers, and J.M. Levine. 2009. Weak effect of climate variability on coexistence in a sagebrush-steppe community. Ecology 90(12): 3303-3312.

Allred, B.W., Bestelmeyer, B.T., Boyd, C.S., Brown, C., Davies, K.W., Duniway, M.C., Ellsworth, L.M., T.A. Erickson, S.D. Fuhlendorf, T.V. Griffiths, V. Jansen, M.O. Jones, J. Karl, A. Knight, J.D. Maestas, J.J. Maynard, S.E. McCord, D.E. Naugle, H.D. Starns, D. Twidwell and D.R. Uden. 2021. Improving Landsat predictions of rangeland fractional cover with multitask learning and uncertainty. Methods in Ecology and Evolution, 12(5): 841-849. https://doi.org/10.1111/2041-210X.13564

Anderson, J.E., and R.S. Inouye. 2001. Landscape-scale changes in plant species abundance and biodiversity of a sagebrush-steppe over 45 years. Ecological Monographs 71(4): 531-556.

Anderson, J.E., and K.E. Holte. 1981. Vegetation development over 25 years without grazing on sagebrush-dominated rangeland in southeastern Idaho. Rangeland Ecology and Management 34(1):25-29.

Applestein, C., M.J. Germino, D.S. Pilliod, M.R. Fisk, and R.S. Arkle. 2018. Appropriate sample sizes for monitoring burned pastures in sagebrush-steppe: how many plots are enough, and can one size fit all? Rangeland Ecology and Management 71(6): 721-726.

Applestein, C. and M.J. Germino. 2021. Detecting shrub recovery in sagebrush steppe: comparing Landsat-derived maps with field data on historical wildfires. Fire Ecology, 17(1): 1-1. https://doi.org/10.1186/s42408-021-00091-7

Ashley, M.V. 2010. Plant parentage, pollination, and dispersal: how DNA microsatellites have altered the landscape. CRC Crit Rev Plant Sci 29(3):148-61. https://doi.org/10.1080/07352689.2010.481167

Barnard, D.M, M.J. Germino, D.S. Pilliod, R.S. Arkle, C. Applestein, B.E. Davidson, and M.R. Fisk. 2019. Cannot see the random forest for the decision trees: selecting predictive models for restoration ecology. Restoration Ecology, 27(5): 1053-1063. https://doi.org/10.1111/rec.12938

Beck, J.L., J.W. Connelly, and C.L. Wambolt. 2012. Consequences of treating Wyoming big sagebrush to enhance wildlife habitats. Rangeland Ecology and Management 65(5):444-55. https://doi.org/10.2111/REM-D-10-00123.1

Beever E.A., D. Simberloff, S.L. Crowley, R. Al-Chokhachy, H.A. Jackson, S.L. Petersen. 2019. Social–ecological mismatches create conservation challenges in introduced species management. Frontiers in Ecology and the Environment 17(2):117-125. https://doi.org/10.1002/fee.2000

Bohrer, G., G.G. Katul, R. Nathan, R.L. Walko, and R. Avissar. 2008. Effects of canopy heterogeneity, seed abscission and inertia on wind-driven dispersal kernels of tree seeds. Journal of Ecology 96(4): 569-580. https://doi.org/10.1111/j.1365-2745.2008.01368.x

Booth, D.T., S.E. Cox, and R.D. Berryman. 2006. Point sampling digital imagery with 'SamplePoint'. Environmental Monitoring and Assessment, 123(1): 97-108. https://doi.org/10.1007/s10661-005-9164-7

Boswell, A., S. Petersen, B. Roundy, R. Jensen, D. Summers, and A. Hulet. 2017. Rangeland monitoring using remote sensing: comparison of cover estimates from field measurements and image analysis. AIMS Environmental Science, 4(1): 1-6. https://doi.org/10.3934/environsci.2017.1.1

Borchert, M., M. Johnson, D. S. Schreiner, and S.B. Vander Wall. 2003. Early postfire seed dispersal, seedling establishment and seedling mortality of Pinus coulteri (D. Don) in central coastal California, USA. Plant Ecology 168(2):207–20. https://doi.org/10.1023/A:1024447811238

Boyd, C.S., and K.W. Davies. 2010. Shrub microsite influences post-fire perennial grass establishment. Rangeland Ecology and Management 63(2):248-252.

Brabec, M.M., M.J. Germino, and B.A. Richardson. 2017. Climate adaption and post-fire restoration of a foundational perennial in cold desert: insights from intraspecific variation in response to weather. Journal Applied Ecology 54(1): 293-302.

Bradley, B.A., J.M. Allen, M.W. O'Neill, R.D. Wallace, C.T. Bargeron, J.A. Richburg, and K. Stinson. 2018. Invasive species risk assessments need more consistent spatial abundance data. Ecosphere, 9(7): e02302. https://doi.org/10.1002/ecs2.2302

Bradley, B.A., C.A. Curtis, and J.C. Chambers. 2016. Bromus response to climate and projected changes with climate change. Pages 257-274 in M.J. Germino, J.C. Chambers, C.S. Brown, editors. Exotic brome-grasses in arid and semiarid ecosystems of the western. Springer International Publishing, Cham, Switzerland.

Briske, D.D., S.D. Fuhlendorf, and F.E. Smeins. 2006. A unified framework for assessment and application of ecological thresholds. Rangeland Ecology & Management, 59(3): 225-236. https://doi.org/10.2111/05-115R.1

Brooks, S.P., and A. Gelman. 1998. General methods for monitoring convergence of iterative simulations. Journal of Computational and Graphical Statistics 7(4):434-455.

Brudvig, L.A., R.S. Barak, J.T. Bauer, T.T. Caughlin, D.C. Laughlin, L. Larios, J.W. Matthews, K.L. Stuble, N.E. Turley, and C.R. Zirbel. 2017. Interpreting variation to advance predictive restoration science. Journal of Applied Ecology 54(4): 1018-1027.

Bullock, J.M., and R.T. Clarke. 2000. Long distance seed dispersal by wind: Measuring and modelling the tail of the curve. Oecologia 124: 506-521.

Bürkner, P.C. 2017. brms: An R package for Bayesian multilevel models using Stan. Journal of Statistical Software 80(1): 1-28.

Cain, M.L., B.G. Milligan, and A.E. Strand. 2002. Long-distance seed dispersal in plant populations. American Journal of Botany 87(9):1217-27. https://doi.org/10.2307/2656714

Caughlin, T.T., J.M. Ferguson, J.W. Lichstein, S. Bunyavejchewin, and D.J. Levey. 2014. The importance of long-distance seed dispersal for the demography and distribution of a canopy tree species. Ecology 95(954): 952–62. https://doi.org/10.1890/13-0580.1

Caughlin, T.T., S. Elliott, and J.W. Lichstein. 2016. When does seed limitation matter for scaling up reforestation from patches to landscapes? Ecological Applications 26(8):2439-50. https://doi.org/10.1002/eap.1410

Chambers, J.C., R.F. Miller, D.I. Board, D.A. Pyke, B.A. Roundy, J.B. Grace, E.W. Schupp, and R.J. Tausch. 2014. Resilience and resistance of sagebrush ecosystems: implications for state and transition models and management treatments. Rangeland Ecology and Management 67(5): 440-454.

Chu, C., and P.B. Adler. 2015. Large niche differences emerge at the recruitment stage to stabilize grassland coexistence. Ecological Monographs 85(3):373-392.

Clark, J.S., C. Fastie, G. Hurtt, S.T. Jackson, C. Johnson, G. A. King, M. Lewis, J. Lynch, S. Pacala, and C. Prentice, and E.W. Schupp. 1998. Reid's paradox of rapid plant migration: dispersal theory and interpretation of paleoecological records. BioScience 48(1):13-24.

Clark, J.S., M. Silman, R. Kern, E. Macklin, and J. HilleRisLambers. 1999. Seed dispersal near and far: patterns across temperate and tropical forests. Ecology 80(5):1475–94. https://doi.org/10.1890/0012-9658(1999)080[1475:SDNAFP]2.0.CO;2

Cohen, J. 1960. A coefficient of agreement for nominal scales. Educational and Psychological Measures 20: 37-46

114

Corbin, J.D., and K.D. Holl. 2012. Applied nucleation as a forest restoration strategy.
Forest Ecology and Management 265: 37-46.
https://doi.org/10.1016/j.foreco.2011.10.013

Costello, C.T. and W.J. Kenworthy. 2011. Twelve-year mapping and change analysis of
eelgrass (Zostera marina) areal abundance in Massachusetts (USA) identifies
statewide declines. Estuaries and Coasts, 34(2): 232-242.
https://doi.org/10.1007/s12237-010-9371-5

Cramer, W., A. Bondeau, F.I. Woodward, I.C. Prentice, R.A. Betts, V. Brovkin, P.M.
Cox, V. Fisher, J.A. Foley, A.D. Friend, C. Kucharik, M.R. Lomas, N.
Ramankutty, S. Sitch, D. Smith, A. White, and C. Young-Molling. 2001. Global
response of terrestrial ecosystem structure and function to CO2 and climate
change: Results from six dynamic global vegetation models. Global Change
Biology 7(4):357-373.

Dale, V.H., L.A. Joyce, S. McNulty, R.P. Neilson, M.P. Ayres, M.D. Flannigan, P.J.
Hanson, L.C. Irland, A.E. Lugo, C.J. Peterson, and D. Simberloff. 2001. Climate
change and forest disturbances: climate change can affect forests by altering the
frequency, intensity, duration, and timing of fire, drought, introduced species,
insect and pathogen outbreaks, hurricanes, windstorms, ice storms, or landslides.
BioScience 51(9): 723-734.

Dark, S.J. and D. Bram. 2007. The modifiable areal unit problem (MAUP) in physical
geography. Progress in Physical Geography, 31(5): 471-479.
https://doi.org/10.1177/0309133307083294

Dauer, J.T., D.A. Mortensen, and M.J. Vangessel. 2007. Temporal and spatial dynamics
of long-distance Conyza canadensis seed dispersal. Journal of Applied Ecology
44:105–14. https://doi.org/10.1111/j.1365-2664.2006.01256.x

Davies, G.M., J.D. Bakker, E. Dettweiler-Robinson, P.W. Dunwiddie, S.A. Hall, J.
Downs, and J. Evans. 2012. Trajectories of change in sagebrush steppe vegetation
communities in relation to multiple wildfires. Ecological Applications 22(5): 562-
577. https://doi.org/10.1890/10-2089.1

Devendra, D., N.J. Pastick, S. Parajuli, and B.K. Wylie. 2021. Fractional estimates of exotic annual grass cover in dryland ecosystems of western United States (2016 – 2019): U.S. Geological Survey data release, https://doi.org/10.5066/P9XT1BV2.

DiCristina, K., and M. Germino. 2006. Correlation of neighborhood relationships, carbon assimilation, and water status of sagebrush seedlings establishing after fire. Western American Naturalist 66(4): 441-450.

Dietze, M.C., A. Fox, L.M. Beck-Johnson, J.L. Betancourt, M.B. Hooten, C.S. Jarnevich, T.H. Keitt, M.A. Kenney, C.M. Laney, L.G. Larsen, and H.W. Loescher. 2018. Iterative near-term ecological forecasting: Needs, opportunities, and challenges. Proceedings of the National Academy of Science of the United States of America 115(7): 1424-1432.

Dilling, L., and M.C. Lemos. 2011. Creating usable science: Opportunities and constraints for climate knowledge use and their implications for science policy. Global Environmental Change 21(2):680-689.

DiVittorio, C.T., J.D. Corbin, and C.M. D'Antonio. 2007. Spatial and temporal patterns of seed dispersal: an important determinant of grassland invasion. Ecological Applications 17(2):311-6. https://doi.org/10.1890/06-0610

Donovan, L.A., and J.R. Ehleringer. 1991. Ecophysiological differences among juvenile and reproductive plants of several woody species. Oecologia 86:594-597.

Driese, K.L., and W.A. Reiners. 1997. Aerodynamic roughness parameters for semi-arid natural shrub communities of Wyoming, USA. Agricultural Forest Meteorology 88:1-4. https://doi.org/10.1016/S0168-1923(97)00055-5

Elmore, A.J., J.F. Mustard, and S.J. Manning. 2003. Regional patterns of plant community response to changes in water: Owens Valley, California. Ecological Applications 13 (2), 443–460. https://doi.org/10.1890/1051-0761(2003)013[0443:RPOPCR]2.0.CO;2

Enright, N.J., J.B. Fontaine, D.M. Bowman, R.A. Bradstock, and R.J. Williams. 2015. Interval squeeze: altered fire regimes and demographic responses interact to threaten woody species persistence as climate changes. Frontiers in Ecology and Environment 13(5):265-272.

Franzese, J., L. Ghermandi, and B. Donaldo. 2009. Post-fire shrub recruitment in a semi-arid grassland: the role of microsites. Journal of Vegetative Science 20(2):251-259.

Fernández-Manso, A., C. Quintano, and O. Fernández-Manso. 2011. Forecast of NDVI in coniferous areas using temporal ARIMA analysis and climatic data at a regional scale. International Journal of Remote Sensing 32(6):1595-1617.

Fotheringham, A.S., and D.W. Wong. 1991. The modifiable areal unit problem in multivariate statistical analysis. Environmental Planning 23(7): 1025–1044. https://doi.org/10.1068/a231025

Germino, M.J., D.M. Barnard, B.E. Davidson, R.S. Arkle, D.S. Pilliod, M.R. Fisk, and C. Applestein. 2018. Thresholds and hotspots for shrub restoration following a heterogeneous megafire. Landscape Ecology 33(7):1177–1194. https://doi.org/10.1007/s10980-018-0662-8

Germino, M.J., A.M. Moser, and A.R. Sands. 2019. Adaptive variation, including local adaptation, requires decades to become evident in common gardens. Ecological Applications 29(2).

Gill, N.S., T.J. Hoecker, and M.G. Turner MG. 2020. The propagule doesn't fall far from the tree, especially after short-interval, high-severity fire. Ecology 102(1); e03194. https://doi.org/10.1002/ecy.3194

Greene, D.F., and C. Calogeropoulos. 2002. Measuring and modelling seed dispersal of terrestrial plants. In Bullock JM, Kenward RE, Hails RS (eds). Dispersal ecology: the 42nd symposium of the British Ecological Society, Blackwell Science Ltd, Berlin, Germany, pp 3-23.

Griffiths, J.I., P.H. Warren, and D.Z. Childs. 2015. Multiple environmental changes interact to modify species dynamics and invasion rates. Oikos 124(4): 458-68.

Hammill, K.A., R.A. Bradstock, and W. Allaway. 1998. Post-fire seed dispersal and species re-establishment in proteaceous heath. Australian Journal Botany 46(4):407–219. https://doi.org/10.1071/BT96116

Hansen, M.C., and T.R. Loveland. 2012. A review of large area monitoring of land cover change using Landsat data. Remote Sensing of the Environment 122: 66–74. https://doi.org/10.1016/j.rse.2011.08.024.

Hardegree, S.P., J.M. Schneider, and C.A. Moffet. 2012. Weather variability and adaptive management for rangeland restoration. Rangelands 34(6): 53-57.

Harvey, P.H., R.K. Colwell, J.W. Silvertown, and R.M. May. 1983. Null models in ecology. Annual Review of Ecology, Evolution, and Systematics 14(1): 189-211.

Heydel F., S. Cunze, M. Bernhardt-Römermann, and O. Tackenberg. 2015. Seasonal synchronization of seed release phenology promotes long-distance seed dispersal by wind for tree species with medium wind dispersal potential. Journal of Vegetation Science 26(6):1090-1101. https://doi.org/10.1111/jvs.12305

Hilbe, J.M. 2011. Negative binomial regression. Cambridge University Press, New York.

Hill, J.P., C.J. Willson, and W.K. Smith. 2005. Enhanced photosynthesis and flower production in a sagebrush morphotype associated with animal burrows. Plant Ecology 177(1):1-12. https://doi.org/10.1007/s11258-005-2233-8

Holl, K.D. 1999. Factors Limiting Tropical Rain Forest Regeneration in Abandoned Pasture: Seed Rain, Seed Germination, Microclimate, and soil. Biotropica 31(2);229-242. https://doi.org/10.1111/j.1744-7429.1999.tb00135.x

Hoppes, W.G. 1988. Seedfall pattern of several species of bird-dispersed plants in an Illinois woodland. Ecology 69(2): 320-329. https://doi.org/10.2307/1940430

Houlahan, J.E., S.T. McKinney, T.M. Anderson, and B.J. McGill. 2017. The priority of prediction in ecological understanding. Oikos 126(1):1-7.

Irvine, K.M., W.J. Wright, E.K. Shanahan, and T.J. Rodhouse. 2019. Cohesive framework for modeling plant cover class data. Methods in Ecology and Evolution 10(10): 1749-1760.

James, J.J., R.L. Sheley, E.A. Leger, P.B. Adler, S.P. Hardegree, E.S. Gornish, and M.J. Rinella. 2019. Increased soil temperature and decreased precipitation during early life stages constrain grass seedling recruitment in cold desert restoration. Journal of Applied Ecology 56(12): 2609-2619.

Jacobs, J., J.D. Scianna, and S.R. Winslow. 2011. Big sagebrush establishment: US Department of Agriculture Natural Resources Conservation Service. Plant Materials Technical Note MT–68.

James, J.J., and T. Svejcar. 2010. Limitations to postfire seedling establishment: the role of seeding technology, water availability, and invasive plant abundance. Rangeland Ecology and Management 63(4):491–495. https://doi.org/10.2111/REM-D-09-00124.1

Jin, X.M., Y.K. Zhang, M.E. Schaepman, J.G. Clevers, Z. Su, J. Cheng, J. Jiang, J. van Genderen. 2008. Impact of elevation and aspect on the spatial distribution of vegetation in the Qilian mountain area with remote sensing data. In: XXIth ISPRS Congress, Beijing, 3 July 2008 - 11 July 2008. International Society of Photogrammetry Remote Sensing: 1385–1390. https://doi.org/10.5167/uzh-77426

Jones, H.P., P. C. Jones, E.B. Barbier, R.C. Blackburn, J.M.R. Benayas, K.D. Holl, M. McCrackin, P. Meli, D. Montoya, D.M. Mateos. 2018. Restoration and repair of Earth's damaged ecosystems. Proceedings of the Royal Society B 285: 2-8. https://doi.org/10.1098/rspb.2017.2577

Katul, G.G., A. Porporato, R. Nathan, M. Siqueira, M.B. Soons, D. Poggi, H.S. Horn, and S.A. Levin. 2005. Mechanistic analytical models for long-distance seed dispersal by wind. American Naturalist 166(3):368-81. https://doi.org/10.1086/432589

Keane, R.E., G.J. Cary, M.D. Flannigan, R.A. Parsons, I.D. Davies, K.J. King, C. Li, R.A. Bradstock, and M. Gill. 2013. Exploring the role of fire, succession, climate, and weather on landscape dynamics using comparative modeling. Ecological Modeling 266: 172-86.

Keeley, J.E., C.J. Fotheringham, and M. Baer-Keeley. 2005. Factors affecting plant diversity during post-fire recovery and succession of mediterranean-climate shrublands in California, USA. Diversity and Distributions 11(6):525-537.

Kim, J.B., B.K. Kerns B.K., R.J. Drapek, G.S. Pitts, and J.E. Halofsky. 2018. Simulating vegetation response to climate change in the Blue Mountains with MC2 dynamic global vegetation model. Climate Services 10: 20-32

Kleinhesselink, A.R., and P.B. Adler. 2018. The response of big sagebrush (*Artemisia tridentata*) to interannual climate variation changes across its range. Ecology 99(5): 1139-1149.

Krivoruchko, K. and A. Gribov. 2019. Evaluation of empirical Bayesian kriging. Spatial Statistics 32: 100368. https://doi.org/10.1016/j.spasta.2019.100368.

Kuhn, M. 2012. Variable importance using the caret package. http://citeseerx.ist.psu.edu/viewdoc/download?doi=10.1.1.168.1655&rep=rep1&type=pdf.

Lamberty, B.B., A.G. Bunn, and A.M. Thomson. 2012. Multi-year lags between forest browning and soil respiration at high northern latitudes. PLoS ONE 7(11): e50441.

Lazarus, B.E., M.J. Germino, and B.A. Richardson. 2019. Freezing resistance, safety margins, and survival vary among big sagebrush populations across the western United States. American Journal of Botany 106(7):922-934.

Lechner, A.M., Langford, W.T., Jones, S.D., Bekessy, S.A., Gordon, A., 2012. Investigating species–environment relationships at multiple scales: Differentiating between intrinsic scale and the modifiable areal unit problem. Ecological Complexity 11: 91–102. https://doi.org/10.1016/j.ecocom.2012.04.002

Leirfallom, S.B., R.E. Keane, D.F. Tomback, and S.Z. Dobrowski. 2015. The effects of seed source health on whitebark pine (Pinus albicaulis) regeneration density after wildfire. Canadian Journal of Forest Research 45(11):1597–606. https://doi.org/10.1139/cjfr-2015-0043

Lesica, P., S.V. Cooper, and G. Kudray. 2007. Recovery of big sagebrush following fire in southwest Montana. Rangeland Ecology and Management 60(3), 261-269.

Ludwig, J.A., G.N. Bastin, J.F. Wallace, T.R. McVicar. 2007. Assessing landscape health by scaling with remote sensing: when is it not enough? Landscape Ecology 22(2):163–169. https://doi.org/10.1007/s10980-006-9038-6.

Makowski, D., M.S. Ben-Shachar, S.A. Chen, and D. Lüdecke. 2019. Indices of effect existence and significance in the Bayesian framework. Frontiers in Psychology 10:2767. https://doi.org/10.3389/fpsyg.2019.02767

Mansour, K., O. Mutanga, T. Everson. 2012. Remote sensing based indicators of vegetation species for assessing rangeland degradation: opportunities and challenges. African Journal of Agricultural Research 7(22): 3261–3270. https://doi.org/10.5897/AJAR11.2316.

McIlroy, S.K. and D.J. Shinneman 2020. Post-fire aspen (Populus tremuloides) regeneration varies in response to winter precipitation across a regional climate gradient. Forest Ecology and Management 455: 117681.

McIver, J., and M. Brunson. 2014. Multisite evaluation of alternative sagebrush-steppe restoration treatments: the SageSTEP project. Rangeland Ecology and Management 67(5): 435-440.

McKenzie, D., Z.E. Gedalof, D.L. Peterson, and P. Mote. 2004. Climatic change, wildfire, and conservation. Conservation Biology 18(4): 890-902.

McNellie, M.J., I. Oliver, S. Ferrier, G. Newell, G. Manion, P. Griffioen, M. White, T. Koen, M. Somerville, and P. Gibbons. 2021. Extending vegetation site data and ensemble models to predict patterns of foliage cover and species richness for plant functional groups. Landscape Ecology 36(5): 1391–1407. https://doi.org/10.1007/s10980-021-01221-x.

Melgoza, G., R.S. Nowak, and R.J. Tausch. 1990. Soil water exploitation after fire: competition between Bromus tectorum (cheatgrass) and two native species. Oecologia 83:7–13.

Meng, R., P.E. Dennison, C. Huang, M.A. Moritz, and C. D'Antonio. 2015. Effects of fire severity and post-fire climate on short-term vegetation recovery of mixed-conifer and red fir forests in the Sierra Nevada Mountains of California. Remote Sensing of the Environment 171: 311-325.

McCune, B., and J.B. Grace. 2002. Analysis of ecological communities. MjM Software, Gleneden Beach, OR, USA 304 p

Miller, J.. 2005. Incorporating spatial dependence in predictive vegetation models: residual interpolation methods. Professional Geography 57(2): 169–184. https://doi.org/10.1111/j.0033-0124.2005.00470.x.

Miller, R.F., S.T. Knick, D.A. Pyke, C.W. Meinke, S.E. Hanser, M.J. Wisdom, and A.L. Hild. 2011. Characteristics of sagebrush habitats and limitations to long-term conservation. Greater sage-grouse: ecology and conservation of a landscape species and its habitats. Studies Avian in Biology 38:145-84.

Mkrtchyan, A. 2004. Spatial interpolation of field data on plant abundance. In Natural Forests in the Temperate Zone of Europe-Values and Utilisation. In: Proceedings of International Conference 2003 Oct, pp. 13–17.

Mitchell, R.M., J.D. Bakker, J.B. Vincent, and G.M. Davies. 2017. Relative importance of abiotic, biotic, and disturbance drivers of plant community structure in the sagebrush steppe. Ecological Applications 27(3): 756–768. https://doi.org/10.1002/eap.1479.

Monnahan, C.C., J.T. Thorson, and T.A. Branch. 2017. Faster estimation of Bayesian models in ecology using Hamiltonian Monte Carlo. Methods in Ecology and Evolution 8(3):339-48. https://doi.org/10.1111/2041-210X.12681

Mueggler, W. 1956. Is sagebrush seed residual in the soil of burns or is it wind- borne? Res. Note 35 Intermountain for. and Range Exp, pp.9. Upper Snake River Exp. Range, U.S.Sheep Exp. Sta., Dubois, Idaho

Myneni, R.B., S. Maggion, J. Iaquinta, J.L. Privette, N. Gobron, B. Pinty, D.S. Kimes, M.M. Verstraete, and D.L. Williams. 1995. Optical remote sensing of vegetation: modeling, caveats, and algorithms. Remote Sensing of the Environment 51(1): 169–188. https://doi.org/10.1016/0034-4257(94)00073-V.

Nathan, R., H.S. Horn, J. Chave, and S.A. Levin. 2009. Mechanistic models for tree seed dispersal by wind in dense forests and open landscapes. In Seed dispersal and frugivory: ecology, evolution and conservation. Levey, D.J., W.R. Silva, M. Galetti (eds). CABI New York pp 69-82.

Nathan, R., G.G. Katul, G. Bohrer, A. Kuparinen, M.B. Soons, S.E. Thompson, A. Trakhtenbrot, H.A. Horn. 2011. Mechanistic models of seed dispersal by wind. Theoretical Ecology 4:113–32. https://doi.org/10.1007/s12080-011-0115-3

Neeson, T.M., M.C. Ferris, M.W. Diebel, P.J. Doran, J.R.O. Hanley, and P.B. Mcintyre. 2015. Enhancing ecosystem restoration efficiency through spatial and temporal coordination. PNAS 112(19); 6236-5241. https://doi.org/10.1073/pnas.1423812112

Nelson, Z.J., P.J. Weisberg, and S.G. Kitchen. 2014. Influence of climate and environment on post-fire recovery of mountain big sagebrush. International Journal of Wildland Fire 23(1): 131-142.

Neubert, M.G., and H. Caswell. 2000. Demography and dispersal: calculation and sensitivity analysis of invasion speed for structured populations. Ecology 81(6):1613-28. https://doi.org/10.1890/0012-9658(2000)081[1613:DADCAS]2.0.CO;2

Nuttle, T., and J.W. Haefner. 2017. Seed Dispersal in Heterogeneous Environments: Bridging the Gap between Mechanistic Dispersal and Forest Dynamics Models. American Naturalist 165(3); 336-349.

O'Connor, R.C., M.J. Germino, D.M. Barnard, C.M. Andrews, J.B. Bradford, D.S. Pilliod, R.S. Arkle, and R.K. Shriver. 2020. Small-scale water deficits after wildfires create long-lasting ecological impacts. Environmental Research Letters 15(4): 044001.

Ogle, K., and J.F. Reynolds. 2004. Plant responses to precipitation in desert ecosystems: integrating functional types, pulses, thresholds, and delays. Oecologia 141(2): 282-294.

Ogle, K., J.J. Barber, G.A. Barron-Gafford, L.P. Bentley, J.M. Young, T.E. Huxman, M.E. Loik, and D.T. Tissue. 2015. Quantifying ecological memory in plant and ecosystem processes. Ecological Letters 18(3): 221-235.

Owens, M.K, and B.E. Norton. 1992. Interactions of grazing and plant protection on basin big sagebrush (*Artemisia tridentata ssp. tridentata*) seedling survival. Rangeland Ecology and Management 45(3):257-262.

Ozinga, W.A., J.H. Schaminée, R.M. Bekker, S. Bonn, P. Poschlod, O. Tackenberg, J. Bakker, and J.M. Groenendael. 2005. Predictability of plant species composition from environmental conditions is constrained by dispersal limitation. Oikos 108(3):555-61. https://doi.org/10.1111/j.0030-1299.2005.13632.x

Palma, A.C., and S.G. Laurance. 2015. A review of the use of direct seeding and seedling plantings in restoration: what do we know and where should we go? Applied Vegetation Science 18(4):561-8. https://doi.org/10.1111/avsc.12173

Passey, H.B., V.K. Hugie, E.W. Williams, D.E. Ball. 1982. Relationships between soil, plant community, and climate on rangelands of the Intermountain West. United States Department of Agriculture Economic Research Service Technical Bulletin 53:1689–1699.

Peeler, J.L., and E.A.H. Smithwick. 2020. Seed source pattern and terrain have scale-dependent effects on post-fire tree recovery. Landscape Ecology 35, 1945–1959. https://doi.org/10.1007/s10980-020-01071-z

Peppin, D., P.Z. Fulé, C. Hull, J.L. Beyers, and M.E. Hunter. 2010. Post-wildfire seeding in forests of the western United States: An evidence-based review. Forest Ecology and Management 260:573–86. https://doi.org/10.1016/j.foreco.2010.06.004

Pilliod, D.S., and R.S. Arkle. 2013. Performance of quantitative vegetation sampling methods across gradients of cover in Great Basin plant communities. Rangeland Ecology and Management 66(6): 634–647.

Pilliod, D.S., and J.L. Welty. 2013. Land treatment digital library: US Geological Survey Data Series 806. http://pubs.er.usgs.gov/publication/DS806

Pilliod, D.S., J.L. Welty, and R.S. Arkle. 2017. Refining the cheatgrass–fire cycle in the Great Basin: Precipitation timing and fine fuel composition predict wildfire trends. Ecology and Evolution 7(19): 8126-8151.

Porensky, L.M., J.D. Derner, and D.W. Pellatz. 2018. Plant community responses to historical wildfire in a shrubland–grassland ecotone reveal hybrid disturbance response. Ecosphere 9(8): e02363. https://doi.org/10.1002/ecs2.2363.

Pouyat, R.V., K.C. Weathers, R. Hauber, G.M. Lovett, A. Bartuska, L. Christenson, J.L. Davis, S.E. Findlay, H. Menninger, E. Rosi-Marshall, and P. Stine. 2010. The role of federal agencies in the application of scientific knowledge. Frontiers in Ecology and Environment 8(6):322-328.

PRISM Climate Group. 2017. PRISM Climate Data. http://prism.oregonstate.edu

Pyke, D.A. 1994. Ecological significance of seed banks with special reference to alien annuals. Proceedings – ecology and management of annual rangelands. 197-201. INT-GTR-313. USDA Forest Service, Ogden, UT, USA.

Pyke, D.A., J.E. Herrick, P. Shaver, and M. Pellant. 2002. Rangeland health attributes and indicators for qualitative assessment. Journal of Rangeland Management 55(6): 584–597. https://doi.org/10.2307/4004002.

Rasanen, A., and T. Virtanen, 2019. Data and resolution requirements in mapping vegetation in spatially heterogeneous landscapes. Remote Sensing of the Environment 230(1): 111207 https://doi.org/10.1016/j.rse.2019.05.026

R Core Team. 2017. R: A language and environment for statistical computing. R Foundation for Statistical Computing, Vienna, Austria. https://www.R-project.org/

Rigge, M., C. Homer, L. Cleeves, D.K. Meyer, B. Bunde, H. Shi, G. Xian, S. Schell, M. Bobo. 2020. Quantifying Western US Rangelands as fractional components with multi-resolution remote sensing and in situ data. Remote Sensing 12(3):412. https://doi.org/10.3390/rs12030412

Rigge, M., C. Homer, H. Shi, D. Meyer, B. Bunde, B. Granneman, K. Postma, P. Danielson, A. Case, and G. Xian. 2021. Trends in rangelands fractional components across the western US from 1985–2018. Remote Sensing, 13: 813. https://doi.org/10.3390/rs13040813.

Russell L.F. and A. Roy. 2008. Spatial variation in seed limitation of plant species richness and population sizes in floodplain tallgrass prairie. Oecologia 158:569-578.

San-José, M., V. Arroyo-Rodríguez, P. Jordano, J.A. Meave, and M. Martínez-Ramos. 2019. The scale of landscape effect on seed dispersal depends on both response variables and landscape predictor. Landscape Ecology 34, 1069–1080. https://doi.org/10.1007/s10980-019-00821-y

Sant, E.D., G.E. Simonds, R.D. Ramsey, and R.T. Larsen. 2014. Assessment of sagebrush cover using remote sensing at multiple spatial and temporal scales. Ecological Indicators 1(43): 297–305. https://doi.org/10.1016/j.ecolind.2014.03.014

Schlaepfer, D.R., W.K. Lauenroth, and J.B. Bradford. 2012. Ecohydrological niche of sagebrush ecosystems. Ecohydrology 5(4): 453-66.

Schoennagel, T.L., and D.M. Waller. 1999. Understory responses to fire and artificial seeding in an eastern Cascades Abies grandis forest, USA. Canadian Journal of Forest Research 29(9):1393-401.

Schupp, E.W., R. Zwolak, and L.R. Jones, and R.S. Snell, N.G. Beckman, C. Aslan, B.R. Cavazos, E. Effiom, E.C. Fricke, F. Montaño-Centellas, and J. Poulsen. 2019. Intrinsic and extrinsic drivers of intraspecific variation in seed dispersal are diverse and pervasive. AoB Plants 11(6):plz067. https://doi.org/10.1093/aobpla/plz067

Seaborn, T., K.R. Andrews, C.V. Applestein, T.M. Breech, M.J. Garrett, A. Zaiats, and T.T. Caughlin. 2021. Integrating genomics in population models to forecast translocation success. Restoration Ecology 29(4):e13395. https://doi.org/10.1111/rec.13395

Shinneman, D.J. and S.K. McIlroy. 2016. Identifying key climate and environmental factors affecting rates of post-fire big sagebrush (Artemisia tridentata) recovery in the northern Columbia Basin, USA. International Journal of Wildland Fire 25(9): 933-945.

Shive, K.L., H.K. Preisler, K.R. Welch, and H.D. Safford, R.J. Butz, K.L. O'Hara, S.L. Stephens. 2018. From the stand scale to the landscape scale: predicting the spatial patterns of forest regeneration after disturbance. Ecological Applications 28(6):1626-1639.

Shriver, R.K., C.A. Andrews, R.A. Arkle, D.M. Barnard, M.C. Duniway, M.J. Germino, D.S. Pilliod, D.A. Pyke, J.L. Welty, and J.B. Bradford. 2019. Transient population dynamics impede restoration and may promote ecosystem transformation after disturbance. Ecological Letters 22(9): 1357-1366.

Shryock, D.F., T.C. Esque, and F.C. Chen. 2015. Topography and climate are more important drivers of long-term, post-fire vegetation assembly than time-since-fire in the Sonoran Desert, US. Journal of Vegetative Science 26(6): 1134-1147.

Smith, M.O., J.B. Adams, and D.E. Sabol. 1994. Mapping Sparse Vegetation Canopies In Imaging Spectrometry—A Tool for Environmental Observations 1994. Springer, Dordrecht, pp. 221–235.

Smith, W.K., M.P. Dannenberg, D. Yan, S. Herrmann, M.L. Barnes, G.A. Barron-Gafford, J.A. Biederman, S. Ferrenberg, A.M. Fox, A. Hudson, and J.F. Knowles. 2019. Remote sensing of dryland ecosystem structure and function: Progress, challenges, and opportunities. Remote Sensing of the Environment 233: 111401. https://doi.org/10.1016/j.rse.2019.111401.

Smithson, M., and J. Verkuilen. 2006. A better lemon squeezer? Maximum-likelihood regression with beta-distributed dependent variables. Psychological Methods 11(1), 54.

Snell, R.S., N.G. Beckman, E. Fricke, B.A. Loiselle, C.S. Carvalho, L.R. Jones, N.I. Lichti, N. Lustenhouwer, S.J. Schreiber, C. Strickland, and L.L. Sullivan. 2019. Consequences of intraspecific variation in seed dispersal for plant demography, communities, evolution and global change. AoB Plants 11(4):plz016. https://doi.org/10.1093/aobpla/plz016

Spanhove, T., J.V. Borre, S. Delalieux, B. Haest, and D. Paelinckx. 2012. Can remote sensing estimate fine-scale quality indicators of natural habitats? Ecological Indicators 1(18): 403–412. https://doi.org/10.1016/j.ecolind.2012.01.025

Strassburg, B.B.N., A. Iribarrem, H.L. Beyer, C.L. Cordeiro, R. Crouzeilles, C.C. Jakovac, A.B. Junqueira, E. Lacerda, A.E. Latawiec, A. Balmford, T.M. Brookes, S.H.M. Butchart, R.L. Chazdon, K.H. Erb, P. Brancalion, G. Buchanan, D. Cooper, S. Diaz, P.F. Donald, V. Kapos , D. Leclere, L. Miles, M. Obersteiner, C. Plutzar, D. Alberto de M. Scaramuza, F.R Scarano, and P. Visconti. 2020. Global priority areas for ecosystem restoration. Nature 586:724–9. https://doi.org/10.1038/s41586-020-2784-9

Sullivan, L.L., A.T. Clark, D. Tilman, and A.K. Shaw. 2018. Mechanistically derived dispersal kernels explain species-level patterns of recruitment and succession. Ecology 99(11): 2415-2420. https://doi.org/10.1002/ecy.2498

Svoray, T., A. Perevolotsky, and P.M. Atkinson. 2013. Ecological sustainability in rangelands: the contribution of remote sensing. International Journal of Remote Sensing 34(17): 6216–6242. https://doi.org/10.1080/01431161.2013.793867

Tackenberg, O., F. Heydel, S. Cunze, and M. Bernhardt-Romermann. 2015. Seasonal synchronization of seed release phenology promotes long-distance seed dispersal by wind for tree species with medium wind dispersal potential. Journal of Vegetation Science 26(6):1090–101. https://doi.org/10.1111/jvs.12305

Tamme, R, L. Götzenberger, M. Zobel, J.M. Bullock, D.A. Hooftman, A. Kaasik, and M. Pärtel. 2014. Predicting species' maximum dispersal distances from simple plant traits. Ecology 95(2):505-13. https://doi.org/10.1890/13-1000.1

Thomson, F.J., A.T. Moles, T.D. Auld, and R.T. Kingsford. 2011. Seed dispersal distance is more strongly correlated with plant height than with seed mass. Journal of Ecology 99(6): 1299–307. https://doi.org/10.1111/j.1365-2745.2011.01867.x

Urza, A.K., and J.S. Sibold. 2017. Climate and seed availability initiate alternate post-fire trajectories in a lower subalpine forest. Journal of Vegetation Science 28(1):43–56. https://doi.org/10.1111/jvs.12465

Valley, R.D. 2016. Case Study. Spatial and temporal variation of aquatic plant abundance: Quantifying change. Journal of Aquatic Plant Management 54: 95–101.

van Putten, B., M.D. Visser, H.C. Muller-Landau, and P.A. Jansen. 2012. Distorted-distance models for directional dispersal: a general framework with application to a wind-dispersed tree. Methods in Ecology and Evolution 3(4):642-52. https://doi.org/10.1111/j.2041-210X.2012.00208.x

Warneke, C.R., T.T. Caughlin, E.I. Damschen, N.M. Haddad, D.J. Levey, and L.A. Brudvig. 2022. Habitat fragmentation alters the distance of abiotic seed dispersal through edge effects and direction of dispersal. Ecology 103(2). https://doi.org/10.1002/ecy.3586

Webber, B.L., B.A. Norton, and I.E. Woodrow. 2010. Disturbance affects spatial patterning and stand structure of a tropical rainforest tree. Australian Ecology 35; 423–34. https://doi.org/10.1111/j.1442-9993.2009.02054.x

Welch, B.L., and D.L. Nelson. 1995. Black Stem Rust Reduces Big Sagebrush Seed Production. Journal of Range Management 48(5): 398–401.

Wenger, S.J., and J.D. Olden. 2012. Assessing transferability of ecological models: an underappreciated aspect of statistical validation. Methods in Ecology and Evolution 3(2): 260-267.

Wijayratne, U.C., and D.A. Pyke. 2012. Burial increases seed longevity of two Artemisia tridentata (Asteraceae) subspecies. American Journal of Botany 99(3):438-47. https://doi.org/10.3732/ajb.1000477

Willmott, C.J. 1981. On the validation of models. Physical Geography 2(2):184-194.

Wilson, A.M., J.A. Silander, A. Gelfand, and J.H. Glenn. 2011. Scaling up: Linking field data and remote sensing with a hierarchical model. International Journal of Geographical Information in Science 25(3): 509–521. https://doi.org/10.1080/13658816.2010.522779.

Wilson, C.H., T.T. Caughlin., S.W. Rifai, E.H. Boughton, M.C. Mack, and S.L. Flory. 2017. Multi-decadal time series of remotely sensed vegetation improves prediction of soil carbon in a subtropical grassland. Ecological Applications 27(5), 1646-1656.

Winward, A.H., and E.W. Tisdale. 1977. Taxonomy of the artemisia tridentata complex in Idaho. Bull number 19.

Wright, H.A. 1985. Effects of fire on grasses and forbs in sagebrush-grass communities. Pages 12-21 *in* Rangeland Fire Effects; A Symposium, Boise, ID, USA.

Wu, D., X. Zhao, S. Liang, T. Zhou, K. Huang, B. Tang, and W. Zhao. 2015. Time-lag effects of global vegetation responses to climate change. Global Change Biology 21(9): 3520-3531.

Wu, J., W. Shen, W. Sun, and P.T. Tueller. 2002. Empirical patterns of the effects of changing scale on landscape metrics. Landscape Ecology 17(8): 761–782. https://doi.org/10.1023/A:1022995922992

Xu, M., C.G. Lacey, and S.D. Armstrong. 2018. The feasibility of satellite remote sensing and spatial interpolation to estimate cover crop biomass and nitrogen uptake in a small watershed. Journal of Soil and Water Conservation 73(6): 682–692. https://doi.org/10.2489/jswc.73.6.682.

Young, D.J., C.M. Werner, K.R. Welch, T.P. Young, H.D. Safford, and A.M. Latimer. 2019. Post-fire forest regeneration shows limited climate tracking and potential for drought-induced type conversion. Ecology 100(2): e02571

Young, J.A., and R.A. Evans. 1989. Dispersal and germination of big sagebrush (Artemisia tridentata) seeds. Weed Science 37: 201-206.

Yu, L., L. Liang, J. Wang, Y. Zhao, Q.U. Cheng, L. Hu, S. Liu, L. Yu, X. Wang, P. Zhu, X. Li, Y. Xu, C. Li, W. Fu, X. Li, W. Li, C. Liu, N.A. Cong, H. Zhang, F. Sun, X. Bi, Q. Xin, D. Li, D. Yan, Z. Zhu, M.F. Goodchild, and Gong, P., 2014. Meta-discoveries from a synthesis of satellite-based land-cover mapping research. International Journal of Remote Sensing 35(13): 4573–4588

Zaiats, A., B.E. Lazarus, M.J. Germino, M.D. Serpe, B.A. Richardson, S. Buerki, T.T. Caughlin. 2020. Intraspecific variation in surface water uptake in a perennial desert shrub. Functional Ecology 34(6): 1170-1179. https://doi.org/10.1111/1365-2435.13546

Ziegenhagen, L.L., and R.F. Miller. 2009. Postfire recovery of two shrubs in the interiors of large burns in the Intermountain West, USA. Western North American Naturalist 69(2): 195-205. https://doi.org/10.3398/064.069.0208

APPENDIX A

Supplementary Material for Chapter One

Table A.1 **Pearson's correlation between covariates (row x column are the two variables and the value is the correlation).**

	Percent Sand	Percent Clay	Elevation
Percent Sand	-	-0.27	-0.14
Percent Clay	-0.27	-	0.17
Elevation	-0.14	0.17	-

APPENDIX B

Supplementary Material for Chapter Two

Figure B.1   A photo of seed traps set up along transects at the Soda wildfire.

Table B.1 **Comparisons of different dispersal kernel fits using distance-only (no height) fit using maximum likelihood.**

Fit	Source	AIC	BIC
Gaussian	Clark et al. (1999)	1334.45	1345.75
Ribbens	Ribbens et al. (1994)	1355.87	1367.18
Negative exponential	Greene and Calogeropoulos (2002), Bullock and Clarke (2000)	1279.39	1290.7
2Dt	Clark et al. (1999)	1201.55	1216.62
Inverse power	Bullock and Clarke (2000)	1205.63	1220.703

Table B.2   **Priors on parameter values for the landscape model.**

Parameter	Description	Prior
$\gamma 0$	Intercept	student_t(3, −2, 10)
$\gamma 1$	Effect of height on trapped seed density	normal(0, 1)
$\gamma 2$	Effect of distance on trapped seed density	normal(0, 1)
$\gamma 3$	Height × distance interaction effect on seed density	normal(0, 1)
$\gamma 4$	Effect of total available seed on trapped seed density	normal(0, 1)
$\phi 1$	Dispersion parameter for negative exponential	exponential(1)
sd_transect	A set of variance parameters describing transect-level variance height and distance parameters ($\gamma 1$, $\gamma 2$, $\gamma 3$)	student_t(3, 0, 10

Table B.3   Priors on parameter values for the empirical 2Dt and mechanistic WALD integrated model.

Priors on ω, δ, $v1$ and $v2$ were set weighted more strongly towards 0 with the assumption that transects would not display extremely different dispersal kernels.

Parameter	Description	Prior	Constraint
A	Global parameter governing 2Dt kernel	half-normal(0, 1)	$a \geq 0$
B	Global parameter governing 2Dt kernel	half-normal(0, 1)	$b \geq 0$
F	Total available seed effect	half-normal(0, 1)	None
$\phi2$	Dispersion parameter for negative exponential	exponential(1)	$\varnothing > 0$
ω	Deviation between a and each transect	normal(0, 0.5)	None
δ	Deviation between b and each transect	normal(0, 0.5)	None
$v1$	Transect-level variance for the a parameter	exponential(4)	$v1 > 0$
$v2$	Transect-level variance for the b parameter	exponential(4)	$v2 > 0$
$dist_{wald}$	Latent distance travelled between the trap and the ground	wald(ρ, λ)	$0 \geq dist_{wald} \geq 50$

APPENDIX C

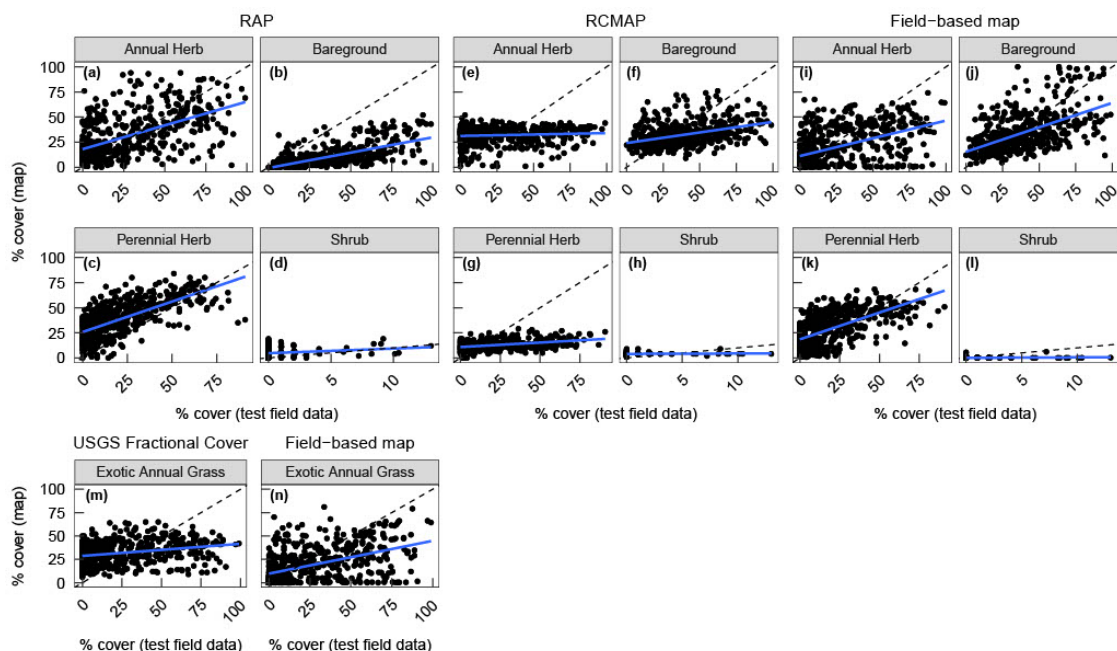**Supplementary Material for Chapter Three**

Figure C.1 **Relationship of satellite- or field-derived modeled vegetation cover (Y) to test field data (X) in 2017.**

Models included the Rangeland Analysis Platform (RAP, a through d), Rangeland Condition Monitoring Assessment and Projection (RCMAP, e through h), a field-based benchmark map (i through l & n), or the USGS fractional cover estimate (m). The diagonal dashed line on each plot shows the one-to-one correspondence (perfect accuracy) and the blue line shows the linear regression line fit for each functional group.
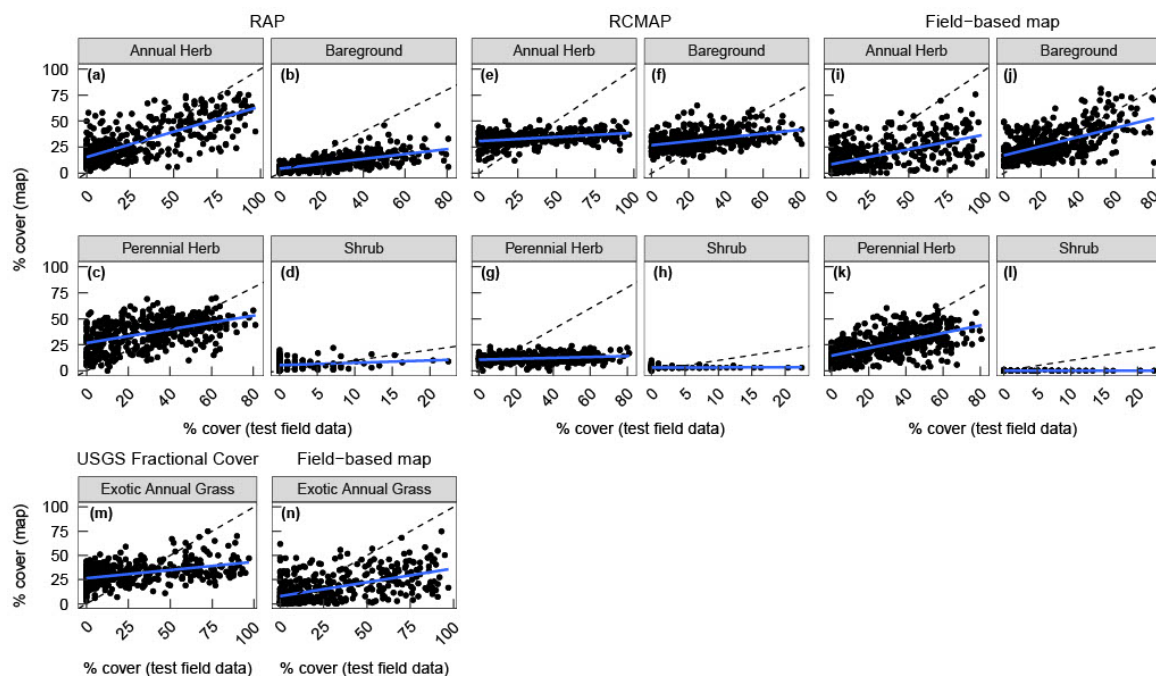
Figure C.2 **Relationship of satellite- or field-derived modeled vegetation cover (Y) to test field data (X) in 2018.**

Models included the Rangeland Analysis Platform (RAP, a through d), Rangeland Condition Monitoring Assessment and Projection (RCMAP, e through h), a field-based benchmark map (i through l & n), or the USGS fractional cover estimate (m). The diagonal dashed line on each plot shows the one-to-one correspondence (perfect accuracy) and the blue line shows the linear regression line fit for each functional group.
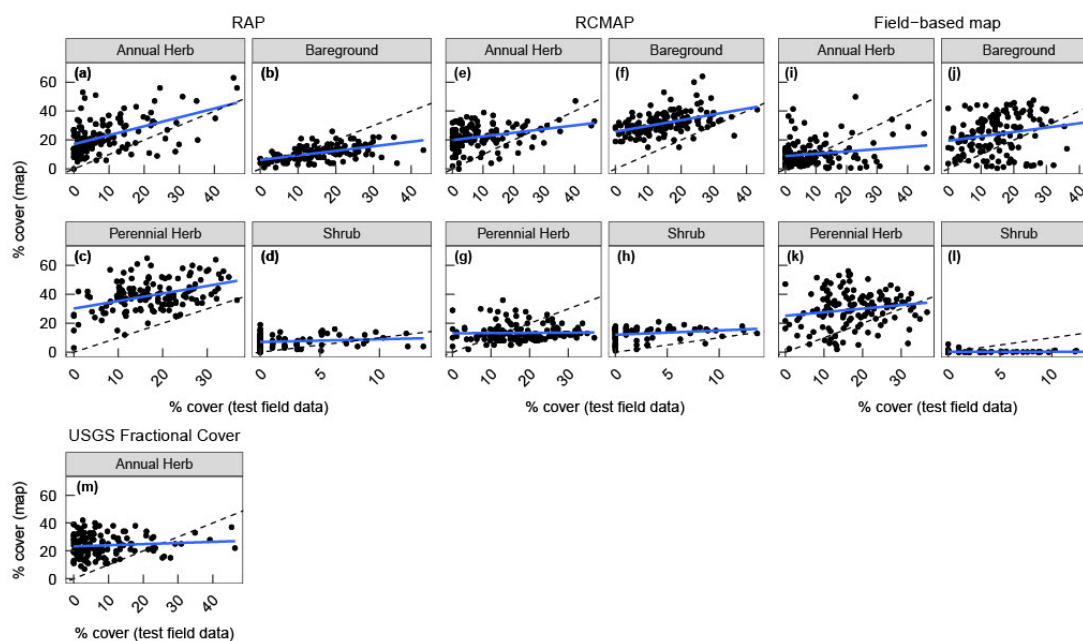
Figure C.3   Relationship of satellite- or field-derived modeled vegetation cover (Y) to test field data (X) in 2020.

Models included the Rangeland Analysis Platform (RAP, a through d), Rangeland Condition Monitoring Assessment and Projection (RCMAP, e through h), a field-based benchmark map (i through l & n), or the USGS fractional cover estimate (m). The diagonal dashed line on each plot shows the one-to-one correspondence (perfect accuracy) and the blue line shows the linear regression line fit for each functional group.